Decarbonising the Transport and Electricity Sectors Using Hydrogen

A thesis submitted to Cardiff University in candidature for the degree of Doctor of Philosophy

By

Oscar Utomo

Institute of Energy, Cardiff School of Engineering

Cardiff University, 2023

Acknowledgements

Alḥamdulillahi waḥdah waṣ-ṣalatu was-salam `alā man lā nabiyya ba`da

The journey towards completing a work of this magnitude would not have been possible by the effort of a single person. If one claims to be capable of completing such a feat by themselves, they are either one of the greatest people to walk the face of this earth or they are simply a liar. I hereby declare with the utmost integrity to be neither.

First and foremost, I would like to express my deepest gratitude to my principal supervisor, Professor Carlos Ugalde-Loo for his constant encouragement, guidance, and belief that I was capable of completing this PhD programme despite all odds.

To my second supervisor, Dr. Muditha Abeysekera, I am truly grateful we crossed paths. Thank you for keeping me on course and supporting me throughout my toughest moments as a trainee researcher.

Having 2 outstanding intellectuals and human beings as my supervisors, I truly learnt a lot and would not be the person I have become today had it not been for this shared experience.

My deepest gratitude to all the senior academics in the energy infrastructure research group (Professor Nick Jenkins, Professor Jianzhong Wu, and Professor Meysam Qadrdan) who have over the course of the PhD provided me with additional guidance and support. This thanks also extends to my friends and colleagues in the CIREGS team for inspiring me every day to become a better researcher.

I would also like to thank, Dr. Tim Farnham of Toshiba Research Europe, Mr. Terence Pycroft of Leeds City Council, Mr. Martin Aizlewood of Rotherham Hospital and the estates department of Queen Elizabeth Hospital for the valuable data and insights.

To my mother, Martha J. Said. Thank you for believing in me and never giving up on my endeavours despite my trials and tribulations as a person. It was your constant belief that I can grow beyond what I am is what has led me to this very moment in life.

To my father, Dr. Wahyu Utomo, I hope I can be the addition to 2 generations of “Dr. Utomos”. You have been one of my greatest inspirations and heroes growing up and you remain so to this very day. Your exemplary work ethic and belief that there is always a solution to any problem in life is what I held on to during the difficult periods of my research journey.

To my sister, Calista A. Utomo, thank you for always being there for me and reminding me that I am capable of great things when I put my mind to it. You're awesome and I honestly think that you'll be a very successful architect in the future. I wish you all the happiness life can give.

To my office mates, Dr. Hector Bastida, Dr. Davide Pinzan, Sofia Mavidou, Kai Zhang, Dr. Saad Khalaf, Dr. Athanasios Mermigkas, Konstantinos Stamatis, Krzysztof Jakubiak and those who have graced E.1.24(5) over the years. Thank you for the camaraderie, encouragement, support and coffee breaks! You all have a special place in my heart.

To my friends Alex Robertson, Russell W. Cross, and Vishwajith Lokuhapuarachchige from 43 Daniel Street, thank you for being such loyal housemates even though the pandemic cut the fun short. To my friends from the Indonesian society over the years who I cannot mention one by one as that would probably lead to a document comparable in length to an undergraduate thesis, thank you for giving me a piece of home here in Wales.

To Dr. Baskoro A. Pratomo, thank you for helping me settle in Cardiff. I will miss our philosophical discussions and hope to catch up soon given the opportunity. Also, a very sincere thank you to Francesca L. Saleh and Idzudin bin Mokhtar for always lending an ear and for the loyal friendship which has lasted the test of time and distance.

To the wonderful Alexandra, thank you for the endless encouragement, care, support and love you have shown me throughout the final year of my PhD studies. You have been a source of great inspiration, comfort to me and kept me going when times were hard. I hope to show you the same levels of support, love and dedication come the time where you will be handing in your PhD thesis in the near future.

Lastly, as a person who grew up with a learning disability and struggled with lots of self-doubt, I am dedicating this work to those who struggled with similar issues growing up as it is at times isolating and terrifying when the person who keeps you back and doubts you the most is yourself. Sometimes I wish I could go back in time and tell my younger self: "keep going, you'll

turn out alright” because I did turn out alright. So, to those struggling with the same, let me tell you this: keep going, you’ll turn out alright!

Abstract

Energy systems are becoming increasingly integrated because energy providers need to address the diverse market. As fossil fuel based energy is slowly being phased out in both the electricity sector and the transportation sector, the new sources of energy need to be both renewable and non-polluting. Due to the drive for a clean and renewable energy supply, there has been a marked increase in intermittent renewable electricity generation. However, intermittent renewable electricity generation may cause supply uncertainties and pose other technical challenges. To address this problem, sufficient energy storage is needed to meet the demand. Furthermore, frequent fluctuations in intermittent renewable electricity generation may cause damage to the electricity grid. Hence, a form of clean dispatchable energy is needed to mitigate the negative effects of intermittency. Given that the UK government aims to ban the sales of new fossil-fuel powered vehicles from 2030, the techno-economic feasibility of new energy vectors to meet these conditions must be better understood. This thesis focuses on the use of hydrogen as an energy vector for decarbonising the transport and electricity sectors. The lack of real operational data and high capital costs are the main barriers to understanding the role that hydrogen can play in providing a part of the solution towards contemporary energy issues. Furthermore, methods for obtaining data for hydrogen-based systems can be complex causing technical exposure and awareness to a very select group of people.

Hence, the work in this thesis attempts to address these issues by developing simple but accurate methods to generate representative electricity demand profiles and hydrogen refuelling data. This data can then be used to conduct studies such as cost analyses for transitioning from conventional fuelled vehicles to hydrogen-powered vehicles and/or optimisation studies for integrated energy systems with hydrogen generation, storage and dispatch to provide a more comprehensive view on how hydrogen can be used to decarbonise parts of the transportation and electricity sectors.

Table of Contents

List of Tables

List of Figures

Publications

The following is a list of publications produced during the duration of the research up until the period of thesis submission:

- **O. Utomo**, M. Abeysekera, and C. E. Ugalde-Loo, "Optimal Operation of a Hydrogen Storage and Fuel Cell Coupled Integrated Energy System," *Sustainability*, vol. 13, no. 6, p. 3525, Mar. 2021, doi: 10.3390/su13063525. [Online]. Available: http://dx.doi.org/10.3390/su13063525

Nomenclature

Abbreviations

ALK	Alkaline
ANN	Artificial Neural Networks
API	Application Programming Interface
ARIMA	Auto Regressive Integrated Moving Average
ARMA	Auto Regressive Moving Average Model
BEV	Battery Electric Vehicle
CBC	Branch and Cut Solver
CGE	Computable General Equilibrium
CHP	Combined Heat and Power
CO_2	Carbon Dioxide
COVID	Coronavirus Disease
DT	Decision Tree
ETM	Energy Transition Model
EU	European Union
FCEV	Fuel Cell Electric Vehicle
GAMS	General Algebraic Modelling System
GHG	Green House Gases
GUI	Graphical User Interface
ICE	Internal Combustion Engine
ICEV	Internal Combustion Engine Vehicle

IES	Integrated Energy System
KPI	Key Performance Indicator
LNG	Liquefied Natural Gas
MAPE	Mean Average Percentage Error
MATLAB	MATLAB Programming Software
MILP	Mixed Integer Linear Programming
MIT	Massachusets Institute of Technology
MPG	Miles per Gallon
MSR	Maintenance, Service, Repairs
MSRP	Manufacturer’s Suggested Retail Price
NN	Neural Network(s)
OC	Operational Cost
OPF	Optimal Power Flow
P2G	Power-to-Gas
PEM	Proton Exchange Membrane
QEH	Queen Elizabeth Hospital
RCV	Refuse Collection Vehicle
RV	Residual Value
SL	Storage Level
SOEC	Solid Oxide Electrolyser Cell
SUV	Sport Utility Vehicle
TC	Temperature Constant
TCO	Total Cost of Ownership

TRL	Technological Readiness Level
UI	User Interface
UK	United Kingdom
ULEV	Ultra Low Emission Vehicle
XCORR	Cross-Correlation

Capital Letters (Latin)

A	Area
C	Cost
E	Energy
G	Irradiance
N	Nominal
P	Pressure
S	Distance
T	Temperature
V	Speed

Small Letters (Latin)

n	Number of Elements
t	Time Step

Greek Letters

μ	Average
ε	Energy Content
η	Efficiency

ρ Air Density

Superscripts

H_2/e Hydrogen to Electricity Conversion

H_2 Hydrogen

e/H_2 Electricity to Hydrogen Conversion

$Diesel$ Diesel fuel

e Electricity

Subscript

S_{pu} Per Unit Distance

V_{pu} Per Unit Volume

m_{pu} Per Unit Mass

D Demand

$Dmax$ Maximum Demand

$Dmin$ Minimum Demand

EL Electrolyser

FC Fuel Cell

PV Photovoltaic

$grid$ Electricity Grid Supply

$inj\ store$ Storage Injection (in or out)

Chapter 1: Introduction

1.1 Motivation of Research

As the global economy grows, more people are becoming part of an urbanised middle class, the demand for industrial goods is rising and society is becoming more interconnected. Therefore, the global demand for energy will naturally increase with the passing of time. Historically, with the advent of industrialisation in the mid-eighteenth century and the development of the low-pressure steam engine by James Watt, non-renewable fossil fuels have fulfilled society's needs for manufactured goods, electricity, heating, transport, and logistics. Unfortunately, fossil fuel based primary energy sources are sources of CO_2 (carbon dioxide), which are key to the rising global temperatures. This is predicted to lead to the polar ice caps melting and a rise in global sea-levels. As the global COVID-19 pandemic has demonstrated, the physical and economic wellbeing of wider society can be compromised quite easily. Melting polar ice caps and glaciers can re-introduce many old pathogens, which most people are no longer immune to into the ecosystem [1]. Rising global sea-levels, drought, extreme heat, floods, and storms have also displaced many people [2]. Thus, solutions to stop such ecological catastrophes are in the interest of modern society.

There is currently a significant growth and development in the use of non-polluting energy sources, such as wind and solar power. It is such that in the UK, renewable electricity production share out of the total generation capacity has increased from 9.4% to 47.8% between 2011 and 2023 [3], [4]. Out of the total renewable generation capacity, 94% of this renewable generation capacity comes from wind and solar [3]. It is known that wind and solar power are very dependent on geographical conditions and weather. Thus, it would not be possible to produce electricity via wind and solar power based on demand. To address this issue, a source of dispatchable energy is required to make up for production shortages in times where demand is greater than supply. Similarly, when supply is greater than demand, energy is usually curtailed. Energy storage methods can be used to avoid curtailment and increase renewable energy supply. This in turn will assist in increasing the penetration of renewable generation. Looking at recent UK data, for the first quarter of 2023, fossil fuels made up 35% of the total electricity generation [3]. This puts renewable penetration at 65%

which is still far off from the ideal 100%. Given the relatively high percentage of fossil fuel based generation, it can be assumed that a significant amount of energy from fossil fuel based generation is used to address issues arising from intermittency as fossil fuel based generation is an effective means of dispatchable electricity. Therefore, efforts to provide clean dispatchable electricity must be explored further.

Hydrogen storage presents a non-emitting solution for increasing renewable penetration. Stored hydrogen can be used as a fuel source for long term energy storage and via a fuel cell, can be converted into electricity. This stored hydrogen can then act as a means of providing clean dispatchable electricity to address load mismatches at times when demand is higher than supply and avoid curtailment when supply is higher than demand.

Another significant contributor to air pollution is vehicle transport fuel. Currently, 25% of all greenhouse gas emissions in the UK comes from the transportation sector to which 80% of transport emissions come from road-based transport (cars, taxis, HGVs, Buses) [5]. As of the final quarter of 2022, 94.3% of these vehicles run on fossil fuels [5]. There has been a rise of sales for battery electric vehicles which is a positive trend in the effort for decarbonising the transportation sector. However, this may be difficult to replicate in other heavier transportation sectors. For such vehicles, diesel is the usual fuel. Diesel is very energy-dense which makes it suitable for heavy transport especially over long distances. If batteries were used for this type of transport, the load capacity would need to be limited unless rapid charging is possible for larger battery electric vehicles [6]. Hydrogen on the other hand possesses high energy density and has low refuelling times which would make it more suitable for this type heavy of transport [7]. Hence, there is also potential for using stored clean hydrogen as a source of transportation fuel which would assist in the decarbonisation of both the electricity and transportation sectors simultaneously.

At present, the use of hydrogen as an energy vector is rare when compared to other energy vectors, such as electricity, coal, natural gas and other crude oil derived fuels. Referring to the Hydrogen Net Zero Investment Roadmap, current government projections regarding installed blue and green hydrogen capacity in the UK barely reaches 1GW though this is expected to grow to almost 20GW by 2030 [8]. However, at present, projects where hydrogen storage is used for electricity supply and transportation fuel are rare in comparison to other technologies (i.e., battery storage, pumped-hydro storage, flywheel, compressed air and heat) and limited to small scale demonstration projects [9]. Hence, the availability of operational data is lacking. The lack of operational data poses challenges as it limits the possibility of studying the role hydrogen plays in integrated energy systems and how it affects the behaviour of other energy vectors present (i.e.: electricity) with hydrogen across diverse scenarios related to renewable electricity intermittency. Furthermore, the lack of data on hydrogen-based transportation technologies makes it difficult to assess the potential techno-economic benefits of using hydrogen as a transport fuel. This causes knowledge gaps that hamper the adoption of hydrogen-based technologies as a lack of convincing studies discourages industry from utilising the technology.

This thesis aims to address the knowledge gaps concerning the use of hydrogen-based technologies in integrated energy systems (IESs) and transportation by developing a series of methods which include producing representative electricity load profiles, quantifying hydrogen fuel demand for transportation as well as integrated energy systems modelling to study the potential benefits of using hydrogen for decarbonising the electricity and transport sectors.

1.2 Hydrogen as an Energy Vector

An energy vector by definition is a form of energy that is derived from primary energy sources with a good degree of flexibility, which can be transported and converted at locations of demand at specific times [10].

Hydrogen is an example of an energy vector that can be obtained via conversion. The production paths of hydrogen are varied because it can be derived from an array of primary energy sources. At present, most hydrogen (95%) is produced via steam reformation [11]. Here, steam enriched natural gas or residues from the petroleum industry are converted to hydrogen via high heat and pressure. The problem with the steam reformation method is that it uses non-renewable fossil fuels. Another means of producing hydrogen is via electrolysis of water molecules. This process involves the use of an electric current to split water molecules into its respective elements of hydrogen and oxygen. This process can be fully zero emission given if the source of electricity to execute the process is derived from non-polluting renewable resources (e.g., wind or solar). Furthermore, electrolysis is much more energy efficient than steam reformation. Efficiency rates exceeding 90% for electrolysis were found in [12]. This is by far a better conversion efficiency rate than that of steam reformation, which is around 74% [13].

Comparing hydrogen and fossil fuel derived energy vectors, hydrogen is non-polluting when used as a fuel. When combusted with oxygen, the resultant emission is water vapour. This is also the case for the use of hydrogen as a source for electricity generation via a fuel cell. Another advantage of hydrogen is that hydrogen has an energy density of 120 kJ/g [14], whereas diesel and petrol have energy densities of 45.8 kJ/g and 46.5 kJ/g, respectively [15].

With regards to storing hydrogen, hydrogen requires compression because its volumetric energy density is only 4.7kWh/l, which is around half of that of diesel (10kWh/l) and petrol (9.6kWh/l) [16]. This means that there is risk of hydrogen incurring extra cost in terms of storage because there would need to be further investment made for the gas compressing infrastructure, or a larger storage tank to store the equivalent unit of energy when compared to petrol and diesel.

In terms of use, hydrogen is a versatile energy vector that can be used to power vehicles. Hydrogen can act as a fuel source for fuel cell electric vehicles (FCEVs) and dual fuel vehicles (diesel-hydrogen mix). Hydrogen converted via a fuel cell can also be used to supply electricity to buildings, industries and homes. Furthermore, hydrogen can be used for residential heating through the use of hydrogen boilers or heat pumps, which capture waste heat dissipated by hydrogen conversion systems.

Table 1.1 lists the common energy vectors, their production methods and transport methods.

Table 1.1: List of common energy vectors and performance indicators [10],[17]–[23]

Energy Vectors	Energy Density (kWh/kg)	Storage Duration (Considering Discharge and Shelf Life)	Emits CO_2?	Storage Capacity	Capable of seasonal storage and is non-emitting?
Naturally Occurring					
• Coal	6.1-6.9	Indefinite	Yes	Indefinite (can exceed 100 TWh range)	No
• Natural gas	14.9	Indefinite	Yes	Indefinite (can exceed 100 TWh range)	No
Refined/Processed Energy Sources					
• Crude oil derivatives	12.6-12.9	6-12 months	Yes	≈300 MWh (based on UK average fuel storage tank at fuel pumps)	No

(Table 1.1-Cont)					
• Biodiesel	11.7	4 months-3 years (depending on induction period)	Yes	≈300 MWh (based on UK average fuel storage tank at fuel pumps)	No
Derived Energy					
• Electricity	0.14-0.2 (Lithium-Ion Battery Storage)	4-100 hours	No	5 kWh-10 MWh	No
• Hydrogen	33.3	1 week-1 year	No	1 GWh-1 TWh	Yes

Out of the energy vectors listed in Table 1.1, electricity and hydrogen are the only non-polluting/non-emitting energy vectors at point of use. Both hydrogen and electricity can be used in the transportation, electricity generation and heat sectors. Electricity edges hydrogen in terms of round-trip efficiency because most equipment to which electricity is suppled runs on electricity, which means that energy losses mainly occur in storage. Comparing the round-trip efficiencies of the two energy vectors, electricity has a round-trip efficiency between 75%–90% [24], whereas hydrogen has a round-trip efficiency of around 30%–35% [24], [25]. However, when looking at a longer period of storage, hydrogen is the better energy vector because it can be stored for longer due to its higher discharge time [26]. Given the longer discharge time, hydrogen as an energy vector is more suitable for seasonal energy storage than electricity.

1.3 Integrated Energy Systems and Dispatchable Energy Sources

Urban centres possess an array of infrastructure for transporting various energy vectors to supply energy needs. Distribution networks for electricity and gas are well established in most urban centres in the UK. Taking into consideration the effects of global warming, the ageing infrastructure, and rising fuel costs, new energy carrier systems such as district heating and cooling, electrification of heating and transport, as well as the development of smart electricity grids are being built as a joint effort to tackle these issues [27].

The availability of different energy vectors allows for greater flexibility in the design of energy provision services and also allows for the exploration of using different forms of locally available energy sources. Energy vectors such as hydrogen can be exploited further in a setting where a local energy system can store excess generated renewable electricity because it can be used as an additional source of backup electricity. Stored hydrogen can also be distributed for use in the transport sector as a fuel for hydrogen powered vehicles. Furthermore, hydrogen can also be used for domestic heating applications. In addition, as energy supply infrastructures are becoming increasingly integrated, the impact of design and techno-economic operation of these infrastructures need to be better understood.

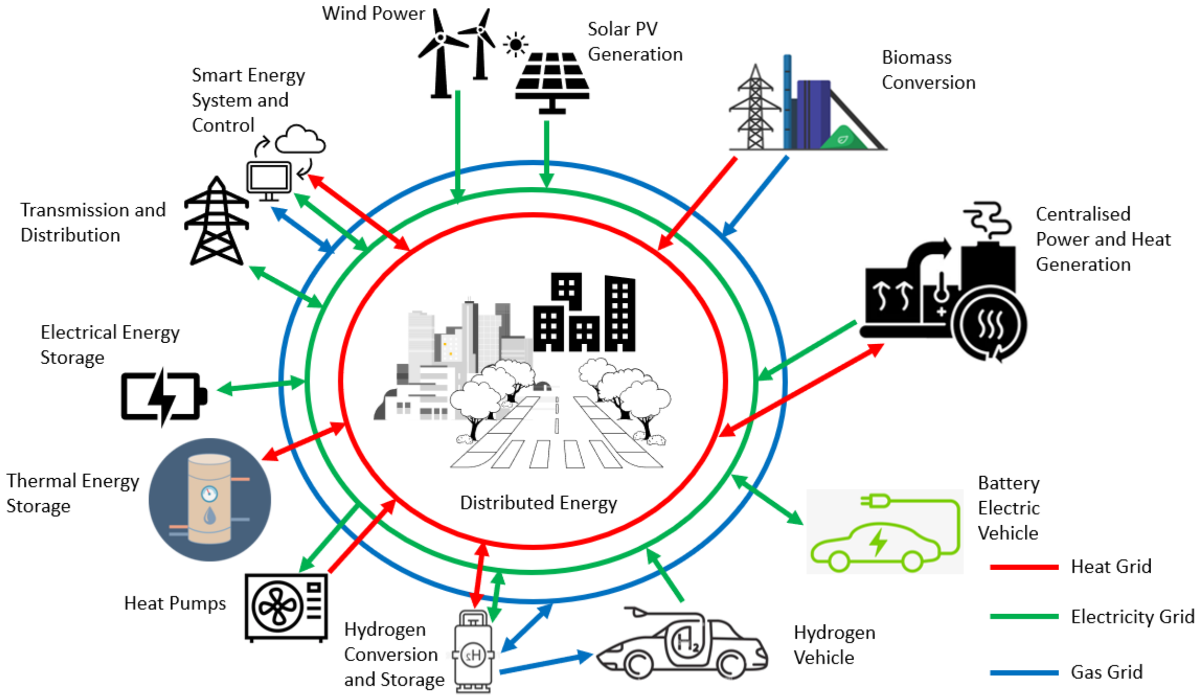

Figure 1.1: Interactions of different energy vectors in an integrated energy system [28]

Figure 1.1 illustrates the possible interactions between different energy supply systems and their interactions in an urban environment. For example, the hydrogen conversion and storage system have interactions with all three present grids (i.e., gas, heat and electricity). The blue arrow denotes hydrogen energy and its interaction with the gas grid and vehicle refuelling. The interconnection of a hydrogen conversion and storage system to the gas grid is possible because hydrogen can be blended into the natural gas mix and transported in existing natural gas networks. The green arrow shows the interdependency between the hydrogen conversion and storage system and the electrical grid. This can be explained by the need for electricity to produce hydrogen and the act of exporting electricity back to the grid via conversion using a fuel cell. The red arrow represents the interactions that the hydrogen conversion and storage system have with the heat grid. The hydrogen conversion and storage system dissipate heat as energy losses, which can be absorbed back into the heat grid. Where the hydrogen conversion system is based on solid oxide technology, heat supply for the conversion processes can be sourced from the heat grid.

Given the example of the various interconnections between the three grids and the hydrogen conversion and storage system, greater flexibility of the energy sources was demonstrated. Integration of the energy systems allows the energy vectors to provide more than one function (i.e.: electricity generation). Due to energy system integration, several energy vectors can be used across different sectors, such as electricity generation, heating, and transport. This allows for faster decarbonisation of three separate sectors simultaneously because the energy sources for both heating and transport can come from renewable energy generated not just directly from the wind turbines and solar PV systems but also from stored electricity and stored hydrogen.

Integration of the energy system, such as that shown in Figure 1.1, provides more freedom to the energy system design. Since more energy sources are being interconnected, the supply for a particular energy source does not need to rely on one specific means of production.

The benefits of IES and the inclusion of hydrogen in IES is elaborated further in chapter 2. These benefits are summarised in the following bullet points.

- Reduction in overall CO_2 emissions as dispatchable energy required for base-load generation can be sourced from hydrogen instead of conventional fossil-fuel based generators.
- High energy density of hydrogen allows for greater storage capacity when compared to other clean energy storage technologies [23].
- Increased flexibility of energy supply sources as hydrogen can be used for addressing load mismatches and provide a source of transport fuel.
- The fast dynamics of hydrogen conversion technologies can provide ancillary services such as frequency support without having to rely on fossil-fuel based generators.
- Reduction of capital expenditure and operational cost savings over time in the case of an independent local energy system as on-site stored hydrogen can provide ancillary services without having to procure them from a service operator.
- Allows for better understanding of interdependencies between energy vectors in which hydrogen will have interactions with (i.e.: electricity and/or heat).
- Provides insights into emerging applications of hydrogen in specific sectors.

1.4 Thesis Structure and Challenges in Integration of Energy Systems and Decarbonisation of the Electricity and Transportation Sectors

The thesis structure is shown in Figure 1.2.

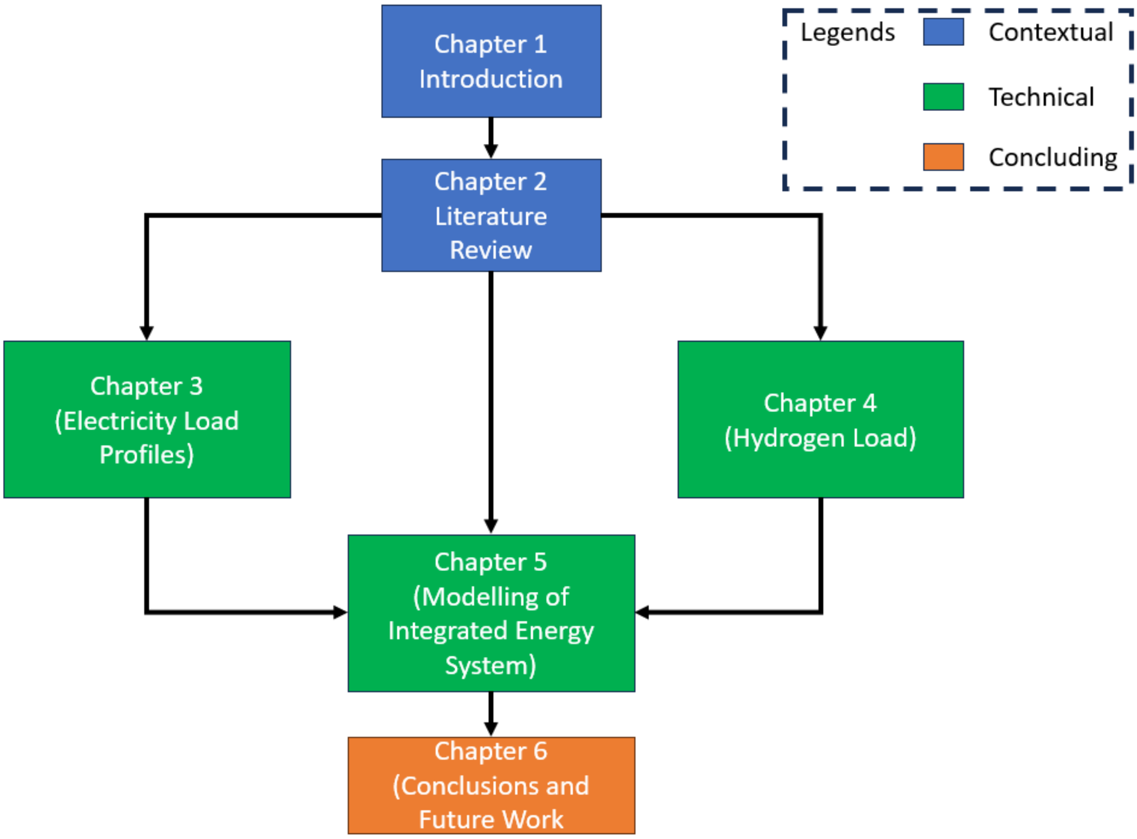

Figure 1.2:: Thesis Structure

The thesis starts off by providing a general overview of the research background, current state of research, challenges, associated research gaps and research objectives (chapter 1). This is then followed by a literature review (chapter 2) where the background and current state of research is discussed in detail. This pans out the work conducted in the subsequent technical contribution chapters (chapters 3,4 and 5) which the findings are then concluded and used to suggest future work.

With regards to general challenges regarding the study of integrated energy systems and the use of hydrogen for decarbonising the transportation and electricity sectors, these are listed below.

- Energy system integration introduces new interactions and interdependencies between different energy vectors that are not understood that well when operating in unison.
- Need for more demonstration projects to obtain a wider range of data to base future studies.
- Lack of sample input profiles for load and renewable electricity supply, only 7% of studies take this into account [29].
- Further studies of IESs that include storage system models accounting for maximum and minimum storage capacities are needed (only 40% of studies include this according to [29]).
- Greater integration of energy sources will result in a more complex energy system due to the different interactions between the different energy sources. This would require better understanding of the various interdependencies and more detailed studies to ensure system robustness.

These challenges are addressed categorically in Table 1.2.

Table 1.2: Summary of challenges in each technical contribution chapter

Technical Contribution Chapter	Challenge(s)
Chapter 3 (Technical Contribution 1)	• Availability of open-access historical demand data for individual building sites. • Complexity of methods for developing representative building energy demand profiles. • Direct monitoring of energy consumption of buildings can be costly due to equipment coupled with risk of equipment being faulty [30].
Chapter 4 (Technical Contribution 2)	• Lack of demonstration projects involving hydrogen for fleet vehicle operations. • Lack of available data surrounding capital costs of hydrogen refuse vehicles, operational costs, and aftersales costs. • Interest in using FCEVs in general is not as high as BEVs. • Studies of demonstration project for hydrogen RCVs mainly involve manufacturers, funding bodies and local councils without university involvement.
Chapter 5 (Technical Contribution 3)	• Lack of demonstration projects involving the use of hydrogen for grid balancing operations. • High capital costs for setting up hydrogen storage and conversion systems. • Low round-trip efficiency of hydrogen systems when compared to other dispatchable energy sources. • Energy storage applications using hydrogen still considered in early technological maturity.

1.5 Research Objectives

The objectives of the research were to develop methods for generating representative on-site electricity, hydrogen fuel consumption profiles and a mathematical model of a hydrogen-coupled integrated energy system to study cost optimal dispatch. This was done to address the lack of real operational data. It also provides a means of developing scenarios and models to study systems that employ hydrogen as an energy source in different sectors (e.g., the electricity and transport sectors).

1.6 Main Contributions

The main contributions of this research work are summarised in the following bullet points.

- A method to generate representative electricity-demand profiles is developed for sites that do not possess adequate monitoring infrastructure. This method is based on and validated using real electricity-demand data provided by the Rotherham and Queen Elizabeth hospital sites (chapter 3).
- Methods for working out the fuel consumption and fuel cost/mile of a hydrogen FCEV are developed. The fuel consumption characteristics of a would-be operational hydrogen powered refuse collection vehicle (RCV) are extrapolated and compared with the real operational data of a diesel powered RCV in the Leeds City Council refuse collection fleet. An overall total cost of ownership (TCO) and TCO/Mile study was conducted to compare the techno-economic competitiveness of operating a hydrogen powered RCV against diesel RCV in present and future scenarios. The sensitivity of the overall TCO and TCO/Mile of the RCVs (hydrogen and diesel powered) to independent variables such as ownership period, discount rates, fuel cell efficiencies and increases in fuel prices are also studied and assessed (chapter 4).
- A steady-state model of an integrated energy system coupled with a hydrogen conversion and storage system is developed and studied. The system on which the model is based is a real demonstration project (i.e., Levenmouth Community Energy Project). This system employs hydrogen for both grid balancing services and vehicle refuelling. A cost minimisation optimisation problem was defined and run on MATLAB. Several scenarios in which renewable energy supply is varied seasonally are developed

to study the system's behaviour and its response to daily changes (across seasons) in renewable energy supply. It also examines how the hydrogen storage and conversion system enhances the use of renewable energy in the system. The techno-economic contributions of the hydrogen storage and conversion system are also studied and summarised (chapter 5).

- Chapter 6 summarises the conclusions of the technical contributions and makes several recommendations for future research.

To summarise the technical contributions, the work in chapters 3 and 4 provide methodologies to produce demand profiles for both electricity and hydrogen. This is done to address situations where there is no data or there are outlier datasets which need to be corrected in order to coherently develop techno-economical analyses and optmisation studies such as that in chapter 5. Therefore, providing a means of developing scenarios and testing models to study systems that employ hydrogen as an energy source in different sectors (e.g., the electricity and transport sectors).

Chapter 2: Literature Review of Hydrogen Use to Decarbonise the Transport Sector and Energy Systems

2.1 Introduction

This chapter will review the technological and economic advantages of utilising hydrogen as an energy source in the transportation sector and as a means of providing reserve energy for immediate dispatch in IESs. State-of-the-art methods in the development of representative electricity generation, demand profile, hydrogen vehicle fuel demand, and performance will also be studied, along with methods of analysing cost optimal operations of IESs. The scope of the studies that are presented in this thesis are limited to electricity, hydrogen, localised energy systems and council vehicle fleets.

2.2 Reducing CO_2 Emissions Associated with Localised Energy Systems

CO_2 emissions should be reduced because of the negative effects of global warming and fuel supply security. Furthermore, many governments are imposing new regulations to curb the use of conventional fossil fuels, for both the transport sector and for power generation. This has led operators of vehicles and power generation to assess best practices in transitioning to more sustainable energy sources in their respective sectors.

The national energy system configuration in the past operated in a unidirectional manner, in which energy produced would be directly supply demand via transmission lines and distribution networks. However, the increase in use of intermittent renewable generation opened opportunities for decentralisation as consumers would be able to participate as prosumers.

An example of this would be how easy it is for a household to purchase and install solar panels on their rooftops and connect that with a battery storage system. To further guarantee energy needs constantly being met, they can also connect to the main grid. This in effect changes the paradigm of having to build one large generator on a single site with very long and elaborate transmission and distribution networks to supply an inflexible national demand.

The emissions caused by conventional generation has necessitated the need for clean energy supply, hence a significant growth in the use of intermittent renewable generation sources combined with energy storage systems. This paves the way for local energy systems as the generation can now be supplied directly to the distribution networks, making the energy generation closer to where the energy is being consumed. Local energy systems and the possibility of them being connected with the wider national level energy system allow them to participate in activities such as energy arbitrage, peer-to-peer energy trading and ancillary service provision [31].

Given the nature of integrated energy systems, different types of energy vectors can then be supplied simultaneously for different uses such as using stored hydrogen or electricity for grid balancing services, transport fuel and heating.

2.2.1 Behaviour of Renewable Electricity Generation

Renewable energy sources, such as wind and solar, are not dispatchable. This means that a certain demand of electricity for "x" kWh cannot solicit the same amount of wind and solar energy to satisfy that demand. Wind and solar energy fluctuate depending on the weather conditions, such as wind speed and solar irradiation. These fluctuations affect the flexibility of the power system. Here, flexibility can be defined as the extent to which a power system can accommodate discrepancies in demand or generation relating to both foreseen and unforeseen variability [32].

Fluctuations in generation impact operational timeframes. Therefore, they should be more thoroughly investigated to enable a better understanding of the flexibility needs of systems that require high penetration of intermittent renewable electricity generation systems, which is summarised in Figure 2.1.

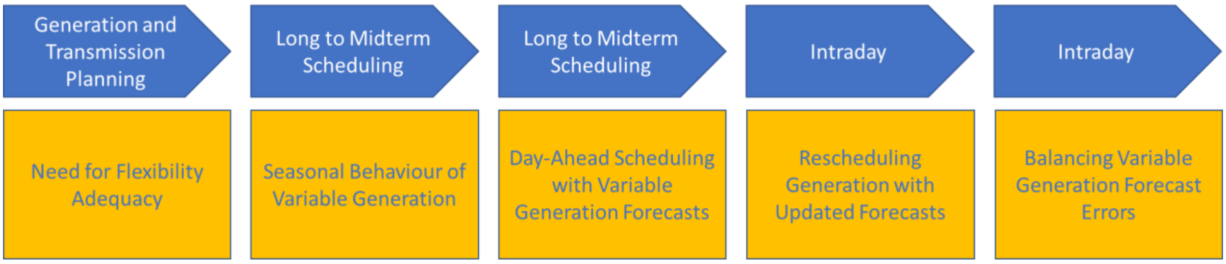

Figure 2.1: Impact of variable generation on flexibility timeline [33]

Traditionally, the planning of power systems has placed emphasis on guaranteeing system adequacy in terms of being able to produce enough power to meet peak demand and energy consumption. In contrast, the measure of adequacy for systems with a high penetration of intermittent renewable energy systems would need a stronger emphasis on providing the necessary flexibility. In particular, the season dependent behaviour of intermittent renewable energy sources needs to be integrated into the long- to mid-term scheduling. This would allow the system to have ample resources to react accordingly to these seasonal changes.

Interday and intraday planning flexibility is essential for flexibility because it indicates which resources are available to allow robust operation given uncertainties in the forecast. Thus, operational flexibility is essential for balancing forecast errors in net demand and fluctuations.

Grid frequency fluctuations are also a product of significant fluctuations in generation. These fluctuations lead to disturbances in voltage stability, transient stability and small signal stability, which may cause damage to any electrical devices that are present in the grid [34]

Looking at UK renewable electricity generation data, wind and solar electricity generation accounted for 47.7% of the UK's renewable electricity generation [35]. This high proportion of highly variable electricity sources may cause disruptions in the grid to become more prevalent. Thus, measures to mitigate grid disruptions are required, such as flexible energy sources, price-responsive demands and optimal operation strategies.

2.2.2 Balancing Electricity Demand

In the case of localised IESs where renewable electricity generation is a significant or main source of electricity supply to the grid, efforts to counteract the negative effects of frequent fluctuations in electricity supply are needed. Demand and generation mismatch must also be addressed. Therefore, a source of dispatchable electricity should be available to the integrated energy system.

Stored energy may be used as a dispatchable renewable energy source. This stored energy can be bought from an off-site source. However, it would be interesting to investigate the case of sourcing this energy on-site in greater depth because of the increasing adoption of on-site renewable generation. In 2020, wind curtailment alone in the UK reached up to 3.8 TWh, which is enough electricity to power every home in Wales [36]. Thus, storing excess wind generation on-site (instead of curtailing it) seems to show significant promise.

Curtailment of variable electricity generation increased from 8% to 15% between the years 2012 and 2016, and the increase of its penetration rose by 405% between 2010 and 2016 for the case of the UK [37]. This trend will continue as time passes due to the necessity of transitioning to renewable electricity generation to offset the depleting supply of non-renewable energy sources and meet CO_2 reduction targets.

Battery storage is another solution to this problem and battery technology that is currently becoming more prevalent. However, batteries have several drawbacks, including the capacity of energy that they can store and their relatively fast discharge rates when compared to hydrogen storage. The discharge rates of various electricity storage methods are shown in Figure 2.2.

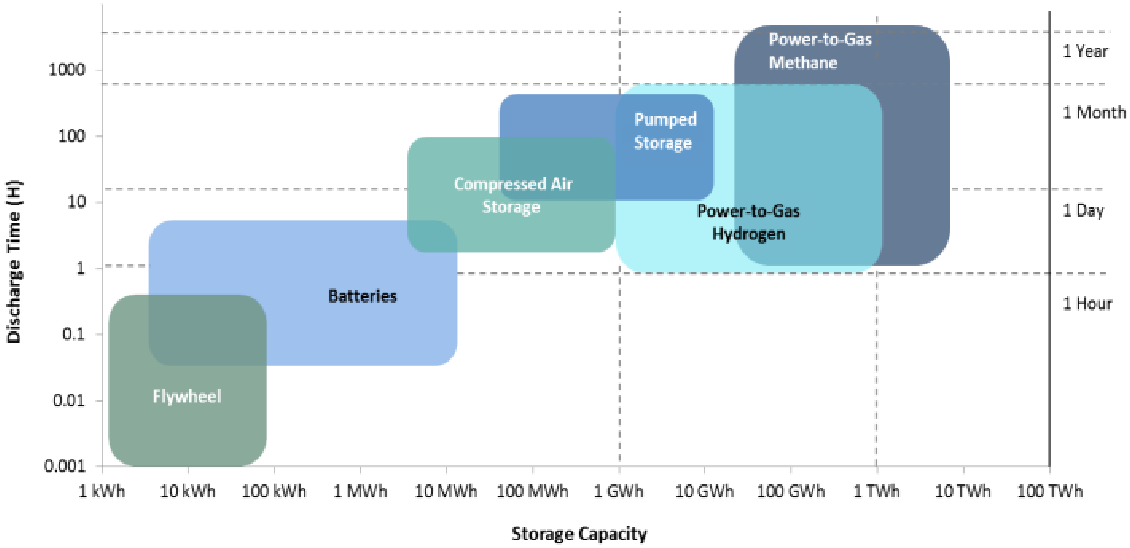

Figure 2.2: Discharge rates of energy storage technologies [23]

It can be seen from Figure 2.2 that hydrogen storage via power-to-gas (P2G) has a higher storage capacity than most of the storage technologies available. In terms of discharge rate, hydrogen storage methods (on average) discharge between the range of days to months. In contrast, electrical batteries mainly have a discharge rate of within hours.

What type of storage technology may be used can be determined by measuring the energetic benefit that the storage system provides to the community receives in exchange for each unit of energy invested in the storage system. This measure can be represented numerically as the ratio $\mathrm{ESOI_e}$, which is the energy dispatched to the grid over its whole lifetime over the energy required to manufacture the storage system [24].

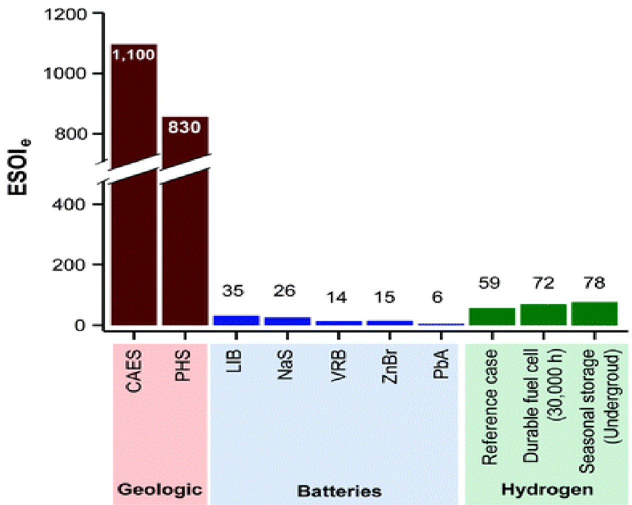

Figure 2.3: $ESOI_e$ values between storage technologies [24]

It can be seen from Figure 2.3 that hydrogen storage provides more energetic benefit than battery storage. However, this comes with the consideration of other factors, such as technology cost and market structure [38], [39]

The technological readiness levels and market maturity of different energy storage technologies are presented in Figure 2.4. This figure consists of an X axis, which shows the market maturity of the storage technology, and a Y axis, which shows the technological readiness level of the storage technology. The storage types are also categorised according to the form of energy stored.

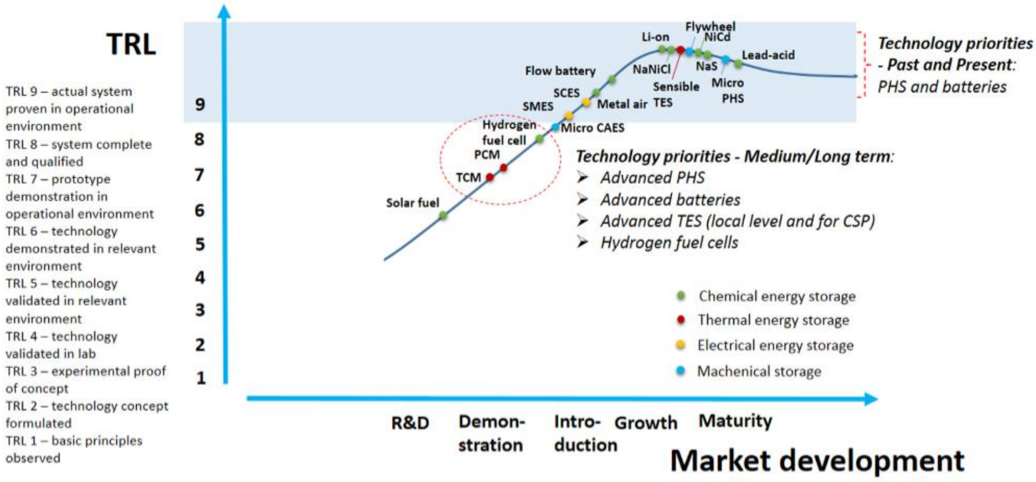

Figure 2.4: Technological readiness and market maturity of energy storage systems [40], [41]

From Figure 2.4, it can be seen that the level of technological readiness of hydrogen storage technologies is quite high at around a TRL of 8. However, its market maturity is still behind battery storage technology and pump-hydro storage. Hydrogen storage technologies are still demonstration projects. This is futher supported by the information in [42]–[45], which shows that none of the hydrogen storage projects in Europe meet the 10 MW capacity limit to be considered a large-scale project, as per the standard of what is considered as a large-scale energy project in [46]. In terms of assessing the technological readiness and market maturity of different hydrogen storage systems, available compressed gaseous and liquid storage are the most technologically ready and mature [47].

2.3 Reducing CO_2 in the Tranport Sector

In 2020, the transport sector contributed 24% of all domestic greenhouse gas (GHG) emissions in Britain [48]. To address this issue, there has been a significant push for the adoption of sustainable means of transportation, which include higher use of public transport, low emission vehicles and manual transport (e.g., walking, cycling, etc.).

2.3.1 Associated Capital and Operational Costs of Ultra Low Emission and Internal Combustion Engine Vehicles

Due to the different powertrain technologies that are employed in ultra low emission vehicles (ULEVs) and internal combustion engine vehicles (ICEVs) of a similar category, their capital and operational costs differ because different technologies used. There is a lack of consensus on the difference in the vehicle capital prices for FCEVs and ICEVs. Analysing the data presented in [49], a hydrogen FCEV is five times more expensive than an ICEV of the same category. Whereas in [50] and [51], a hydrogen FCEV is around three times more expensive than an ICEV of the same category. A fuel cell electric refuse vehicle was developed based on the technical specifications for a 26 tonne fuel cell electric refuse vehicle in [52]. The component costs of this vehicle (e.g., the battery price/kWh, fuel cell system price/kW and storage) were based on the data presented in [53]. The prices for the glider chassis, RCV body and split lifter were based on the prices provided in [54]. Reference [54] also provides a price for an equivalent internal combustion refuse vehicle. Comparing the two vehicles, it was found that the price of the hydrogen fuel cell electric refuse vehicle was 1.9 times higher than the conventional internal combustion engine refuse vehicle. A set of commercially available vehicles of a similar category were listed according to their fuel categories (i.e., battery electric, hydrogen and diesel) in [50]. Comparing the prices of the FCEV available in the publications and the diesel ICEVs, the FCEV was on average two times more expensive.

To provide a direct comparison between the fuel costs for hydrogen and diesel powered vehicles, the cost/kWh can be calculated by dividing the price of the fuel with its energy density. The value for the cost/kWh of each fuel type can then be compared using the same metric. The values for energy density of hydrogen is assumed to be 33.33kWh/kg and diesel as 10.7kWh/L [55], [56]. For hydrogen, in the case where the prices are within the range of £5.30-£7.00 as per the data in [57], the cost/kWh woud be between would be £0.16/kWh-£0.21/kWh. For hydrogen cost/kWh generated from average between grid electricity retail price (baseload and long run variable cost), dedicated on-site generation and curtailed electricity, the figure is £0.12/kWh [58]. It is projected that hydrogen price/kg could fall to £1.26/kg in 2030 [59]. Hydrogen cost/kg in 2030 will thus be around £0.038/kWh. For UK average diesel price/L (retail) in 2022, the figure is around £0.17/kWh [60]. This will change in the future according to projections for crude oil prices, which will rise to arround £99.50/barrel (per current exchange rate) [61]. Looking at the data on diesel price at pump/month for the UK presented in [62], and comparing the current price per barrel/month in [63], an assumption can be made by taking the average of the ratio between diesel price at pump/month and the price of a barrel of crude oil/month. Using the ratio, the price of diesel/L at pump for the year 2030 is approximately £0.24/kWh.

Looking at the cost/kWh of both hydrogen and diesel, there are instances where hydrogen is more expensive/kWh. This is prevalent at present because the use of hydrogen as a fuel is not as widespread. Price variations of hydrogen may also be attributed to different sources of electricity and electrolyser technology being used for hydrogen production among the vendors. In addition, deriving the higher prices of hydrogen recorded in the data in [57], the cost/kWh of hydrogen can also range from £0.26/kWh-£0.32/kWh. This would make hydrogen on average more expensive than diesel. However, the diesel price is expected to rise and hydrogen prices to decrease by 2030, and therefore the cost/kWh of hydrogen fuel will be by far cheaper than diesel. This would enable cheaper operational costs of hydrogen powered vehicles.

2.3.2 CO_2 Emissions in the Case of Waste Collection Operations at a Local Council Level

A variety of vehicles collect waste in local councils. They range from small vans that weigh slightly more than 1 tonne to 26-tonne rigid trucks. It is expected that large 26-tonne rigid vehicles will emit more CO_2 than a smaller 1-tonne van. This thesis is mainly limited to a specialised focus on council fleet operations.

A report regarding a potential pilot study to decarbonise vehicles across seven fleet operators (mainly council) was presented in [64]. The combined fleet size was 920 vehicles, which included of an array of different sized vans, SUVs, large RCVs and tractors. Out of the entire fleet, 14% of the vehicles were 26-tonne RCVs and these vehicles contributed to 31% of the whole fleet's CO_2 emissions. An example of a recent drive to transition fleet vehicles from conventional ICEVs into ULEVs can be found in the government's commitment to have a vehicle fleet comprised of ULEVs (25% of fleet) by 2022 [65].

From a technical perspective, diesel RCVs are not as fuel efficient when compared to vehicles that use electrical powertrains, such as battery electric RCVs and fuel cell electric RCVs. Given that waste collection operations require frequent stop-start cycles, most of the travel will be done at low speeds (i.e., residential waste collection). This implies a frequent use of low gears due to the frequent stop-start cycles, which increases fuel consumption in general [66]. However, RCVs that have electric powertrains can offset this issue because they can reach maximum torque from stationary instantaneously [67], [68]. Furthermore, energy losses attained from braking can be captured and utilised better in both battery electric and fuel cell electric RCVs via regenerative breaking. This energy could then be collected as electricity that can be stored in a battery instead of being lost as heat during braking events, thus improving overall fuel efficiency [69].

2.4 Demonstration Projects Involving Hydrogen as an Energy Vector for Transport and in Integrated Energy Systems

Demonstration projects that utilise hydrogen as a fuel for vehicle transport and/or for electricity grid support functions can help us to assess the technological readiness, costs, and benefits of hydrogen in both sectors. These investigations could also provide a platform for further independent study because they can be helpful in assessing the suitability of hydrogen as a method of energy storage in the respective sectors.

2.4.1 Example Demonstration Projects

Table 2.1 gives a list of projects around Europe, which was compiled via a literature study. It was found that out of 93 projects, there were 49 projects that involved the use of hydrogen in the transport sector and 44 projects involving hydrogen with grid electricity support [42]–[45], [64], [70], [71]. In the UK, out of 10 projects looking at the use of hydrogen in either the transport sector or for grid electricity uses, only four projects looked at the use of hydrogen for transport and grid electricity services together.

Table 2.1: List of Demonstrator Projects (Europe)

Table 2.1 (P.1)-Cont							**Quoted installed capacity**	
Project name	**Country**	**Start**	**End**	**Technology**	**End-use fuel or feedstock - Sector**		**MW_{el}**	**nm^3 H_2/hour**
PVFCSYS Sophia Antipolis	France	2000	2004	ALK	Grid Electricity	Transport	0.0036	0.7
Grimstad Renewable Energy Park	Norway	2000		ALK	Grid Electricity		0.05	10
FIRST - Showcase II	Spain	2000	2004	PEM	Grid Electricity		0.001	0.2
HyFLEET:CUTE, Hamburg	Germany	2003	2011	ALK		Transport	0.39	60
ECTOS	Iceland	2003	2007	ALK		Transport	0.2976	60
HyFLEET:CUTE, Amesterdam	Netherlands	2003	2009	ALK		Transport	0.4	60
Laboratory System at IFE Kjeller	Norway	2003		PEM	Grid Electricity		0.0033	0.7
Porto, CUTE	Portugal	2003		ALK		Transport	0.32	60
CUTE, Stockholm	Sweden	2003	2006	ALK		Transport	0.4	60
PVFCSYS Agrate	Italy	2004	2004	ALK	Grid Electricity		0.0034	0.7
Utsira Island	Norway	2004	2010	ALK	Grid Electricity		0.048	10
GenHyPEM (R&D)	EU	2005	2008	PEM	Grid Electricity		0.03	5
Fronius HyLOG-Fleet (Hydrogen powered Logistic System)	Austria	2006		PEM	Grid Electricity	Transport	0.006	

Table 2.1 (P.2)-Cont							**Quoted Installed Capacity**	
Project Name	**Country**	**Start**	**End**	**Technology**	**End-use fuel or feedstock - Sector**		**MW_{el}**	**nm^3H_2/hour**
HyWindBalance, Oldenburg	Germany	2006		ALK	Grid Electricity		0.006	1
Demo Plant Agricultural University Athens	Greece	2006		PEM	Grid Electricity		0.0002	
CUTE and HyFLEET:CUTE, Barcelona	Spain	2006	2009	ALK		Transport	0.4	60
H2 from the sun, Brunate	Italy	2007		ALK	Grid Electricity		0.0067	1
ITHER	Spain	2007		ALK		Transport	0.065	
RES2H2 Gran Canaria	Spain	2007		ALK	Grid Electricity		0.055	11
HyCycle - Center for renewable H2 (R&D)	Denmark	2008	2011	PEM				
WELTEMP, Water electrolysis at elevated temperature	EU	2008	2011	Unknown PtX				
Stand-alone power system, Neo Olvio of Xanthi	Greece	2008		PEM	Grid Electricity		0.0042	0.7
Hydrogen Wind Farm Sotavento	Spain	2008	2011	ALK	Grid Electricity		0.32	60

Table 2.1 (P.3)-Cont							**Quoted Installed Capacity**	
Project Name	**Country**	**Start**	**End**	**Technology**	**End-use fuel or feedstock - Sector**		**MW_{el}**	**nm^3H_2/hour**
Hidrolica, Tahivilla	Spain	2008	2009	PEM	Grid Electricity		0.041	6
Baglan Energy Park Wales	United Kingdom	2008		ALK	Grid Electricity	Transport		10
AltHytude	France	2009		ALK			0.08	10
Abalone Energie Nantes	France	2009		Unknown PtX	Grid Electricity			
Regenerativer Energipark Ostfalia/hybrid renewable energy park (HREP)	Germany	2009		ALK	Grid Electricity		0.006	1
Primolyzer (R&D)	Denmark	2010	2012	PEM	Grid Electricity		0.00586	1
PROCON (R&D)	Denmark	2010	2013	PEM				
Nukissiorfiit Nuuk Hydrogen Plant	Denmark	2010		ALK	Grid Electricity			
NEXPEL (R&D)	Norway	2010	2012	PEM				
MEDLYS, Medium temperature water electrolysis (R&D)	Denmark	2011	2015	Unknown PtX				
ELYGRID (R&D)	EU	2011	2014	ALK	Grid Electricity		3.5	760
RESelyser (R&D)	EU	2011	2014	ALK	Grid Electricity		0.001	2
Hamburg Hafen City, CEP	Germany	2011	2017	ALK		Transport	0.6	180
EnBW H2 station, Stuttgart	Germany	2011	2016	ALK		Transport	0.3	60

Table 2.1 (P.4)-Cont							**Quoted Installed Capacity**	
Project Name	**Country**	**Start**	**End**	**Technology**	**End-use fuel or feedstock - Sector**		**MW_{el}**	**nm^3H_2/hour**
Commercial Plant Svartsengi/George Olah plant	Iceland	2011		Unknown PtX		Transport	6	1200
RABH2	United Kingdom	2011	2014	ALK	Grid Electricity	Transport	0.005	1.1
Don Quichote	Belgium	2012	2017	ALK	Grid Electricity	Transport	0.3	60
MYRTE	France	2012	2015	PEM	Grid Electricity		0.11	23
H2 research center BTU Cottbus	Germany	2012		ALK	Grid Electricity		0.14	30
Ekolyser (R&D)	Germany	2012	2015	PEM				
LastEISys (R&D)	Germany	2012	2015	PEM				
Agios Efstratios	Greece	2012		Unknown PtX	Grid Electricity		0.1	
Oslo, CHIC	Norway	2012		ALK		Transport	0.64	120
PostBus Hydrogen bus, Brugg, aargau CHIC	Switzerland	2012	2016	ALK		Transport	0.315	60
Brugg PostBus hydrogen bus	Switzerland	2012	2017	Unknown PtX		Transport		
Air Fuel Synthesis pilot plant	United Kingdom	2012	2013	Unknown PtX		Transport		
H2 Logic 5 HRS with on-site electrolysis (Aalborg, Holstebro, Vejle, Gladsaxe, – Køge)	Denmark	2013		ALK		Transport	0.4	75

Table 2.1 (P.5)-Cont							**Quoted Installed Capacity**	
Project Name	**Country**	**Start**	**End**	**Technology**	**End-use fuel or feedstock - Sector**		**MW_{el}**	**nm^3H_2/hour**
RH2 Grapzow, Mecklenburg Vorpommern	Germany	2013		ALK	Grid Electricity		1	210
H2Move, Fraunhofer ISE	Germany	2013		PEM		Transport	0.04	6
Greenhouse heating, solar-H2	Italy	2013	2014	ALK	Grid Electricity		0.0025	0.5
HyNor Lillestrøm, Akershus Energy Park	Norway	2013	2015	ALK	Grid Electricity	Transport		10.66
El Tubo	Spain	2013		PEM	Grid Electricity		0.00265	
Minerve, Nantes	France	2014	2015	SOEC		Transport	0.012	3
MicroPyros	Germany	2014	2017	Unknown PtX		Transport		
Bolzano, CHIC	Norway	2014		ALK		Transport	1	180
Reduction and Reuse of CO_2: Renewable Fuels for Electricity Production- ZHAW	Switzerland	2014	2017	PEM	Grid Electricity	Transport		0.3
SYNFUEL	Denmark	2015	2019	SOEC		Transport		
Hamburg - Schnackenburgallee	Germany	2015		PEM		Transport	0.185	30
Dresden	Germany	2015		SOEC	Grid Electricity		0.01	

Table 2.1 (P.6)-Cont							**Quoted Installed Capacity**	
Project Name	**Country**	**Start**	**End**	**Technology**	**End-use fuel or feedstock - Sector**		**MW_{el}**	**$nm^3 H_2$/hour**
Aberdeen, Hydrogen bus project	United Kingdom	2015	2018	ALK		Transport	1	180
Energy & Smartgrid Corsica	France	2016		ALK	Grid Electricity			10
smart grid solar - arzberg	Germany	2016		PEM	Grid Electricity	Transport	0.075	
Fife, Levenmouth Community Energy Project	United Kingdom	2016		ALK	Grid Electricity	Transport	0.37	
FaHyence	France	2017		ALK		Transport		30
Wyhlen hydroelectric power plant, ENERGIEDIENST, ENBW Group, Center For Solar Energy	Germany	2017		ALK	Grid Electricity			200
Energy in the Container, Fraunhofer IISB, Erlangen, Leistungszentren Elektroniksysteme (LZE)	Germany	2017		PEM	Grid Electricity			
ASKO Midt-Norge	Norway	2017		ALK		Transport		150

Table 2.1 (P.7)-Cont							**Quoted Installed Capacity**	
Project Name	**Country**	**Start**	**End**	**Technology**	**End-use fuel or feedstock - Sector**		**MW_{el}**	**Nm^3H_2/hour**
Surf'n'Turf Orkney	United Kingdom	2017		PEM	Grid Electricity		0.5	
GRHYD (Hythane)	France	2018	2022	Unknown PtX		Transport		
GrInHy	Germany	2018	209	SOEC	Grid Electricity		0.15	37.5
REFLEX	Italy	2018	2020	SOEC	Grid Electricity		0.08	16
Natuurgasbuffer Zuidwending	Netherlands	2018		PEM		Transport	1	
Oxelösund Forklifts	Sweden	2018		PEM		Transport		
NT Bene, Parnu	Estonia	2019		PEM		Transport		185
Balance	EU	2019	2019	SOEC	Grid Electricity		0.008	2
VTT	Finland	2019		PEM	Grid Electricity		0.0184	4.1
GNVert H2 filling station with Engie	France	2019		PEM		Transport		37
eFarm	Germany	2019		PEM		Transport	1.125	
Maximator	Germany	2019		PEM		Transport	0.833	
Duwaal	Netherlands	2019		PEM		Transport	2	
H2 Energy	Switzerland	2019		PEM		Transport	2	
Hydrogen plant - Orkney Islands, Scotland (Building Innovative Green Hydrogen BIG HIT)	United Kingdom	2019		PEM		Transport	1	
Nordic Blue Crude	Norway	2020		SOEC		Transport	20	

Table 2.1 (P.8)-Cont							**Quoted Installed Capacity**	
Project Name	**Country**	**Start**	**End**	**Technology**	**End-use fuel or feedstock - Sector**		**MW_{el}**	**nm^3H_2/hour**
SkyNRG	Netherlands	2022		Unknown PtX		Transport		
Magnum, Eemshaven	Netherlands	2023		Fossil	Grid Electricity			
Samsø	Denmark			ALK		Transport	0.02	
Vendée hydrogène	France			Unknown PtX		Transport	3.425	
Glomfjord Hydrogen AS	Norway			ALK		Transport		2500
Submarines	United Kingdom			PEM				
Tees Valley Demonstrator	United Kingdom			PEM		Transport		1667

It can be seen in Table 2.1 that there is an equal level of interest in Europe in studying the use of hydrogen in both grid electricity applications and transport applications. In terms of the country with the most demonstrator projects, Germany leads with 19 projects. This is followed by Norway, France (10 projects), the UK (9 projects) and Denmark (8 projects).

It is interesting to draw a comparison between Norway and the UK. Norway has an annual primary energy consumption of around 500TWh, whereas the UK has an annual primary energy consumption of around 2,000TWh [72] which is apparent due to the significantly larger population of the UK. Nevertheless, they both share a comparable number of hydrogen demonstration projects. This can be explained by the share of primary energy being produced from renewable sources in the two countries. Norway has around 70% of its primary energy being supplied by renewable energy whereas the percentage in the UK is almost 50% [72], [3]. For green hydrogen production to be economic, there must be a high proportion of renewable electricity generation because this would allow for a greater amount of excess renewable electricity generation to be stored per capita.

Findings from the projects based in Norway and the UK found that despite positive indicators such as a reduction of emissions per kWh of electricity on grid being achieved (73% in the case of [73]), the projects are almost all within the small-scale generation capacity category (<10MW). In some cases, the use of hydrogen technologies for storage and dispatch can be financially feasible such as that demonstrated in [74], there are still challenges that need to be addressed.

Ready solutions for the deployment of local energy systems are not present, thus presenting a challenge in developing a suitable policy environment for the integration of hydrogen into any energy system. Variations in geographies, social dynamics and legacy infrastructure would make the implementation of generic local energy system designs difficult, thus more real case studies would be needed to assist in developing the right policies going forward.

Legislation related accessing electricity grid for the cases of generation and demand as well as the intricacy caused by active network management of local renewable generators make the connection of additional electrolysers difficult [75], [76]. Further specific legislation relating to safety standards and hydrogen purity may no longer be suitable at present as current existing legislation does not address hydrogen in the context it is being intended to use for (electricity and transport). This would mean that there is a possibility under a present scenario where the legislation between the 2 countries do not comply, hence making it difficult to expand the hydrogen supply chain between Norway and the UK. In terms certification schemes to ensure hydrogen supply was sourced from low-carbon/zero-carbon production methods, the UK is currently developing a suitable labelling category via the Department for Energy Security and Net-Zero whereas no such initiative is being done in Norway [77].

In terms of transport, road infrastructure can be a challenge when looking at rural areas such as the Orkney and HAEOLUS projects as it is constrained by the types of vehicles suitable or allowed for haulage. Transporting by sea requires dangerous goods exemption which makes options for travel routes limited thus increasing complexity and costs.

In terms of technical data available, the studies varied in terms of data availability. Some projects had datasets for demands, renewable generation, equipment size and parameters, equipment costs and operational costs whereas others did not. This necessitated some studies to make estimates on technical data such as conversion equipment energy consumption, demand, and generation data (if outlier datasets existed in data sample) as well as operational costs and equipment lifetime.

Out of the projects in Norway and the UK, almost half of those projects are no longer running. This can be attributed to several reasons, benign or detrimental such as the project demonstration period having ended or high capital costs due to a lack of reliable mass-produced components leading to systems being built with components of inappropriate sizes to reduce capital costs [78].

Looking at the technical aspects, the most popular hydrogen conversion technologies that are used across these projects are alkaline (ALK) and proton exchange membrane (PEM). This can be attributed to better capital costs for a minimum stack size of 1MW, and to the lifetime of PEM and Alkaline technologies (PEM: £332/kW, 50,000-80,000 hours—ALK: £225/kW, 60,000 hours) when compared to solid oxide electrolyser cell (SOEC) technologies (capital costs: £1664/kW, lifetime: 20,000 hours) [59].

Pumped-hydropower storage is the most popular energy storage method for grid-related operations [79]. In terms of demand for hydrogen in the transport and mobility sector as per 2020, hydrogen vehicle sales only make up 1% of all ULEV sales [80]. Furthermore, when looking at the list of projects available in the UK from Table 2.1, there are fewer projects involving hydrogen when compared to countries of a similar size, such as Germany and France. Thus, it would be useful to better understand the implications and applicability of hydrogen for both grid and transport operations in a UK context.

2.4.2 Availability of Seasonal Data

Seasonal data for renewable electricity generation and site electricity demand will vary depending on factors such as weather, generation technology, generation capacity and site maximum electricity demand capacity. Most references regarding electricity demand look at the demand values at a national or sectoral level (i.e., sectoral as a whole either regionally, nationally or globally) [81]–[83]. Furthermore, despite relatively high percentages of reporting for electricity-demand data, there are instances where that data that are reported may be missing even from very established sources of information, such as balancing authorities. An example of this can be found in [84], where 2.2% of demand data is missing. For on-site electricity-demand data of smaller energy networks, on-site monitoring may be the best solution. However, monitoring is considered to be expensive [85]. Further disadvantages regarding monitoring include equipment malfunction, privacy concerns and small sample size [30]. In the case of renewable electricity generation, the capacity of generation can be estimated mathematically without the need for historical electricity generation on-site, which is due to the variable nature of renewable electricity generation. Historical electricity generation data may be reflective of dispatchable energy before the advent of variable electricity generation from renewable sources such as wind or solar [86]–[89].

The emphasis of seasonality is important because wind speeds for wind generation are usually higher during winter months and solar irradiation for solar photovoltaic (PV) generation is higher during summer months [90], [91]. This seasonality may reflect the supply of readily available electricity, excess or deficit in renewable electricity production (amongst others). Specifically for the case of hydrogen, excess electricity generation can signify the amount of hydrogen that can be generated. In the case of a deficit in renewable electricity production, this would be the amount of hydrogen needed for conversion to electricity for grid balancing applications in IESs.

2.5 Understanding the Potential Role of Hydrogen in Integrated Energy Systems

Hydrogen is a versatile energy carrier that can be used as a source of energy for fuelling hydrogen powered vehicles or as a means for providing dispatchable electricity to the grid via electrolysis. However, the context of its use in the case of localised energy systems must be better understood because hydrogen is still comparatively less frequently used in these applications.

2.5.1 Increasing the Flexibility of Integrated Energy Systems by Using Hydrogen as an Energy Vector

Flexibility in the context of energy systems can be defined as the ability of a power system to modify electricity production to mitigate intermittency and variability, either foreseen or not [92]. It can also be defined as the ability to adjust generation or consumption behaviours subject to external stimuli, such as price signals or activation signals, to fulfil a service within the energy system [93].

The inclusion of hydrogen as an energy vector in IESs is a means of providing energy flexibility. This can either be in the form of electricity to the grid or hydrogen for vehicle refuelling. Current trends show an increase in the use of battery electric vehicles (BEVs). This may lead to an exacerbation of the peak-power problem. By using hydrogen as a fuel, this issue can be avoided because hydrogen can be stored over longer periods of time and is only generated during over-generation, considering the economics relating to the round-trip efficiency of hydrogen systems. Studies have shown that energy flexibility is indeed achievable via the inclusion of hydrogen within the energy mix. The difference between hydrogen energy system modelling types to assess their common gaps and interrelationship was investigated in [94]. This included specifying grid support actions at different time horizons so as to not overstate the degree of flexibility that hydrogen provides. The use of hydrogen for mitigation efforts was also studied in [94]. The ability of hydrogen to provide flexibility and the impact was studied in [95] via a macro energy model. Meanwhile, both electricity and hydrogen can provide a more flexible, reliable, and cheaper energy system in the case of an office building [96].

2.5.2 Barriers to Adopting Hydrogen as a Means of Providing Energy Flexibility for Grid Operations and Transport

Hydrogen is less popular when compared to other more established means of energy storage. In the transport sector, hydrogen vehicles are not as widespread as BEVs. In terms of providing flexibility in IESs, under current market conditions, the economics of using FCEVs as a distributed source of peak power and spinning reserve are marginal [97]. This may change subject to the increasing value of balancing services as energy systems move towards more intermittent renewable electricity generation. According to [94], there is a lack of suitable and validated data for the purpose of modelling hydrogen-based systems. In [95], it is stated that wind and solar PV generation systems provide significant amounts of free or low-cost electricity, which can be used to power a hydrogen economy. However, expanding the hydrogen economy would require additional generation capacity. This causes higher hydrogen production costs. In the case of hydrogen fuel adoption in the transportation sector, resistance to adoption is mainly due to high capital costs [98], [99]. In general, the challenges for the adoption of hydrogen-based technologies for both applications are listed in [100]. These barriers are given in Table 2.2.

Table 2.2: Barriers to hydrogen technology adoption

Category	
Production	• Majority of H_2 produced is via steam methane gas reformation, which is only 74%-85% efficient according to [101] or even worse at 40% efficiency according to [102] efficient and not fully "green". • Supporting infrastructure is needed for green hydrogen production via electrolysis, which may increase capital costs. • Commercial electrolysers have a lifetime of between 4.5-7 years [103].
Storage	• High energy requirement in compressed H_2 storage due to low volumetric energy density. • Low durability of materials.
Transport	• Existing H_2 transportation pipeline is not sufficient to meet future demand. • Utilising the current natural gas pipeline to transport large amounts of H_2 poses the risk of embrittlement. • Network of refuelling stations is not widespread enough (in the case of the UK for 2022, only 12 [104] compared to 28,375 public electric charging stations [105] and 8,370 petrol filling stations [106]).
Commercialisation	• High overall costs (capital, operational, maintenance). • Supply chain not very well established. • Developing aftersales services for H_2 technology is still needed.

2.6 Review of Methods for Developing Energy Demand Profiles, Vehicle Fleet Analyses, and Integrated Energy Systems Modelling

This section reviews the literature in terms of the current methods of modelling and analysis, which will be discussed and used in the subsequent technical contribution chapters. The rationale behind the selection of the analysis methods for each chapter is specified in order of the technical contribution chapters.

2.6.1 Developing Building Site Electricity-demand Profiles

When developing electricity-demand profiles, two approaches are usually used:

- Top-down approach
- Bottom-up approach

Top-down approaches depend on aggregated data and do not take into consideration individual buildings or the end use. This approach sees the building stock as an energy sink [107]. Meanwhile, the bottom-up approach uses disaggregated data to model the many constituents of the site being studied, be it an individual building or multiple buildings which is then extrapolated to the whole case study [107], [108].

Both approaches are demonstrated in [109] for a case study of the residential and non-residential electricity demands in 14 countries (large scale). Meanwhile, [110] focuses on a bottom-up approach because the scales used in this study range from individual buildings to multiple buildings. Bottom-up approaches tend to use more of an engineering-economic approach, unlike top-down approaches which are more macro-economic [111]. Hence, a bottom-down approach may be more suitable for the case of smaller scale projects (i.e., individual buildings). In [112], the bottom-down approaches are categorised into three types of models:

- Physics-based models/“White-box”
- Data-driven models/“Black-box”
- Hybrid models/“Grey-box”

Physics-based models use physics-based equations to depict the energy behaviour of buildings. Data-driven models use time-series statistical analyses and incorporate machine learning algorithms to conduct forecasts of building energy demands. Finally, hybrid models combine both approaches. Figure 2.5 summarises these model types.

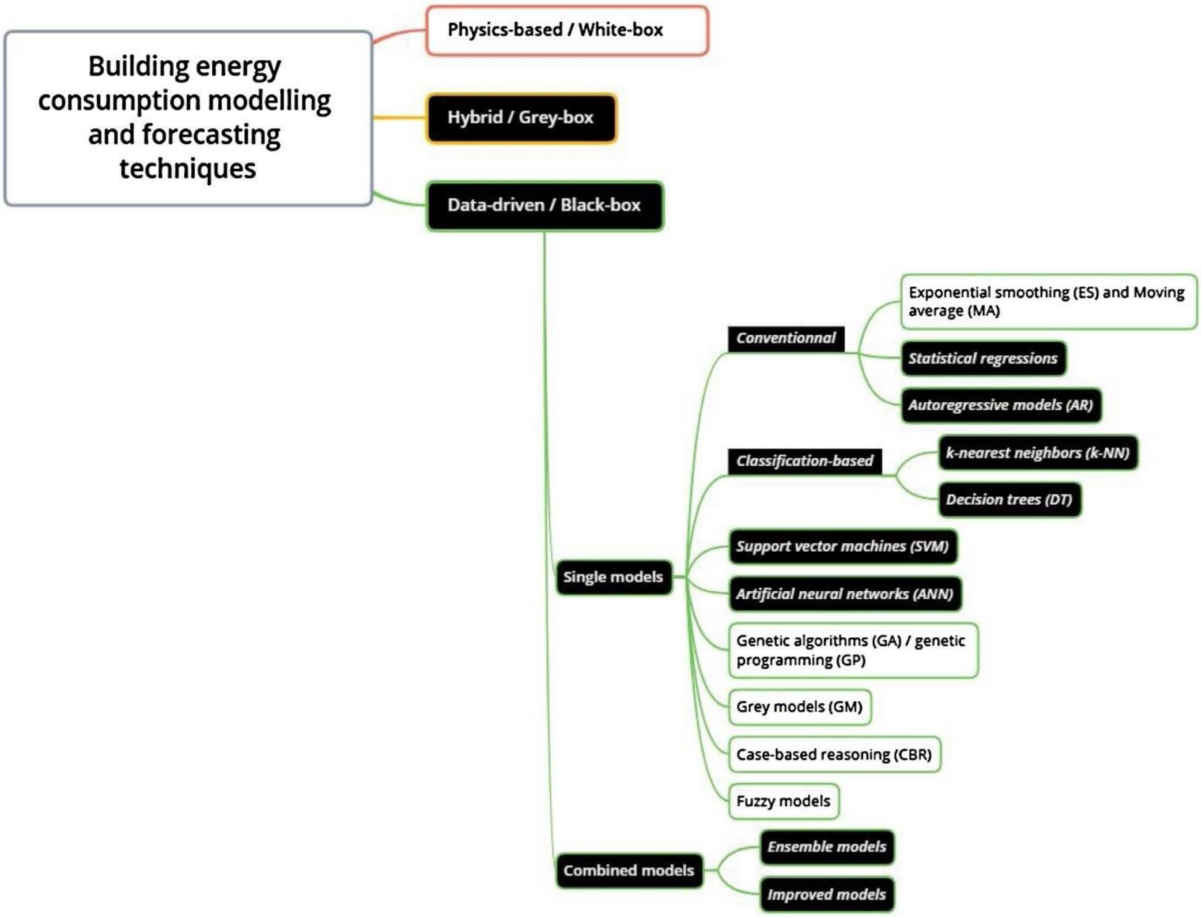

Figure 2.5: Building energy consumption modelling and forecasting methods [112]

Figure 2.5, data-driven models are categorised into two main groups: single models and combined models. Single models are data-driven techniques that use a predictive algorithm for forecasting problems. Single models are further categorised into two methods: conventional and classification based. Conventional methods can be autoregressive models or statistical regressions. They are simple to implement and have good accuracy but are limited with regards to their forecasting horizon and their ability to model nonlinear data patterns. Autoregressive models are based on statistical analysis of time-series. The statistical properties of the time-series in autoregressive models are time-invariant. This means that in the case of modelling energy demand, the energy demand at a specific time is expected to be like that of the recent past. Meanwhile, statistical regressions model the relationship of inputs and an output via an equation.

Classification-based methods are usually expressed by the k-nearest neighbours (k-NN) technique or the decision tree (DT) technique. The k-NN technique identifies and classifies similar patterns according to their properties (e.g., energy demand being related to weather conditions, occupancy, etc.). DT begins with a root node which leads to consequent nodes. Tests are performed at each node taking into consideration specific conditions or a certain input variable. The branches of the nodes continue to split until a possible value of the predicted output is obtained.

Support vector machines are employed for solving nonlinear problems. The process of a support vector machine is like that of regression, in which it tries to obtain a best-fit function. Artificial neural networks (ANNs) are nonlinear machine learning techniques where information coming from a processing element is transmitted with a weight via a link to subsequent processing element. The information received is combined with information from other processing elements via a combining function. The combination of the weighted information is then sent to other receivers depending on a transfer function. The process is repeated several times until the model matches the data.

Combined models focus on forecasting technique optimisation in the pursuit of prediction accuracy. Combined models can consist of several single algorithms in a group. This is known as an ensemble model. If a combined model consists of several optimisation methods, then it is called an improved model [112], [113].

This literature review also examined works related to forecasting methods to assess the current body of knowledge in data-driven modelling. For example, short-term electricity demand has been predicted using an Auto Regressive Moving Average Model (ARMA) on a Fog computing framework, where several peripheral devices are connected to a cloud [114] Data-driven methods, such as that proposed by [115], allow the development of predicted electricity-demand profiles for a city. Other methods, such as Auto Regressive Integrated Moving Average (ARIMA), predict future points of event regarding historic time-series data [116]. These methods require rather complex computing, as well as the use of extensive monitoring and historical data. In the XCORR method (the returning of the cross-correlation of two discrete-time sequences), movements of two or more sets of time-series data relative to one another are tracked [117]. This method is not as reliant on historical data but still requires a comprehensive site monitoring system and complicated computing.

2.6.2 Quantifying Hydrogen Demand for Vehicle Fleet and Total Cost of Ownership

Quantifying hydrogen demand in terms of individual vehicles or a fleet of vehicles can be done in three ways:

- Direct monitoring
- Physics-based modelling
- Hybrid modelling

Figure 2.6 shows the relationship between the three quantification methods.

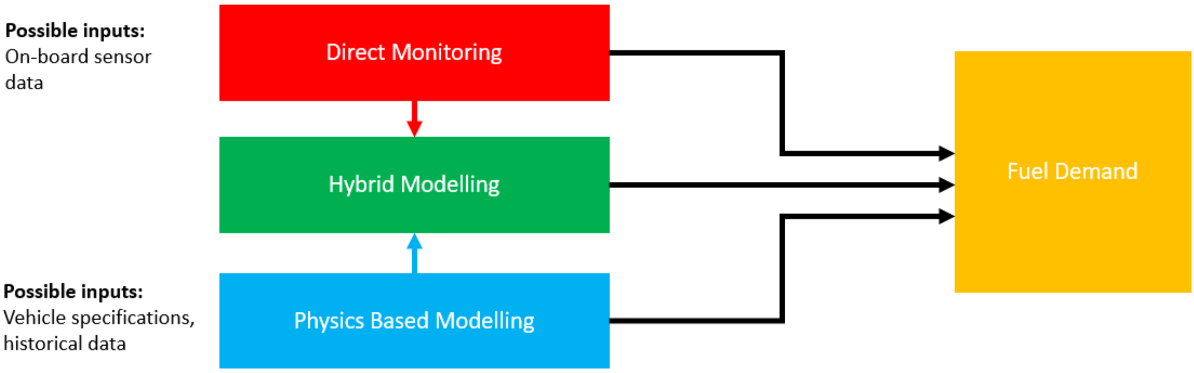

Figure 2.6: Methods of quantifying fuel demand

Direct monitoring installs measurement equipment to either monitor the fuel tank level or measure the fuel flow rate into the engine. However, it would cost an additional amount of money to install, and the accuracy of the measurements may vary. In [118], it is specified that the accuracy for on-board diagnostic systems for fuel consumption in vehicles should meet a ±5% accuracy limit as per European Union regulations. However, this limit may not be met depending on the road conditions. The accuracy limit is often not met because of the road conditions, such as frequent inclines on the road, rural road conditions and frequent occurrences of stop-start cycles [118]–[120].

Physics-based modelling can include detailed considerations of vehicle components, such as engine efficiencies, vehicle weight, aerodynamics, distance travelled, road conditions, driving behaviours and others. The complexities in which these factors are calculated depend on how accurate the fuel consumption estimate is meant to be.

Hybrid modelling can incorporate data derived from direct monitoring with physics-based models to achieve better accuracy. Physics-based models may miss some of the nuances of actual vehicle operation because they are based a lot on assumptions. Incorporating data from direct monitoring methods can include these nuances in the physics-based model.

In terms of advantages, both physics-based and hybrid models can be used to develop fuel demand profiles for future predictions because they do not rely solely on real-time fuel measurements. The main difference between the two is the complexity of the models which would hinge on the availability of data. Vehicle fuel consumption can be estimated by modelling the factors that cause energy losses, such as aerodynamic friction, rolling friction, energy dissipated from braking; and factors such as individual component efficiencies and drive cycles [121]–[123]. Meanwhile, [124] took a more simplistic approach in terms of factors considered where vehicle payload was the main indicator of performance related to fuel consumption instead of accounting for all possible losses in the entire architecture of the vehicle. The technical report in [125] takes more of a high-level approach by making direct assumptions of fuel consumption for alternative fuelled vehicles by determining the fuel tank size (i.e., on-board hydrogen tank) to meet average or maximum daily mileage achieved by already operating refuse vehicles.

The adoption of hydrogen vehicles for transport—or more specifically in the scope of this thesis refuse collection operations—has some problems. The main problem hampering the quick adoption of hydrogen technology for this purpose is high capital costs. Thus, to assess the economic feasibility of owning and operating fuel cell electric RCVs, all of the associated costs in owning and operating these vehicles must be analysed.

The associated costs, which will always be present in a techno-economical study of such vehicles, can be broken down as follows:

- Capital costs (unit cost of vehicle)
- Fuel costs
- Maintenance costs

The capital costs of hydrogen refuse vehicles are still not clearly established (see Section 2.3.1). In terms of such vehicles being available for purchase, there are several vendors who provide fuel cell electric refuse vehicles for the 26-tonne weight category. Looking at the available information, the three main vendors are Ballard Motive Solutions, Faun-Zoeller and Hyzon. However, the actual retail price for these vehicles is not available publicly (hence the assumption made in Section 2.3.1). The fuel costs for hydrogen and maintenance costs have also been discussed in Section 2.3.1. However, there is some uncertainty about the maintenance costs. Most work derived from peer-reviewed sources, research laboratories and professional institute reports suggest that the maintenance costs for hydrogen fuel cell vehicles are lower than those of ICE vehicles [50], [126], [127]. However, Ballard Motive Solutions state that at present the maintenance cost of a FCEV is still higher than that of a diesel vehicle [128].

The TCO method can incorporate these costs. This was done in [129], where the TCO of buses of a different type of powertrain (diesel, battery electric and fuel cell electric) were compared in terms of annual cash flow and a separate sensitivity analysis to TCO against mileage. The work in [130] presented a TCO analysis of battery electric vehicles and ICE vehicles of the same category to establish the break-even capital cost of the BEV in relation to the capital cost of the ICE vehicle depending on annual distance travelled. TCO calculations can also be used to analyse the effectiveness of the policies that have been implemented to stimulate public desire for transitioning to ULEVs. For example, in [131] the effects of incentives provided by the Norwegian government caused an increase in ULEV purchase. A specific study for decarbonising a refuse collection vehicle fleet was conducted in [132], where TCO analysis of diesel RCVs was compared against that of electric refuse vehicles.

2.6.3 Analysis of Integrated Energy Systems and the Interdependencies Between Energy Vectors

With the further integration of different energy sources in energy systems, the comprehensive study of understanding their behaviour under a single system must be better understood. Hence, the analysis and modelling of energy systems is shifting from individual analysis to a combined analysis of all energy production and/or storage systems present.

Contemporary reviews studying the modelling of energy systems can be better understood by observing how they have been conducted and what their focus areas are. The work in [133] describes this by setting out categories via the following divisions:

- Category 1 (Descriptive overview): Provides a descriptive overview of the technical properties of modelling tools. These include their methodological approach, mathematical formulation, and resolution.
- Category 2 (Classification): Provides a novel scheme for classifying and/or grouping of modelling tools for the purpose of outlining current modelling topologies based on their technical properties and modelling approaches.
- Category 3 (Practical application): Assesses the use of energy system modelling tools based on previous applied studies and indicates areas where these modelling tools are suitable for tackling present and future issues based on the modelling tool's capabilities.
- Category 4 (Inter-comparison and suitability): Compare the modelling features directly to identify their suitability for a specific application.
- Category 5 (Transparency, accessibility, and usability): Identify transparency and licensing or availability of the tool, singling out issues such as result replicability, validation and testing, open-source code and user interaction.
- Category 6 (Policy relevance): Identify the policy relevance of the modelling tools according to real-world applications and policy-making case studies.
- Category 7 (Model linking): Single out combined capabilities of modelling approaches via the linking of modelling frameworks.

A survey was conducted by the Sustainable Energy group at Aalborg University that listed 55 energy system modelling tools according to the categories listed above. Tools that look at local energy systems for cost minimisation and study the interdependencies of different energy vectors where is hydrogen is used for energy storage are summarised in Table 2.3, which was adapted from [134].

Table 2.3: Summary of available energy systems modelling tools [134]

Modelling Tool	Modelling Method	Purpose of Model	Accessibility of the Tool
Energy Transition Model	Simulation/Other: The ETM is a simulation model with a simple merit order optimisation for electricity flexibility, and heat.	Multi-criteria analysis/Other: Explore the impact of input assumptions on major KPIs. Learn about the interactions between carriers and sectors in the energy system.	Open source/Free (freeware)
EnergyPLAN	Simulation	Investment cost minimisation, dispatch cost minimisation, electricity import, export minimisation, social welfare maximisation, fuel minimisation.	Free (Freeware)
EnergyPRO	Simulation	Dispatch cost minimisation.	Commercially (paid) licensed
Enertile	Optimisation	Investment cost minimisation, dispatch cost minimisation, electricity import, export minimisation.	Other: only for internal use
TransiEnt Library	Simulation	Multi-criteria analysis/Other: Resilience maximisation, emission minimisation.	Open source/Free (freeware)

It can be seen from Table 2.3 that the two functions that the modelling tools execute are optimisation and simulation. Optimisation is the mathematical approach of decision-making to find an optimal or best possible value of a state variable, while satisfying all constraints imposed on the objective. Simulation evaluates a significant number of alternatives given varying realistic scenarios, which are identified via decision making variables. In essence, simulation evaluates via pre-determined options but does not necessarily result in the best possible value or result [135]. In the context of IES, optimal operation of the system is an essential aspect to be studied. The relationship between the intermittent renewable energy sources and optimal dispatch of stored energy for grid balancing and transportation is essential because energy demands must be met while keeping operational costs low.

It can also be seen in Table 2.3 that most of these tools use simulation for cost minimisation. This gives the advantage of a stronger analysis because the results will be an aggregate of individual events. However, using simulation, true optimality cannot be guaranteed. Meanwhile, optimisation provides greater validity in terms of results because optimality is guaranteed. By observing the results obtained by studies conducted using the tools listed in [134], it was found that temporal resolution was important in simulation and optimisation studies. On many occasions, low temporal resolution resulted in over estimation of renewable energy supply [136]–[138]. Considering situations where renewable energy supply is not as high as expected, energy storage can be part of a solution to address this problem. Thus, a more interconnected energy system where different sectors are linked would help to accommodate an intermittent renewable energy supply. Some studies using the tools in Table 2.3 also looked at sector coupling such as in [139], [140]. In [140], sector coupling resulted in no load losses for a 6-year simulated period. These findings suggest that for better modelling of renewable energy systems, sectoral coupling and high temporal resolutions are needed. The energy hubs concept can be used to analyse IESs and sectoral coupling. Energy hubs analyses multiple energy vectors present in a localised energy system simultaneously by assessing the interconnections and interdependence of the energy vectors. An example of an energy hub is shown in Figure 2.7.

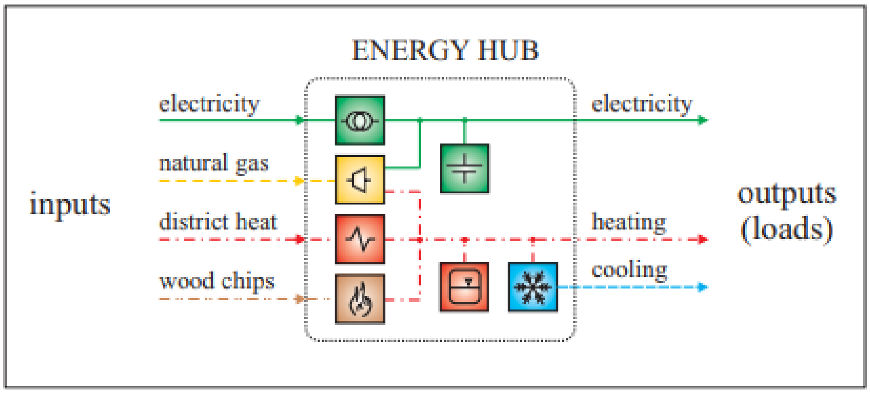

Figure 2.7: Energy hub example [110]

As shown in Figure 2.7, the energy hub looks at the various interactions that multiple energy vectors have with each other. In this case, the three energy vectors that interact with one another are electricity, heat, and cooling. Furthermore, the energy hub concept is flexible in its application because it can be used for both simulation and optimisation studies [141], [143]. The energy hub concept enables a steady-state representation of an integrated energy system by observing the conversion of a specific type of input energy to fulfil a specific load demand within a network that has different power delivery routes [142], [144]. The direct connection serves the purpose of transporting an input energy vector to the output (demand/load) without having to convert it into a different form of energy. The converters transform a certain energy vector α into another form β to fulfil the energy demand of vector β. Alternatively, vector α can be stored in a storage device. Multiple storage devices can be installed for each type of energy vector.

Mathematically, the input-output notation of energy conversion in an energy hub can be expressed by Equation (2.1) [145].

$$E_{out}^{\beta} = \eta^{\alpha/\beta} E_{in}^{\alpha} \tag{2.1}$$

where E_{in}^{α} is the input energy of vector α, $\eta^{\alpha/\beta}$ is the conversion efficiency of converting input energy vector α to an output energy vector β, and E_{out}^{β} is an output energy of vector β.

An energy hub can also be mathematically expressed in a matrix representation by Equation (2.2) [145].

$$\underbrace{\begin{bmatrix} E_{out}^{\alpha} \\ E_{out}^{\beta} \\ \vdots \\ E_{out}^{\zeta} \end{bmatrix}}_{\mathrm{E}_{out}} = \underbrace{\begin{bmatrix} c_{\alpha\alpha} & c_{\beta\alpha} & \cdots & c_{\zeta\alpha} \\ c_{\alpha\beta} & c_{\beta\beta} & \cdots & c_{\zeta\beta} \\ \vdots & \vdots & \ddots & \vdots \\ c_{\alpha\zeta} & c_{\beta\zeta} & \dots & c_{\zeta\zeta} \end{bmatrix}}_{\mathrm{C}} \underbrace{\begin{bmatrix} E_{in}^{\alpha} \\ E_{in}^{\beta} \\ \vdots \\ E_{in}^{\zeta} \end{bmatrix}}_{\mathrm{E}_{in}} \tag{2.2}$$

The purpose of the matrix representation is to provide a simple and compact form of the potential multiple input-output relationships in an energy hub. Matrix “C" is the coupling matrix and contains the converter efficiencies and/or dispatch factors, which are denoted as "c_{ij}".

There are many references in the literature to IESs that include hydrogen. For instance, [146], [147], and [148] demonstrate the cost optimal operation of hydrogen-coupled IESs using the concept of an energy hub, which enables a steady-state analysis of the systems under study. However, in these references, hydrogen is a by-product of excess electricity production because hydrogen demand is not defined. Thus, an understanding of how the integrated energy system could optimally dispatch hydrogen as an energy vector either for storage or direct consumption cannot be established.

An example of a system linking electricity, gas and hydrogen as energy vectors is presented in [149]. An optimal energy flow problem formulation is employed to assess hydrogen economy issues, such as production, distribution, and utilisation. Reference [96] showcases an integrated energy system including hydrogen and electricity as energy vectors, where a hydrogen storage system and a fuel cell are considered. The problem is formulated as a mixed integer linear programming (MILP) optimisation problem, which is used to demonstrate what the model can do for the optimal management of the system. The mathematical modelling approach that is used in both references is based on energy hub modelling. However, [149] does not account for energy storage, and neither of these references look at electrolyser input and fuel cell output against electricity export and import prices.

Reference [96] demonstrates that introducing hydrogen into an integrated energy system allows for a higher penetration of renewable electricity. Along the same line, [150] presents a study of an integrated energy system that uses hydrogen for seasonal storage and assesses its variation depending on season. However, as opposed to [144], the optimisation exercise in [151] considers a fully renewable energy run system that is isolated from the main electrical grid supply. Furthermore, a buy-back period using operational, maintenance and installation costs is considered. The robust scheduling of an integrated energy system is presented in [152], where it is found that operational costs decrease by up to 7.8% when hydrogen is included. Similarly, an integrated energy system considering hydrogen is studied for optimisation in [153]. However, in both [152] and [153], the systems under study do not consider the use of fuel cells and they look at a time scale of 24 hours only, which may not be sufficient to provide a detailed assessment of system behaviour. Furthermore, reference [145] states that greater utilisation times are necessary for hydrogen systems to be economically viable. Hence, the more renewable energy that is available, the greater the utilisation times would be—resulting in a marked difference in the system's total operational cost.

An essential reason for adding hydrogen into IESs as a means of energy storage is to avoid curtailment of renewable electricity, and thus maximise its potential. This is successfully demonstrated in [154] and [155]. This also allows for the energy system to be almost fully run with renewable energy only. However, the findings in [156] are important because it is shown that the stored hydrogen available for conversion via a fuel cell cannot meet annual shortcomings in electrical supply. This causes the system to import 70% of electricity to make up for the shortcomings.

Reference [157] studies an integrated energy system used to charge a fleet of electric vehicles. The main idea behind this work is to assess the optimal dispatch of the available energy source for vehicle refuelling. A similar idea is demonstrated in [158], thus providing insight on the practical use of renewable energy resources for vehicle refuelling, where hydrogen is a biproduct of stored excess electricity production. A hydrogen vehicle refuelling system within an integrated energy system is presented in [159], but there is no historical data available for comparison. All of the references mentioned in this paragraph are relevant because they involve the optimal management of renewable energy sources, where the energy hub is used as the modelling approach.

Reference [160] looks at the optimal sizing and operational optimisation of an off-grid integrated energy system that fully runs on renewable energy. However, system sizing is an important challenge, regardless of the system being connected or not to the grid. For instance, in grid-connected systems featuring hydrogen, it is paramount to assess the suitability of the on-site renewable generation capacity and hydrogen storage and conversion systems. This helps to determine the best way to operate the system and the optimal system size to achieve 100% renewable generation.

Flexibility offers many advantages to IESs. For instance, the inclusion of hydrogen and hydrogen storage can help to achieve an optimal system operation that guarantees 100% renewable energy supply [161], [162], which may be more challenging in systems only considering electrical energy storage. Reference [163] also looks at optimising the operation of an integrated energy system with hydrogen to achieve 100% renewable energy supply; however, only a 24-hour window is assessed. As discussed previously, a longer optimisation horizon would be needed, not only to fully understand system behaviour but also to assess the ability of the system to conduct day-ahead scheduling. Day-ahead scheduling is important because it accounts for the uncertainty of intermittent renewable energy supply, while still meeting energy demand.

2.7 Identification of Key Challenges and Research Gaps

The realisation of the potential benefits of using hydrogen for decarbonising the electricity and transport sector can be hampered if solid conclusions on its suitability for its use in the respective sectors cannot be demonstrated. From the literature review, a list of current challenges for arriving to conclusive studies to support the argument for hydrogen use in the electricity and transport sector are listed in the following bullet points.

- Site electricity demand data for specific customer categories are not widely available as most open access data require official data requests which cause delays in acquiring relevant data due to request processing times.
- Developing site electricity demand data and hydrogen demand data using stochastic methods requires a large amount of training data and bespoke knowledge on complex computing methods which may cause further time delays in being able to produce the data.
- A lack of demonstration projects makes coming to strong conclusive arguments in support of the use of hydrogen-based technologies in IESs difficult.

- Real historical site data availability for hydrogen coupled integrated energy systems are not widely available and require collaboration between university researchers and industry making it difficult for independent researchers to make their own studies.
- Hydrogen conversion and storage systems have lower round-trip efficiency when compared to other means of energy storage and provision of dispatchable energy (e.g., battery storage and pump-hydro storage is still more efficient than hydrogen) thus causing it to be lagging in terms of popularity in its use.
- Higher capital costs of hydrogen vehicles when compared to other non-polluting vehicles in the context of decarbonising the transport sector.
- Lack of commercially available hydrogen vehicles available for purchase making it difficult to conduct cost studies for the deployment of hydrogen vehicles at a wider scale.
- Uncertainty in hydrogen fuel price (prices can be very high when compared to conventional fossil fuels).
- Hydrogen economy is in its infancy, thus data relating to the techno-economic advantages of large-scale hydrogen generation, equipment aftersales market and factors effecting hydrogen price is still very speculative and difficult to model.

Research gaps that require addressing were identified are addressed by the technical contribution chapters in this thesis, as described in Table 2.4.

Table 2.4: Summary of research gaps in each technical contribution chapter

Technical Contribution Chapter	Research Gaps
Chapter 3 (Technical Contribution 1)	• Lack of modelling methods that do not require complex computing. • Lack of extensive historical data for specific sites (some sites may have only been operational quite recently and may not have abundant seasonal electrical data). • The intermittent nature of renewable energy production is heavily dependent on geographical conditions when assessing peak and low generation times within a day and/or a season.
Chapter 4 (Technical Contribution 2)	• A study assessing the TCO of converting a diesel ICE refuse collection vehicle fleet to a fuel cell electric refuse collection has not yet been studied in the current available literature. In the case of TCO studies of a refuse collection fleet, there are only studies that addresses the comparative study of a diesel fleet conversion to battery electric [164], [165]. • There is a significant lack of available data regarding the performance of current fuel cell electric RCVs (i.e., fuel consumption and fuel efficiency). • Sensitivity of TCO of fuel cell electric RCVs with respect to fuel cell efficiency and hydrogen price needs further investigation. • Economic feasibility of operating a fuel cell electric refuse collection vehicle fleet needs to be studied further.

Chapter 4 (Technical Contribution 2-Cont)	• Capital cost of fuel cell electric RCVs, estimated fuel costs/unit distance and maintenance costs must be studied better due to a lack of reliable information regarding these costs.
Chapter 5 (Technical Contribution 3)	• Lack of sectoral coupling technologies between electricity heat and transport sector, which calls for the development of an energy system optimisation model that incorporates all energy sectors at hourly resolution, regional spatial resolution, seasonal storage options and technological learning [166]. • Lack of hourly resolution capturing of intermittent renewable energy production and related potentials [166]. • A better understanding of the techno-economic benefits of using hydrogen for storage of excess electricity generation, and its potential for electricity export and import to assess revenue streams and calculate buy-back periods is needed. • A further understanding of the role that hydrogen can play in both electrical grid balancing and hydrogen fuel supply for transport is required.

2.8 Summary of the Literature Review

This chapter has introduced the basic aspects of the challenges surrounding intermittent renewable energy supply, energy storage, costs of fuel and emission reduction via renewable energy use in different business sectors. The hydrogen energy projects around Europe were listed (Table 2.1) and compared with hydrogen projects in the UK. It was found that almost all operational hydrogen projects in Europe did not exceed a generation capacity of 10MW. Furthermore, the findings from the operational projects faced challenges relating to regulatory uncertainty, equipment availability, high capital costs and transport. The literature on the capital costs and operational cost of a large hydrogen vehicle was also studied for in the UK context and at present, it was difficult to determine the manufacturer retail price of large hydrogen vehicles as there are no mass-produced models and current manufacturers are not public about their prices. The challenges of hydrogen production, storage, transport, and commercialisation were also explained according to current literature. These challenges related to the scaling up of production, effect of hydrogen equipment levelized cost of energy for the whole energy system, equipment availability and clear standards certification and legislation. Finally, the barriers for adopting hydrogen-based technologies in the transport sector and its relation to high capital costs were also presented.

The methods that were previously used to develop electricity-demand profiles were categorised and discussed in length. The three main categories of modelling methods for electricity-demand forecasting (i.e., physics-based, data driven, and hybrid) were defined and explained. These methods were mainly stochastic methods which required large data input and complex computing. Methods for quantifying vehicle fuel demand were categorised and based on the type of model (i.e., direct monitoring, physics-based modelling, hybrid modelling). A method (TCO analysis) for assessing the techno-economic benefits of operating hydrogen vehicles in the transport sector was discussed and explained.

A list of energy simulation and optimisation tools used in the study of IES is compiled in Table 2.3. The use of these tools was reviewed in the literature. In addition, the studies that have used these tools to look at systems that have large amounts of renewable energy supply and sectoral coupling of the constituent energy systems were discussed. From reviewing the tools, it was found that temporal resolution as well as the ability to couple different sectors greatly improved the quality of the results presented in the studies.

Furthermore, present methods of IES analysis were divided into seven categories (Section 2.6.3). A method for modelling and analysing IES with sectoral coupling (energy hubs concept) was also presented and discussed. The energy hubs concept was found to be suitable for creating an optimisation study of high temporal resolution and allowed for sector coupling. Finally, this chapter established the general situation, current challenges, and benefits of hydrogen-based technologies in terms of adoption in the case of IES and the transport sector.

Chapter 3: Methods for Developing Representative Renewable Electricity Generation and Demand Profiles

3.1 Introduction

Accurate profiles of renewable electricity generation are essential for the analysis of multi-vector energy systems. Historical site data for both renewable energy resource, electricity generation and electricity-demand can give an insight into how an energy system operates in certain conditions. At present, stochastic methods such as machine learning are popular for developing electricity generation and demand profiles; however, these methods require large datasets to train the machine learning systems. Furthermore, machine learning systems take a considerable amount of time to develop, train and deploy also necessitating the user to be well versed in complex computing methods. Hence simpler methods for developing electricity demand profiles using minimum input data which can be used to produce representative profiles of a considerable level of accuracy would be beneficial for users who require who require this data at short notice without having to acquire complex computing skills.

This chapter will describe the methods to create representative renewable electricity generation profiles using calculations of solar panel efficiency and sizing, as well as wind turbine power output. A method of creating a representative profile for electricity-demand using an arithmetical method of scaling against historical data is then presented and discussed.

The purpose of generating representative profiles is to provide sufficient information for when a specific site does not have energy monitoring data with a good granularity. Without this data, it would be difficult to undertake a comprehensive study of the behaviour of the energy sources supply with site energy demand. Furthermore, collecting data from sites can be time consuming because it may take a considerable amount of time (e.g., a year) to collect full seasonal data. This may require expensive monitoring systems to be installed. Sites that do not have monitoring infrastructure in place can use the methods presented in this chapter to generate representative profiles for renewable power generation and site electricity-demand, which can then be used for energy system improvement studies.

3.2 Methods of Generating Renewable Electricity Generation Profiles

The methods for generating representative renewable electricity profiles are presented in this section, which are explained with the aid of an example. The geographical data will be described in the subsequent subsections.

3.2.1 Solar PV Modelling

Solar PV profiles can be derived from calculating the total PV collection area via Equation (3.1) [86].

$$T_{PV} = T_a + \frac{N_{OCT}20}{0.8}G \tag{3.1}$$

Where:

- T_{PV}: Temperature of the PV panel (°C)
- T_a: Ambient temperature (°C)
- G: Solar irradiance $(\mathrm{W/m^2})$
- N_{OCT} : Nominal cell operating temperature (°C)

The nominal operating temperature is derived from data determined by solar PV panel manufacturers. For the values of irradiance and ambient temperature, an average of monthly values for an entire year is provided by the CIBSE Guide A [167]. Upon determining the temperature of the panel, its efficiency with respect to temperature is calculated using Equation (3.2) [87].

$$\eta_e = \eta_{module}(1 - TC(T_{PV} - 25)/100) \tag{3.2}$$

Where:

- η_{module}: PV module efficiency from manufacturer data
- TC: Temperature coefficient $(\%/\mathrm{K})$

Values for panel efficiency and the temperature coefficient are based on the data provided by the solar PV panel manufacturer. An average value for efficiency is then calculated with the average value of irradiance. The rated power of the PV system should be determined to allow for the calculation of the effective area of solar PV collection. This is achieved with [88]

$$A_D = Q/(\mu\, \eta_e \times \mu_{Ir}) \tag{3.3}$$

Where:

- Q: Rated generation capacity of whole solar PV system (kW)
- A_D: Demand area (m^2)
- $\mu\, \eta_e$: Average annual panel efficiency (%)
- μ_{Ir}: Average annual solar irradiance $(\mathrm{W/m}^2)$

The product of the demand area with the hourly solar irradiance values and panel efficiency allows for the hourly values of PV electrical generation to be obtained.

An example of a PV electrical generation profile using Equations (3.1–3.3) was demonstrated. The results for this example are shown in Figure 3.1. The example was based on geographically specific data for irradiation values and ambient temperature values in Fife, Scotland [167], [168]. The value of nominal operating cell temperature that was used was 46°C, as per the datasheet in [169]. The values of irradiance and ambient temperature were the average of monthly values for an entire year and were provided in [167]. Once the temperature of the panel was obtained, the panel efficiency with respect to the panel temperature was calculated using Equation (3.2). The values for panel efficiency and the temperature coefficient are based on the Hyundai HiS-S260MG PV module, being 16.1% and 0.45 %/K, respectively [169]. An average value for η_e was found and the average value of seasonal irradiance based on hourly irradiance values for a specific season was derived from data in [168], whereas the rated power of the PV system was determined to be 200 kW. Hence, the effective area of PV collection is then found using Equation (3.3). The hourly values for PV electrical generation were obtained by multiplying the demand area with the hourly irradiance values obtained from [167] and the panel efficiency, as shown in Figure 3.1.

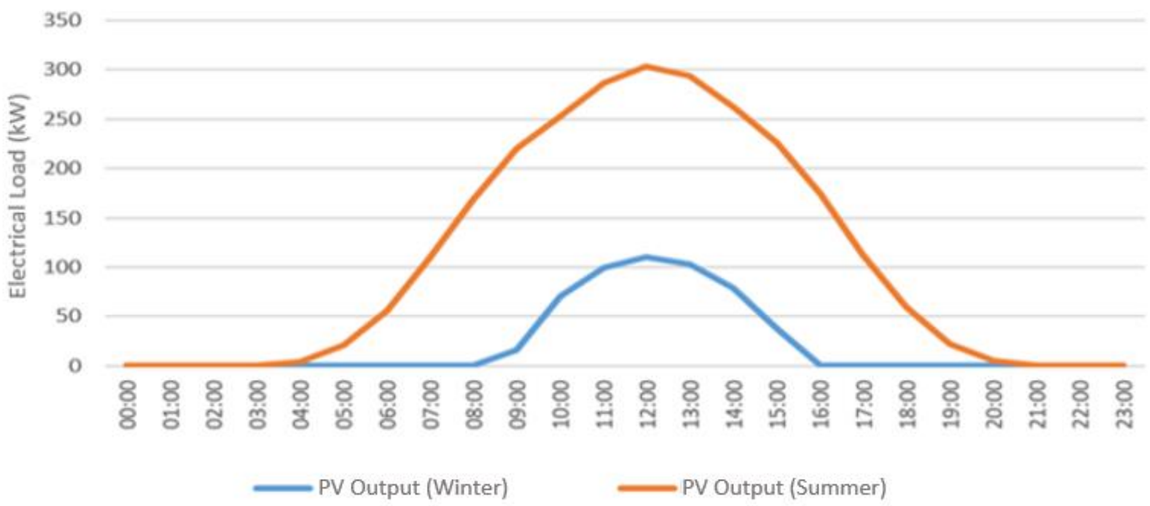

Figure 3.1: Daily PV output across seasons

Due to expected higher solar irradiance on a typical summer day, Figure 3.1 indicates a higher level of PV generation, as can be seen in the orange trace at 12:00 hours, where the solar PV output is almost 200 kW higher than the output in winter (blue trace).

3.2.2 Wind Generation Profile

The power extracted from the wind by a wind turbine can be obtained through Equation (3.4) [89].

$$P_{avail} = \frac{1}{2}\rho A V^3 C_p \tag{3.4}$$

Where:

- ρ: air density $(\mathrm{kg/m^3})$
- A: total swept area of turbine $(\mathrm{m^2})$
- V: wind speed $(\mathrm{m/s})$
- C_p: power coefficient

The power coefficient of the wind turbine is based on the wind turbine make and should not exceed 0.59, which is known as the Betz limit [170]. Wind speed is defined by obtaining the average wind speed according to the geographical location of the turbine. Air density is calculated using the ideal gas law [171]:

$$\rho = \frac{P}{R_{sp}T} \tag{3.5}$$

Where:

- ρ: Air density $(\mathrm{kg/m^3})$
- P: Pressure (Pa)
- R_{sp}: Specific gas constant $\mathrm{J/kg \cdot K}$
- T: Ambient temperature (K)

A more accurate value of air density is obtained by using the average ambient temperature for the geographical location at a given time because temperature has an inversely proportional relationship with air density.

A wind turbine with a rated power output of 750 kW was selected to demonstrate the calculations. To demonstrate the proposed wind turbine output, the NEG Micon NM 48/750 wind turbine was selected because it has a maximum generation capacity of 750 kW. From its datasheet, the swept area obtained, and the performance coefficient were determined from the average wind speed for each seasonal profile and compared to the power curve graph provided in [89], [171]. The performance coefficients were calculated as 0.37 (summer) and 0.33 (winter). Hourly wind speeds provided in [172], with historical weather wind speed data from Fife, Scotland were selected.

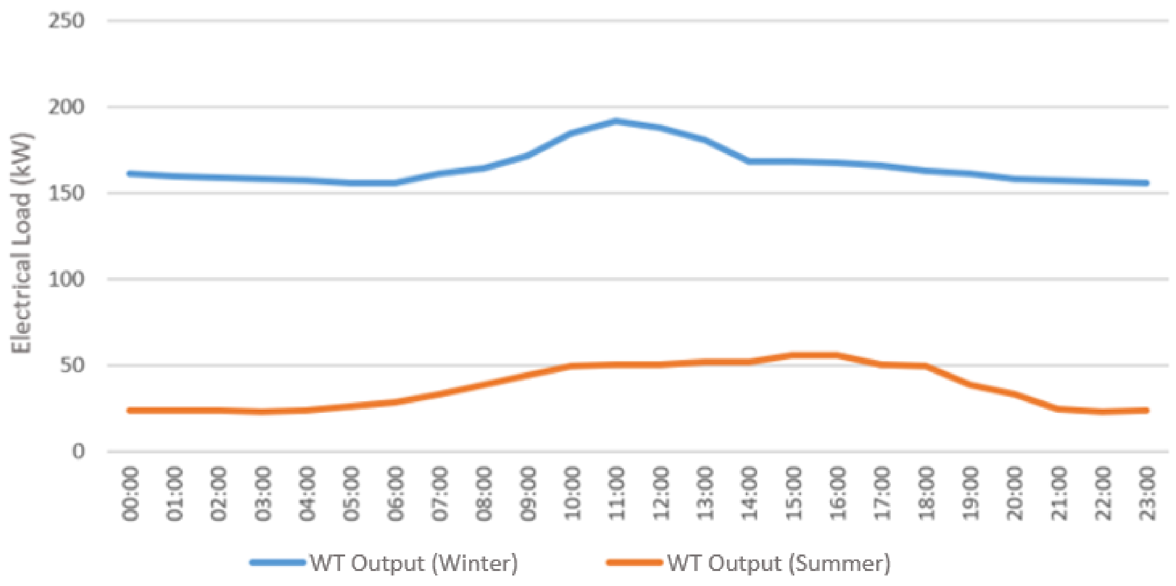

Figure 3.2: Daily wind turbine output across seasons

Figure 3.2 shows representative winter and summer profiles of wind turbine generation, which were obtained using the method discussed. The winter months have a higher generation in comparison to the summer months. This is attributed to higher wind speed and colder temperature.

3.3 Methods of Building Electricity-demand Profiles

3.3.1 Electricity Demand Scaling Methodology

The literature reviewed in Section 2.4.1 discusses the various challenges related to obtaining good electricity-demand data. These methods usually involve monitoring electricity demand on a national or regional scope. Electricity-demand data can also be forecasted. The methods of forecasting usually involve complex computing (e.g., ARIMA or XCORR) and may also combine the use of historical data. These methods were discussed in Section 2.6.1.

Alternatively, available representative electricity demand profiles can be found such as those provided by Elexon [173]. These electricity demand profiles are based on consumer categories which are metered half-hourly readings. The consumer categories are broadly described as either domestic or non-domestic consumers with varying peak load factors. In fact, consumers within a single category may exhibit very different consumption patterns if looked at in more detail as the categorisation is mainly based on the annual consumption data. Given the broad categorisation of the Elexon profiles, the representative profiles provided by Elexon may not reflect site specific characteristics of a singular building/building type of interest as it is very generalised.

In terms of data availability, the demand data is available on their website. However, to access the data, parties must develop their own bespoke solutions or outsource the conversion/analysis to a secondary provider. This is due to the data being provided in a pipe-deliminated flat file which is a legacy format adopted by the industry. The only available Elexon demand profile readily available in a spreadsheet format is data from 1997 [174]. Hence this may not be a good set of data for comparison with a more recent demand profile.

To address the complexity of developing representative electricity demand profiles, the method presented in this section develops representative electricity-demand profiles and does not employ complex computing. The purpose of this is to allow a greater range of users who may not be familiar with the various complexities present in machine learning, complex computing or having limited access to specific datasets.

In the proposed method, the scaling factor is an average between maximum energy between weekdays and weekends. First, the average maximum demand between every weekday and weekend is calculated. Average electricity demand for each hour of the day for both weekdays and weekends is determined as Equation (3.6)

$$\mu E_{D(t)}^{weekday/weekend} = \frac{\sum E_{D(t)}^{weekday/weekend}}{n_{days}} \tag{3.6}$$

Where:

- $\mu E_{\mathrm{D(t)}}^{weekday/weekend}$: Average electricity demand at each hour for weekdays or weekends (kW)
- $\sum E_{\mathrm{D(t)}}^{weekday/weekend}$: Total electricity demand for weekdays or weekends (kW)
- n: number of days.

This will result in two separate sets of values for average hourly electricity demand corresponding to two 24-hour datasets: the first for weekdays and the second for weekends. The highest value between the two datasets becomes the scaling factor, with $SF_{(t)}^{weekday/weekend} = 1$.

The average scaling factor for each hour of the day is then obtained for weekdays and weekends as

$$SF_{(t)}^{weekday/weekend} = \frac{\mu E_{D(t)}^{weekday/weekend}}{\mu E_{Dmax}^{weekday/weekend}} \tag{3.7}$$

Where:

- $SF_{(t)}^{weekday/weekend}$: Hourly scaling factor for weekdays or weekends
- $\mu E_{\mathrm{Dmax}}^{weekday/weekend}$: Average maximum electricity demand for weekdays or weekends (kW)

Hourly profiles are then obtained by multiplying the average scaling factor for the specific time of day with the average maximum electricity demand value for weekdays and weekends.

$$E_{D(t)}^{weekday/weekend} = \mu E_{Dmax}^{weekday/weekend} \times SF_{(t)}^{weekday/weekend} \quad (3.8)$$

A second method of deriving representative electricity-demand profiles is demonstrated using hourly data for each day of the week present in a specific month. First, the average electricity demand for each hour of a particular day of the week is determined.

The average of $E_{\mathrm{D(t)}}^{day}$ for *n* days gives the value of average electricity demand at time *t* for a specific day (i.e., for time 00:00 across all Mondays that occur in a month):

$$\mu E_{D(t)}^{day} = \frac{\sum \mu E_{D(t)}^{day}}{n_{days}} \quad (3.9)$$

To calculate the scaling factor, the following formula is used:

$$SF_{(t)}^{day} = \frac{\mu E_{D(t)}^{day}}{\mu E_{Dmax}^{day}} \quad (3.10)$$

Where:

- $\mu E_{\mathrm{D(t)}}^{day}$: Average hourly electricity demand on that day of the week (kW)
- $\mu E_{\mathrm{Dmax}}^{day}$: Average maximum electricity demand on that day of the week (kW)

The highest value of electricity demand in each specific day of the week is represented by $SF_{(t)}^{day} = 1$.

Given the daily scaling factors, calculation of the hourly electricity demand specific for that day of the week is:

$$E_{(t)day}^{d} = \mu E_{max\,day}^{d} \times SF_{(t)day} \quad (3.11)$$

To summarise, Equations (3.6–3.8) constitute the first method to derive representative electricity-demand profiles, which is referred to here as the "weekly scaling factor method". Equations (3.9-3.11) are referred to as the "daily scaling factor method". The purpose of developing these two methods is to determine which form of data aggregation provides better accuracy when used to generate representative electricity-demand profiles.

The possibility of using the scaling factors between two different sites was also investigated. For this to happen and result in better accuracy, the historical electricity demand data of the site that the scaling factors were based on were corrected against the minimum and maximum electricity demand of the site whose representative electricity-demand profile is being developed, using the following condition:

$$E_{Dmin}^{Site\ B} \leq E_{D(t)}^{Site\ A} \leq E_{Dmax(t)}^{Site\ B} \quad (3.12)$$

Where:

- $E_{D(t)}^{Site\ A}$: Electricity demand of site the scaling factors are generated from at time "t" (kW)
- $E_{Dmin(t)}^{Site\ B}$: Minimum electricity demand of site who's demand profile is to be developed (kW)
- $E_{Dmax(t)}^{Site\ B}$: Maximum electricity demand of site who's demand profile is to be developed (kW)

3.3.2 Historical Data Scenario Study

The data that are compared in this section are based on two existing sites: Rotherham Hospital and the Queen Elizabeth Hospital (QEH). The purpose of comparing two sites of similar function is to observe if the electricity consumption profiles are similar given that they are both hospitals. The assumption is that due to the similar roles the sites play, the times of day where the electricity consumption is at its lowest and when it is at its highest are likely to be similar. The comparisons between the two hospitals are not expected to be a near mirror of each other, due to differing minimum and maximum demands per site and any given hour (QEH: 800-1600 kWe, Rotherham: 160-900 kWe). Comparing two sites of a different category with similar maximum demand may not give a good comparison because (for instance) residential dwellings and office sites may have different consumption peaks [116].

Scenarios were developed to observe the daily demand profiles across seasons of the real electricity-demand profiles and the scaling factors. This was done in anticipation that electricity consumption during winter months is expected to be higher than during summer months, as per the historical data. Other examples in the literature also indicate this trend [117], [175]. These scenarios are shown in the Table 3.1.

Table 3.1: Description of Scenarios for Demand Data Analysis

Scenario	**Description**
QEH Daily Winter Month Data with QEH Winter Scaling Factors	QEH daily winter month data both real and averaged are compared against the representative profile derived by the corresponding winter scaling factors.
QEH Daily Summer Month Data with QEH Summer Scaling Factors	QEH daily summer month data both real and averaged are compared against the representative profile derived by the corresponding summer scaling factors.
Rotherham Daily Winter Month Data with Rotherham Winter Scaling Factors	Rotherham daily winter month data both real and averaged are compared against the representative profile derived by the corresponding winter scaling factors.
Rotherham Daily Summer Month Data with Rotherham Summer Scaling Factors	Rotherham daily summer month data both real and averaged are compared against the representative profile derived by the corresponding summer scaling factors.
QEH Winter Daily Month Data with Rotherham Winter Scaling Factors	QEH daily winter month data both real and averaged are compared against the representative profile derived from the Rotherham winter scaling factors.
Rotherham Daily Summer Month Data with QEH Summer Scaling Factors	Rotherham daily summer month data both real and averaged are compared against the representative profile derived from the QEH summer scaling factors.
QEH Daily Summer Month Data with Rotherham Summer Scaling Factors	QEH daily summer month data both real and averaged are compared against the representative profile derived from the Rotherham summer scaling factors.

For each of the scenarios, the specific scaling factors (weekly and daily) are used to create a representative electricity demand profile which the resultant representative electricity demand profile is compared to both averaged real data and the actual hourly real data. The purpose of averaging the real data is to smoothen out any outlier data from the actual hourly readings. This will then allow a comparison of the accuracy provided by the scaling factor method when compared to the actual hourly readings.

3.4 Results and Discussion of Historical Data Scenario Studies

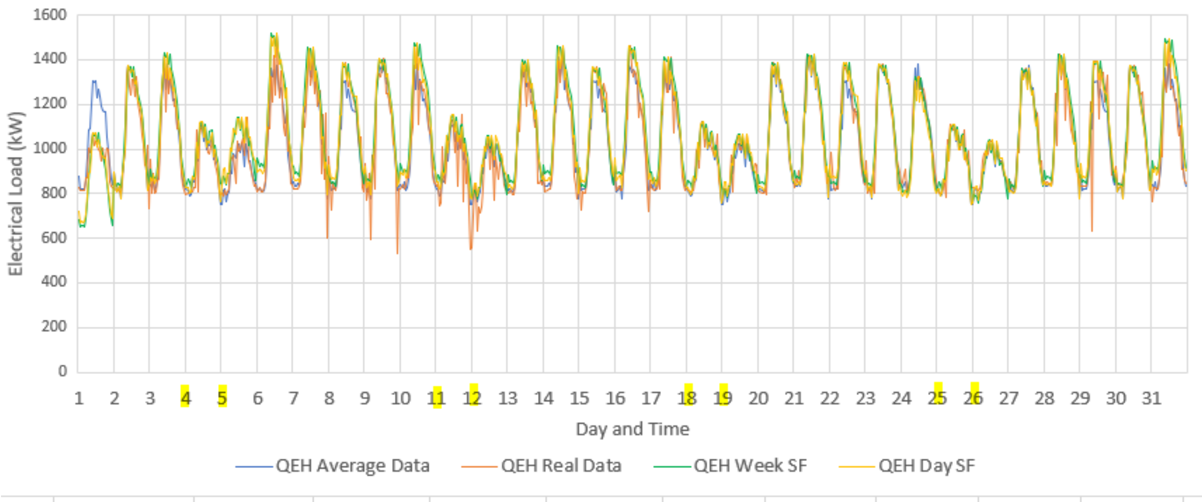

Figure 3.3: QEH daily winter month data with QEH winter scaling factors

The information presented in Figures 3.3–3.8 show a month's worth of data, where weekdays and weekends are distinctly identified. Weekends are highlighted in the x-axis labels in yellow for clarity. This aims to show the variance of electricity demand between weekdays and weekends.

By comparing the real data with the averaged data presented in Figure 3.3, it can be observed on the first day of the winter month that the difference between averaged and real data is apparent. This may be due to bad quality data because sudden dips in demand occur again on days 8, 9, 12 and 29. However, for the most part, the averaged data and real data are a better match.

The profiles generated using the scaling factor methods seem to almost match both the averaged data and the real data throughout the month. This gives an indication that the scaling factor is a simple but effective means of generating a representative electricity-demand profile. Both of the scaling factor methods in this example seem to arrive to a good match when compared to the averaged and real data. This is possible due to the high quality and relatively stable electricity consumption pattern throughout the month. Thus, for this example it can be said that the method leads to an accurate representative electricity-demand profile.

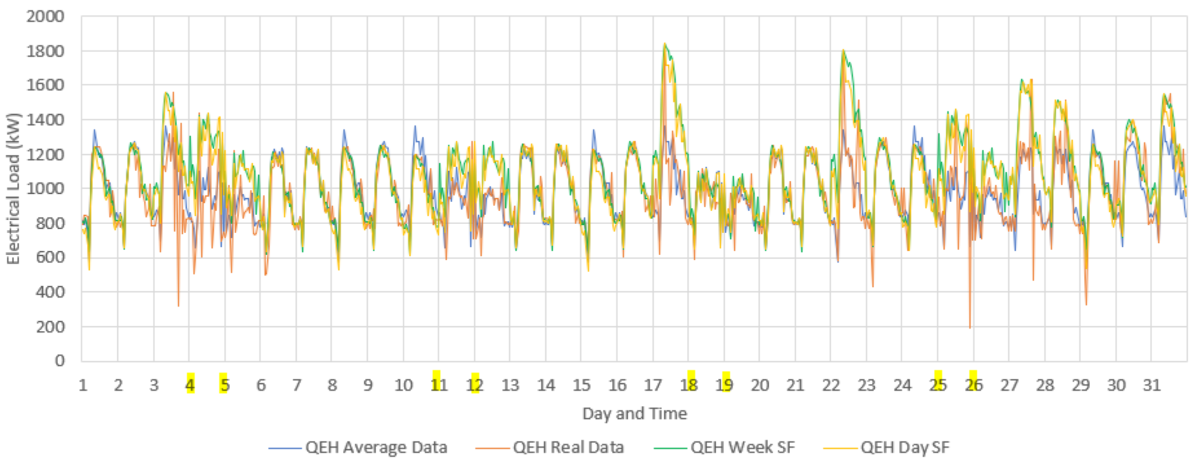

Figure 3.4: QEH daily summer month data with QEH summer scaling factors

Similarly, Figure 3.4 shows similar characteristics with those mentioned in Figure 3.3 regarding the accuracy of the scaling factors when compared to the averaged and real data. However, the profiles derived from the scaling factors are less accurate when compared to the accuracy demonstrated in Figure 3.3. One of the main reasons for this is the quality of historical data. This is apparent from the fluctuations of electricity demand (e.g., see days 17 and 22). These outlier electricity-demand peaks can be attributed to irregular high activity in the hospital site occurring on those instances because it does not seem to be a recurring incident throughout the month. Nonetheless, when creating a representative profile for the site, the accuracy shown in Figure 3.4 is still considered to be acceptable.

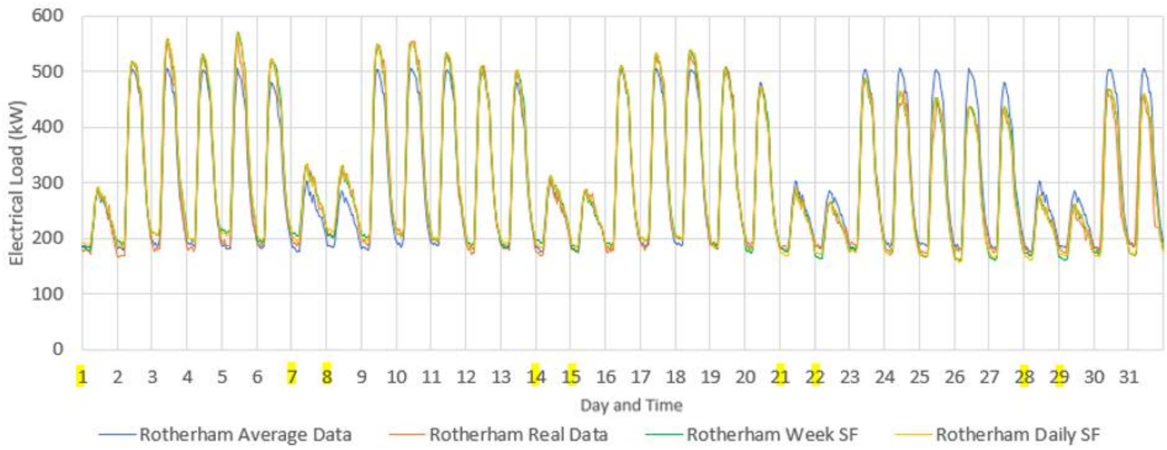

Figure 3.5: Rotherham daily winter month data with Rotherham winter scaling factors

Figure 3.5 looks at the data from the Rotherham site for a winter month. This graph indicates that the electricity-demand profiles derived from the scaling factor method align well with both the averaged and real data for the winter month. This level of accuracy was possible due to the effect of the installed combined heat and power (CHP) unit installed in the Rotherham site being corrected. Had the effect of CHP not been addressed, then there would be significant fluctuations because CHP operation would lead to higher average electricity-demand peaks.

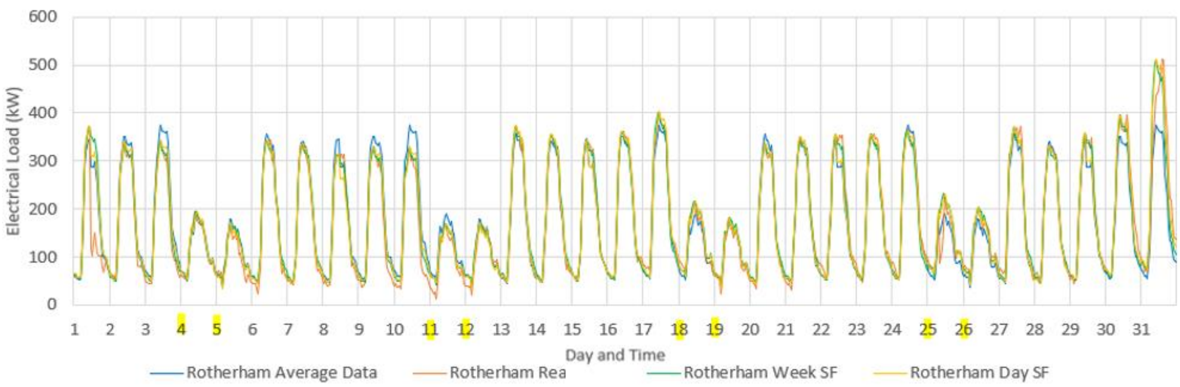

Figure 3.6: Rotherham daily summer month data with Rotherham summer scaling factors

Figure 3.6 shows a more closely matched profile between the real and averaged data, and hence a better matched profile produced by the scaling factors is obtained. There is a higher peak on day 31, which can be attributed to CHP operation. This conclusion was made as the baseline minimum throughout the days following that indicate a significantly lower value.

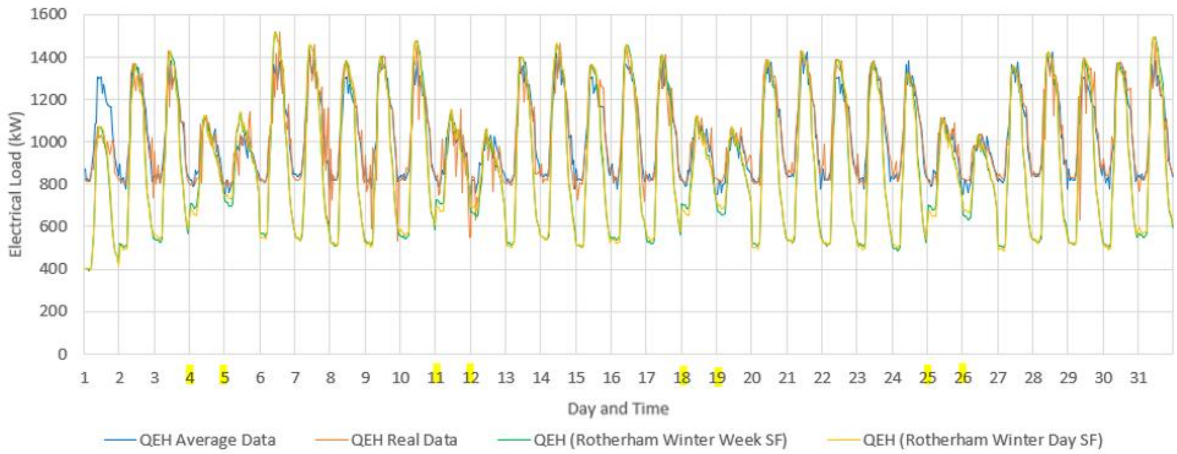

Figure 3.7: QEH daily winter month data with Rotherham winter scaling factors

Figure 3.7 shows the results of a scenario where the scaling factors of the Rotherham site for a winter month were used to generate representative electricity-demand profiles for the QEH site. The logic behind this was to observe if the scaling factors can be used interchangeably between sites that serve similar functions.

Looking at the results in Figure 3.7, there is a frequent mismatch of demand dips between the representative profiles generated by the scaling factor methods when compared to the averaged and real data for the QEH site. This can be attributed to the fact that sites operate at specific capacities (QEH: 1600 kWe max, Rotherham: 900 kWe max). This is the reason why there is a mismatch in the data comparison because this leads to different scaling factors. Furthermore, the quality of data for the Rotherham hospital in the winter month is not as consistent as for the QEH site. This inconsistency in data quality reflects the point brought up regarding CHP operation and the addition of electric chillers, as mentioned previously when discussing Figure 3.5.

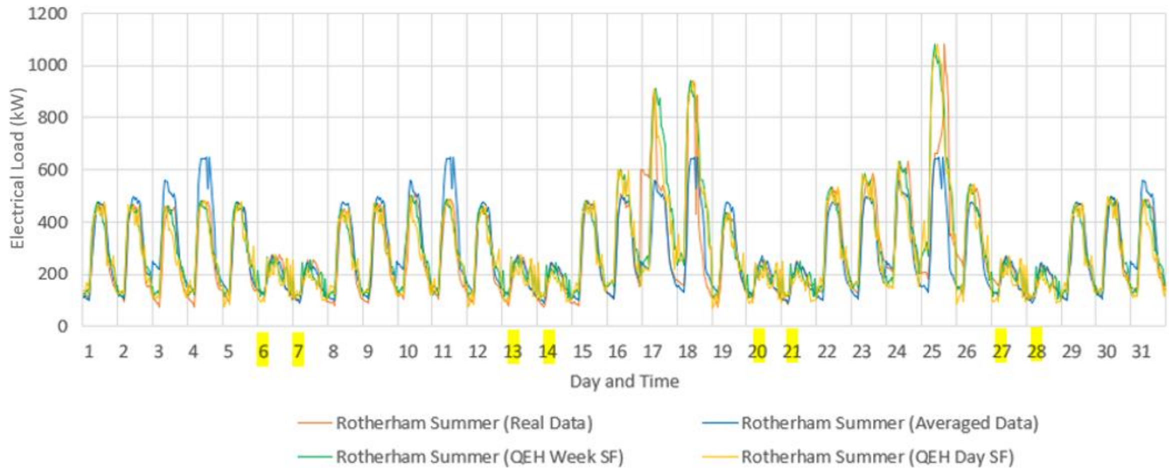

Figure 3.8: Rotherham daily summer month data with QEH summer scaling factors

Figure 3.8 shows the results of interchangeably using scaling factors between two different sites. In this example, the scaling factors for the QEH data are used to generate a representative profile based on the Rotherham data (summer month). This result is similar to Figure 3.7, where the representative profiles generated from the scaling factors do not fit well with the averaged and real data of the site despite using a scaling factor from the same month.

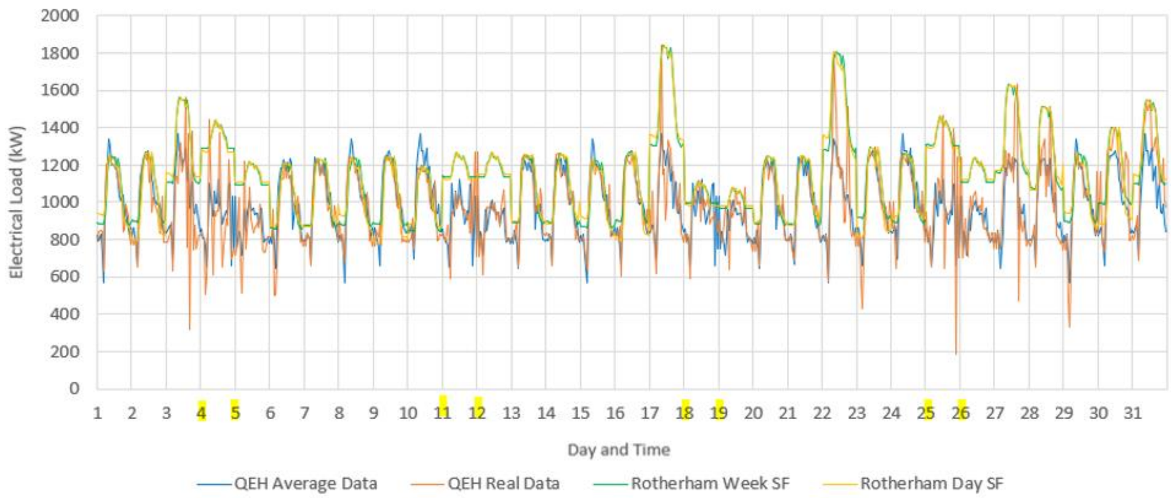

Figure 3.9: QEH daily summer data with Rotherham summer scaling factors

Again, observing the results presented in Figure 3.9, the traces of the profiles generated by the scaling factors do not seem to match those of the real and averaged datasets. The mismatch seen in the profiles and compared with real and average datasets are significant at a glance because the minimum points of the representative profiles are quite far from the minimum points of the real and average datasets on each day shown. These results are consistent with those previously seen in Figure 3.8, where the site's real and averaged datasets are compared to a representative profile generated by the other site's scaling factors.

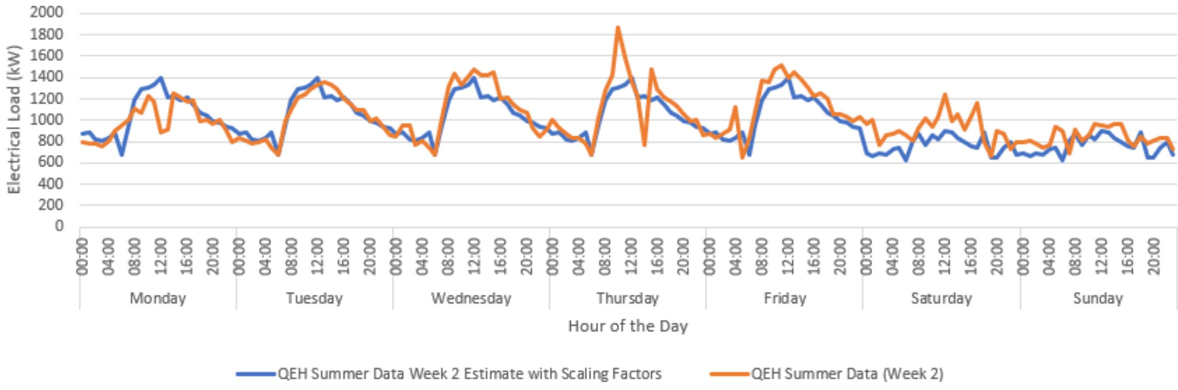

Figure 3.10: QEH daily summer week data with QEH summer scaling factors

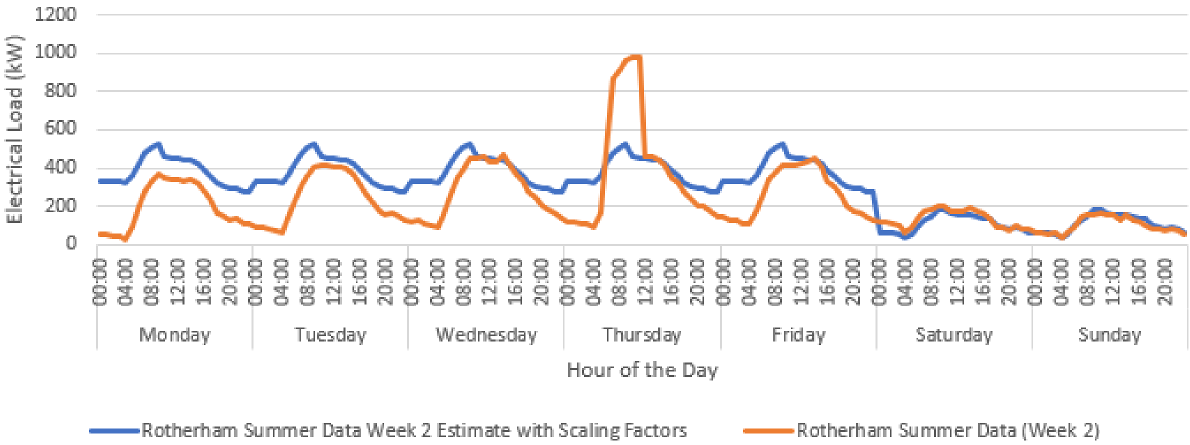

Figure 3.11: Rotherham daily summer week data with Rotherham summer scaling factors

In Figures 3.10 and 3.11, a week's representative electricity-demand profile was generated by using the scaling factor method and the previous week's weekly data. This profile (orange line) was compared to the real data for the subsequent week.

In Figure 3.10, the representative profile generated by the scaling factors fits rather well with a mean absolute error of around 10% when compared to the error margin limit of 20%. However, the error margin is around 80% in Figure 3.11. When taking a closer look, the error margin for the Rotherham site (Figure 3.11) in the weekend is 7.8%. Therefore, the representative profiles generated by the scaling factor method requires it to be based on good quality historical data.

Looking at the Figures 3.3-3.9, for all scenarios, electricity consumption peaks at around the same time in both sites (16:00-17:00) and decreases until the end of the day. Electricity consumption then increases gradually during the start of the day until the peak hours. This pattern also occurs between weekdays and weekends. Electricity consumption during weekdays is significantly larger than that during weekends. This is due to more activity being done over the weekdays. Hence, there is a need to define two different sets of scaling factors when using the first method. The difference of electricity consumption during weekdays and weekends is significant.

Calculating an average throughout the entire week to base the scaling factors on would lead to a representative profile that does not reflect the difference of electricity consumption between weekdays and weekends. For both sites, when seasons are compared, the consumption of electricity is significantly higher during the winter months than the summer months. This can be attributed to higher electricity consumption for heating purposes, higher hospital activities that are specific winter months (e.g., imaging) and generally higher hospital admission rates during the winter months [176].

In terms of the two weekly profiles (Figures 3.10 and 3.11), it can be observed that the QEH data when compared to the profile generated based on the scaling factors is a better fit than that of the Rotherham site. Therefore, data quality is the main limitation of the scaling factor method. However, if the real data has a good quality, then the scaling factor method can be a very easy and simple method to generate representative profiles of a specific site (or sites).

This is most apparent when observing the QEH winter site data where the representative profile based on the scaling factor method aligns well with the averaged and real data. Meanwhile, the Rotherham winter data shows the opposite because the profiles generated by the scaling factor method do not match very closely with the averaged and real data. This is due to the number of fluctuations between the days in this month. These fluctuations result in a significant skewing of the averaged data that are used to build the scaling factors and lead to the very apparent inaccuracy.

When using the scaling factor method, it is important to note that the scaling factors for each site should be unique to that specific site for greater accuracy. It would be possible to use the scaling factors of two different sites interchangeably. This does require further adjustment of the historical data that is being used to develop the scaling factors to be corrected in proportion to the minimum and maximum electricity demand per hour at the targeted site whose electricity-demand profile is to be developed (as explained in Section 3.3.1). Interchanging scaling factors between two sites that fulfil the same function (in this case, two hospital sites) will lead to a less accurate representative electricity-demand profile. This is due to the scaling factors being based on a scaling up of the site's hourly consumption and maximum peaks, which may differ from site to site. This is most apparent in Figure 3.8 given that the average accuracy of the results is above 20%.

The scaling factor can also be used to create a site's representative profile, which can be adjusted in potential changes of a site's maximum demand if that changes with time. This can be used as a benchmark for comparison if any changes in terms of the maximum energy demand of the system changes in real time. The scaling factor method allows a close enough estimate of a representative electricity-demand profile for a specific system that does not have enough electricity consumption monitoring infrastructure. It is also an easier method to use than machine learning, which would require an individual to possess advanced computing knowledge. The accuracy of the results that are obtained using the scaling factor methods will be discussed in the following subsection.

3.5 Analysis of Mean Absolute Percentage Error to Determine Accuracy

Representative profiles are considered to be more accurate if the value of error is closer to zero (perfect forecast) when compared to the real data. Furthermore, the advantage of using available real historical data to base representative electricity-demand profiles on is that operational uncertainties are considered. Using historical data leads to a more accurate representation of the system's electricity consumption behaviour. Reference [177] considers anything exceeding a 5% mean absolute percentage error to be inaccurate for their purpose of measuring the accuracy of a forecasted electricity-demand profile with historical data. However, for the study undertaken with the scaling factor method, the limit for accuracy is set to anything below 20% as the benchmark (comparing representative profile to actual/averaged data).

Accuracy between profiles derived from scaling factors is compared with the average daily data and the actual daily data using the mean absolute percentage error (MAPE), as shown in Equation (3.13)

$$MAPE = \frac{100\%}{n}\sum_{t=1}^{n}\left|\frac{E_{D(t)}^{SF} - E_{D(t)}^{actual\ or\ average}}{E_{D(t)}^{actual\ or\ average}}\right| \tag{3.13}$$

The results of the accuracy tests are shown in the Table 3.2.

Table 3.2: Measure of Accuracy for Scenarios under Study

	QEH Daily Winter Month Data with QEH Winter Scaling Factors	QEH Daily Summer Month Data with QEH Summer Scaling Factors	Rotherham Daily Winter Month Data with Rotherham Winter Scaling Factors	Rotherham Daily Summer Month Data with Rotherham Summer Scaling Factors	QEH Winter Daily Month Data with Rotherham Winter Scaling Factors	Rotherham Daily Summer Month Data with QEH Summer Scaling Factors	QEH Daily Summer Month Data with Rotherham Summer Scaling Factors
% Error Average Data vs Week SF	6%	13%	7%	9%	13%	24%	20%
% Error Average Data vs Day SF	4%	12%	7%	7%	13%	27%	20%
% Error Real Data vs Week SF	7%	12%	4%	14%	13%	24%	22%
% Error Real Data vs Day SF	6%	15%	4%	13%	13%	25%	22%

Looking at the results presented in Table 3.2 and the graphs showing the demand profiles, the QEH data has a lot of sudden fluctuations and outliers, whereas the Rotherham data seem to be more stable. It can also be observed that the second scaling factor method is more accurate (daily averaged scaling factors). For the case of using scaling factors to produce representative profiles most optimally, they must be used in a site-specific manner. Although the scaling factors can be interchangeable between sites, this will be very dependent on the quality of data provided.

Direct application of scaling factors of one site to work out the representative electricity-demand profile of another site was attempted without imposing the condition mentioned in (3.13). This led to a MAPE value of 37–38% in the scenario where historical data of the Rotherham site was compared with the resultant representative electricity-demand profile generated via the scaling factors of the QEH site (summer month). The reverse of this scenario (Rotherham historical data, QEH scaling factors) was also investigated, and the resultant MAPE was 104–116%, which is significantly worse. Thus, to maintain accuracy of results when using scaling factors interchangeably between two sites, the conditions set in (3.13) must be fulfilled.

It is, however, worth noting that aggregating the data helps in achieving better accuracy. For the scenario observing the demand profiles for the Rotherham hospital during winter, aggregating the data helps to bring the accuracy closer to the 20% mean absolute error mark that was the designated benchmark for tolerance. Thus, for the best results when using the scaling factors, the second scaling factor method should be used against a set of aggregated data (this is especially important for when the real datasets have significant outlier data).

In the case of the QEH data, the summer historical values are the least reliable. However, this can be corrected by using the QEH summer scaling factors to generate profiles for the days with fluctuations by basing it on more stable days where these fluctuations are not as contrasting. Looking more closely at the Rotherham data, there are also few instances where there are contrasting values (e.g., in Figure 3.11). The weekend data for the real and scaling factor estimate is close and upon calculating MAPE the value is 7.8%, which is well below the 20% limit.

Other work where electricity-demand profiles were being generated from historical data and data-driven models show accuracy levels that vary significantly. For example, the work in [175] presented the use of a linear regression model for day-ahead electricity-demand forecasting of 700 households in Japan. The absolute mean error of the results of their model when compared to the real data was between 6–12%. Another method of data-driven modelling is to use a convolution neural network and a gated recurrent unit. This was demonstrated in [178], where the MAPE of different machine learning models were compared against two sets of electricity-demand data. The resultant MAPE from this work was between 24–33%. For further comparison, the results shown in [179] give a value of 40.38% for the MAPE between historical and predicted electricity-demand profiles and in [117] the mean percentage error was between 9%–11% in their best-case scenario. These values are reasonably close to some of the results obtained from the scaling factor methods proposed in this chapter.

It is important to stress that the accuracy of data depends on the purpose that the representative profiles are used for. It is also equally important to stress that knowing the quality of the historical datasets will impact the accuracy of the representative profile generated by the scaling factor methods. In the case of this work, the accuracy of the representative profile in terms of actual values of peaks and minimums does not have to be pinpoint accurate. It is important for this study that the pattern of consumption is a standardised daily profile across different seasons because this allows for an idealised image of how the system works.

3.6 Chapter Summary

Methods for obtaining representative renewable energy generation profiles and electricity generation profiles were studied and discussed. A methodology to develop representative electricity profiles was investigated further with the aid of real historical data. The results show that the method can be applied to produce representative electricity demand profiles albeit with limitations. Seeing how aggregating the historical real data and using the daily scaling factor method (2nd method), a relatively accurate representative profile can be obtained. However, the accuracy of the estimates derived from the scaling factors are very dependent on the quality of the historical data. The purpose of obtaining a more generalised representative electricity demand profile aided the contributions presented in this thesis.

Firstly, aggregating historical real data and using the scaling factor method can smoothen the effect of outlier data in the dataset. Also, a more generalised representative electricity demand profile when optimised gives a more generalised view of the system behaviour. This is essential when attempting to analyse a system's general behaviour, as it provides the user a better overall understanding of how the system works.

The scaling factor method can also be used to fill in missing entries in datasets for a specific day or hour as it allows the generation of a close representation of the averaged demand profile based on the seasonal scaling factor. Furthermore, the scaling factor method assists in data selection as it generates a profile which is based on an aggregated profile. This allows for easier seasonal data selection as it shows what a typical demand profile for that season should look like.

The best way of using the scaling factors would be to use site specific scaling factors for which representative demand profiles are to be generated from. The results shown in Figures 3.3-3.6 indicate this to be the case. When scaling factors are used interchangeably between sites, the results are most likely reflective of that seen in Figures 3.7-3.9, where mean percentage errors exceed the 20% error tolerance limit defined for the study. Looking at the MAPE analysis, it can be said that for almost all scenarios, the scaling factor method is fit for purpose as it meets the MAPE measure of accuracy (≤20%).

The use of scaling factors interchangeably between 2 different sites is technically possible but will really depend on the quality of data provided and correcting the difference between minimum and maximum electricity demand between the 2 sites. Correcting the difference between the minimum and maximum electricity demand of the 2 sites is useful for generating more accurate scaling factors.

Using the scaling factor method, a more detailed look at what a daily or weekly profile of an electricity demand for a specific site can be obtained. Having a representative profile on a daily, weekly, and seasonal basis enables the selection of appropriate data sets to be used for optimisation problems.

Chapter 4: Hydrogen Powered Refuse Collection Vehicles: Total Cost of Ownership Analysis and Sensitivity Analysis

4.1 Introduction

A significant step at reducing harmful vehicle emissions was introduced in 2019 when the Mayor of London initiated the Ultra-Low Emissions Zone (ULEZ). The introduction of the ULEZ in London aimed to improve upon the previous policy of Toxicity Charge (T-Charge), which acts as a deterrent for operating older, more emission intensive vehicles and encourages non-polluting or lower polluting means of transport (e.g., walking, cycling and public transport). However, the T-Charge was only enforced during weekdays, whereas ULEZ is meant to be implemented every day of the year.

In anticipation of the possibility of similar measures being introduced in other cities UK-wide, local councils will need to adjust their current vehicle fleets to comply with the emission requirements of such policies. Local councils are responsible for collecting and disposing of all domestic waste (recyclable, non-recyclable and compostable), as well as a portion of commercial waste. Due to the proximity principle, waste is to be disposed of near the point of generation. This requires a means of mass transporting this waste via heavy-duty RCVs. Most of the RCVs that are currently in operation run on diesel. This releases a significant amount of CO_2, NO_x and particulate matter emissions into the air. Given the proximity of operation (i.e., being close to residential areas) and the frequent stop-start cycles due to idling and revving to run equipment for emptying bins and waste compacting, local residents are inevitably exposed to significant amounts of pollution on their doorstep. Given the layout of streets in some residential areas or commercial areas with tall buildings flanking the street, air movement may be restricted and this increases the concentration of harmful emissions in the ambient air.

In the study shown in [64] which was based on council vehicle fleet data in the Tees Valley area, 80% of harmful emissions were caused by only 47% of the vehicles present in the RCV fleet. The largest contributor of harmful emissions in this fleet were the 26-tonne RCVs. Consequently, a quick fix to this issue would be to substitute these vehicles with ones that run on non-polluting fuels. However, these vehicles, specifically vehicles for refuse collection operations, are not widely available and are considerably more expensive than diesel powered options.

In 2017, the UK government released its clean growth strategy, which states by the year 2022 vehicle fleets should comprise of at least 25% ULEVs [65], and will eventually ban the sale of petrol and diesel vehicles in 2030 [180]. Therefore, the techno-economic feasibility of using non-polluting fuelled vehicles for refuse collection operations needs to be better understood.

The study that is presented in this chapter investigates the techno-economic feasibility of operating 26-tonne fuel cell electric RCVs in a local council's refuse collection fleet. The vehicle fleet studied is the refuse collection fleet of Leeds City council in where fuel consumption and mileage data of their 26-tonne refuse collection vehicles is used to develop an estimated equivalent hydrogen fuel demand. The estimated hydrogen demand of the fleet is then used to compare the lifetime TCO and TCO/Mile of the diesel-fuelled RCVs present in the fleet against an equivalently sized fuel cell electric (hydrogen-powered) RCV to assess the cost competitiveness and techno-economic feasibility of operating a hydrogen powered RCV under present and future (2030) technical and economic conditions.

4.2 Methods of Developing Hydrogen Fuel Consumption Profiles and Techno-Economic Assessment

The lack of available operational data for FCEVs relating to running costs requires this data to be mathematically generated. This can be achieved by using available operational data from vehicles running on conventional fuels, which are given complete data on fuel consumption for a unit of distance, and distance travelled. The data from these vehicles is then used to calculate the hydrogen fuel consumption for a unit mile and the hydrogen cost for the given distance travelled. These hydrogen fuel consumption profiles are meant to reflect a direct equivalent for the conventional fuelled vehicles consumption profiles on which they are based. A simple method is proposed that considers the tank-to-wheel (TtW) efficiency of the diesel vehicle and then uses this generated value of useful energy as the energy provided to move the vehicle for one unit of distance. This allows for a direct conversion of the fuel consumption per unit distance from a diesel-powered vehicle to a hydrogen-powered vehicle.

Figure 4.1: A diesel vehicle's components and energy flows

Figure 4.1 is a basic block diagram of a diesel-powered vehicle, where diesel is injected from the diesel fuel tank into the diesel engine. The fuel-air mixture in the diesel engine is compressed by pistons and ignited. The expansion of the gases for combustion then pushes the pistons. Via a network of gears in the transmission, the crankshaft then enables rotation of the vehicle's wheels. In the combustion process, a lot of energy initially represented by $E_{S_{pu}}^{Diesel}$ is lost as heat. Thus, the measure of energy that effectively moves the vehicle is represented as E_{Useful}.

Given need to reduce CO_2 emissions that are generated by the combustion of fossil fuels, hydrogen can be used as an alternative fuel for motor vehicles. A simple block diagram of a fuel cell electric vehicle is shown in Figure 4.2.

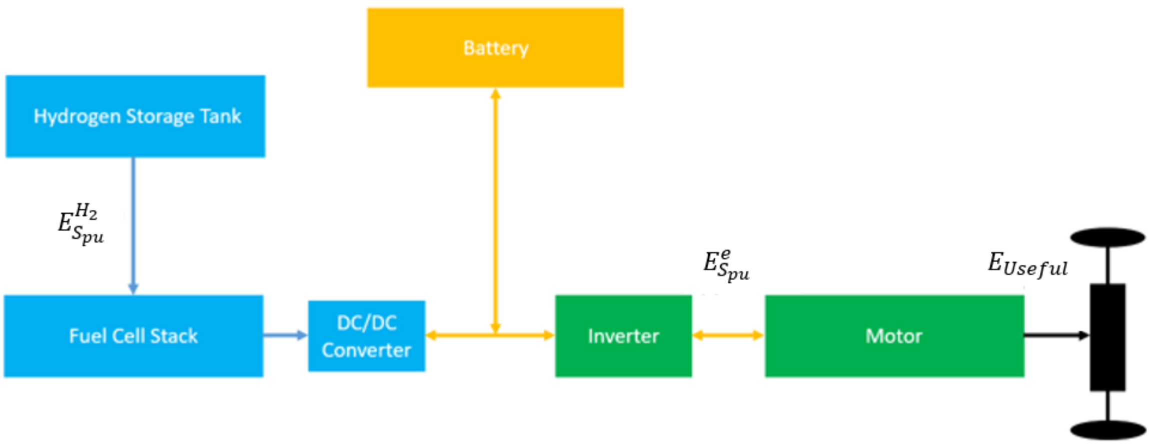

Figure 4.2: A fuel cell electric vehicle's components and energy flows

Fuel cell electric vehicles use hydrogen as a primary fuel, where it is converted into electricity via a fuel cell stack. This gives off no harmful tailpipe emissions. The resultant electricity that is generated from this conversion is then stored in a battery, where the electricity will be dispatched to a stator in the motor causing the rotor to turn when required. This will provide the mechanical energy to move the crankshaft of the vehicle to rotate the wheels. This process suffers energy losses because the fuel cell stack has a hydrogen to electricity efficiency rate. The resultant E_{Useful} is the energy required to move the crankshaft of the vehicle upon considering energy losses from converting $E_{S_{pu}}^{H_2}$ into $E_{S_{pu}}^{e}$.

At present, large 26-tonne RCVs run on diesel. Thus, it would be of interest to assess the techno-economic feasibility of operating a non-polluting RCV, such as a hydrogen fuelled RCV. The calculations for generating a fuel cell electric vehicle equivalent of a diesel vehicle are described in the following equations:

The energy consumption per mile of a diesel vehicle is first calculated by Equation (4.1).

$$E_{S_{pu}}^{Diesel} = \frac{\varepsilon_{V_{pu}}^{Diesel}}{MPG} \tag{4.1}$$

Where:

- $\varepsilon_{V_{pu}}^{Diesel}$: energy in one gallon of diesel (≈43.69kWh)
- MPG : Miles per gallon (MPG) of diesel vehicle

The value of $E_{S_{pu}}^{Diesel}$ is then used to figure out the energy required to move the vehicle for 1 mile. This is calculated in Equation (4.2).

$$E_{Useful} = E_{S_{pu}}^{Diesel} \times \eta_{Diesel} \tag{4.2}$$

Where:

- η_{Diesel} : Tank to wheel efficiency of diesel engine

It is assumed that the useful energy (E_{Useful}) is equivalent to the required electrical energy from the electric powertrain of a FCEV in Equation (4.3). The electrical energy required at the input to the electric power train is calculated as:

$$E_{S_{pu}}^{e} = \frac{E_{Useful}}{\eta^{e}} \tag{4.3}$$

Where:

- η^{e} : Electric drivetrain efficiency

The required hydrogen energy per unit distance is then calculated by dividing $E^{e}_{S_{pu}}$ by the efficiency of the fuel cell, as shown in Equation (4.4).

$$E^{H_2}_{S_{pu}} = \frac{E^{e}_{S_{pu}}}{\eta^{FC}} \tag{4.4}$$

Where:

- η^{FC}: Efficiency of fuel cell

The cost of hydrogen per unit energy (kWh) is calculated by dividing the cost of 1 kg of hydrogen by the gravimetric energy density of hydrogen. This is shown in Equation (4.5).

$$C^{H_2}_{E_{pu}} = \frac{C^{H_2}_{m_{pu}}}{\varepsilon^{H_2}_{m_{pu}}} \tag{4.5}$$

Where:

- $\varepsilon^{H_2}_{m_{pu}}$: Gravimetric energy density of hydrogen (33.33kWh/kg)
- $C^{H_2}_{E_{pu}}$: Price per unit mass (kg) of hydrogen

Now that the cost per unit energy (kWh) of hydrogen has been calculated, the cost per mile of a hydrogen powered vehicle is as follows:

$$C^{H_2}_{S_{pu}} = E^{H_2}_{S_{pu}} \times C^{H_2}_{E_{pu}} \tag{4.6}$$

The hydrogen demand of a vehicle after a certain distance (kg) may also be quantified. This is done by the multiplying the hydrogen energy per unit distance with the distance travelled divided by the gravimetric energy density of hydrogen.

$$E^{H_2}_{D} = \frac{E^{H_2}_{S_{pu}} \times S}{\varepsilon_{m_{H_2}}} \tag{4.7}$$

Where:

- S: Distance travelled

The cost per unit energy (kWh) of diesel is calculated by dividing the cost per gallon of diesel with the volumetric energy density of 1 gallon of diesel.

$$C_{E_{pu}}^{Diesel} = \frac{C_{V_{pu}}^{Diesel}}{\varepsilon_{V_{pu}}^{Diesel}} \tag{4.8}$$

Where:

- $C_{V_{pu}}^{Diesel}$: Price of diesel/gallon

Thus, like in the calculation of the cost per mile of the hydrogen RCV, the cost per mile of the diesel RCV is obtained by multiplying the energy per mile value with the cost per unit energy (kWh) of the diesel fuel.

$$C_{S_{pu}}^{Diesel} = E_{S_{pu}}^{Diesel} \times C_{E_{pu}}^{Diesel} \tag{4.9}$$

To calculate the diesel demand (gallon) of a vehicle at a certain distance, the diesel fuel required per unit distance is multiplied by the distance travelled.

$$E_{D}^{Diesel} = \frac{S}{MPG} \tag{4.10}$$

Equations (4.6) and (4.9) represent the fuel cost per unit distance, which is one of the several operational costs of a vehicle. However, further costs must be considered to comprehensively study the cost competitiveness of hydrogen RCVs against diesel RCVs. Therefore, capital costs and other related operational costs are taken into consideration. This leads to a TCO calculation of each individual vehicle. The general formula for the TCO calculation is given as follows [50]:

$$TCO = (MSRP - RV) + \sum_{x=1}^{3} \sum_{n=0}^{9} \left(OC_{x_n} \times \frac{1}{(1+i)^n} \right) \tag{4.11}$$

Where:

- $MSRP$: Manufacturer's suggested retail price.
- RV: Residual value (product of residual percentage "y" for year "n").
- OC_1: Vehicle tax (according to emissions per UK government).
- OC_2:Fuel costs/mile ($C_{S_{pu}}^{Diesel}$& $C_{S_{pu}}^{H_2}$)

- OC_3: MSR (Maintenance, Service and Repairs)
- i: Discount rate to UK gilt yield (10 years)

The assumed values for $MSRP$, RV, OC_1, OC_3, and i are shown in Table 4.1.

Table 4.1: Assumed values (MSRP, OC_1, OC_3)

MSRP-£	Vehicle Tax (OC_1)-£	MSR (OC_3)-£
• 152,500 (Diesel)	• 615/annum (Diesel)	• 0.56/mile
• 288,616.51 (Hydrogen)	• 0/annum (Hydrogen)	• 0.39/mile

The MSRP of the hydrogen powered RCV considered the costs of the chassis, RCV body and split lifter in [54]. This was then followed by basing the fuel cell system, battery and auxiliary systems was based on the hydrogen powered RCV presented in [52] for which the costs for the fuel cell system, battery and auxiliary system were then quantified based on the component costs in [53]. Given government regulations on purchase subsidies for ULEVs, the MSRP of the hydrogen powered RCV includes a purchase subsidy of £25,000 [181]. For the MSRP of the diesel powered RCV, this was based on the diesel powered RCV in [54] The value for $\boldsymbol{OC_1}$ was based on the prescribed vehicle tax rates set out by the UK government in [182]. The value for $\boldsymbol{OC_3}$ (MSR) of the diesel RCV was derived from [54]. The hydrogen RCV's MSRP value was pegged to 70% of the diesel RCV's MSR value. This is consistent with the less moving parts theory, in which a vehicle with less moving parts in its powertrain would require less maintenance, as stated in [127]. The value i represents the discount rate, which enables the calculation of the present value of expected future cashflows for a specified duration of time [183]. Two values of discount rate were used in this study: first, the risk-free rate (i=1.4%) is assumed to be the 10-year gilt yield of UK government bonds; and second, all scenarios were run again considering a high-risk discount rate set at 10%.

The residual values of the vehicle are assumed to be a percentage of the monetary value the vehicle possesses after a certain duration of time. The residual values of hydrogen vehicles only differ by around 0.8% per year when compared to the residual values of diesel vehicles

[184]. Thus, due to the very low difference the residual values in this study were assumed to be the same between the diesel RCVs and the hydrogen RCVs because the difference in the residual value was not detrimental to the overall TCO of the individual vehicles. The TCO analysis considers a lifetime cycle of 10 years for each vehicle and the values for these are based on residual values mentioned in [50] and are shown in Table 4.2.

Table 4.2: Residual values of vehicle

Year	0	1	2	3	4	5	6	7	8	9
RV	100%	66%	54%	49%	38%	34%	31%	27%	25%	22%

RV (for year n: 0-9):

The TCO analysis was conducted to compare the cost competitiveness and techno-economic feasibility of operating a hydrogen powered RCV and a diesel RCV. In terms of being able to see actual benefits of operating a hydrogen RCV, the TCO analysis is done with sensitivity to annual mileage. Thus, the comparison of the two fuel modes is done by looking at the TCO/Mile of each vehicle over a certain annual mileage.

4.3 Background of the Fleet Study

To assess the cost competitiveness and techno-economic feasibility of a hydrogen powered RCV to be operated in a local council's refuse collection fleet, the TCO study required the comparison of a hydrogen powered RCV operating under similar conditions (i.e., carried weight, distance and operational frequency) to that of a diesel powered RCV. Given the lack of operational data for large 26-tonne hydrogen powered RCVs, the fuel consumption patterns of the hydrogen powered RCV had to be modelled via the Equations (4.2– 4.6). This required data of an average 26-tonne diesel RCV to figure out an average value for E_{Useful}.

Real operational data for the average 26-tonne diesel RCV were provided by the Leeds City Council in [185], [186]. The Leeds City Council operates 76 vehicles for waste and refuse operations. Of these 76 vehicles, 57 are 26 tonne RCVs. Vehicle fleet data such as hourly fuel consumption per mile, distance travelled, mileage and registration period of the vehicles present in their refuse collection fleet is recorded. The average fuel consumption in miles/gallon (MPG) of the 26-tonne diesel RCV in the Leeds City Council fleet was used to obtain the value for average E_{Useful}, which was then used to model the fuel consumption of the hydrogen powered RCV and the eventual fuel cost per unit distance (OC_2). For the diesel powered RCV, the fuel consumption data is given from the Leeds City Council data. This was used to calculate the (OC_2) for the average diesel RCV via Equations (4.1–4.2) and (4.8–4.9).

Given the values of MSRP, OC_1 and OC_3 for both the hydrogen powered RCV and the diesel powered RCV, a TCO analysis between the two types of RCVs was conducted to observe if the TCO/Mile of the average hydrogen powered RCV can reach parity with the average diesel RCV after a certain annual mileage.

4.4 Definition the of Scenarios

The scenarios that were designed for this study took into consideration the fuel cell efficiency values and fuel prices for both present and future cases. Fuel cell efficiency values currently available from manufacturers to operators and the current fuel prices served as a basis for assessing the cost competitiveness and techno-economic feasibility of operating hydrogen RCV units at present.

The value parameters in the future scenarios targeted fuel cell efficiency achievable by the year 2030 [187]. It was important to consider this value because it is a significantly higher efficiency value than the maximum attainable manufacturer efficiency value for 2022. In terms of fuel cost of hydrogen, it is also expected that the price of hydrogen will drop to approximately the value stated in Table 4.4 [59].

The operational costs and TCO/Mile of the vehicles of these two scenarios were compared to determine if it would be economically competitive or feasible to operate a hydrogen fuelled RCV fleet at a specific annual mileage, fuel cell efficiency and fuel prices. These scenarios are described in Table 4.3.

Table 4.3: Description of the scenarios studied

Scenario	Description
Baseline scenario with current average fuel cell efficiency and average hydrogen price (Scenario 1)	• TCO analysis was made based on the assumption of an average value for fuel cell efficiency to present the most likely TCO values for a set of hydrogen RCVs that can be introduced as replacements of the current diesel RCVs in the Leeds City Council RCV fleet. • Hydrogen price used in this scenario is the current average hydrogen price/kg. • Diesel price is set on average current retail price (year 2022).
Current maximum fuel cell efficiency with high hydrogen price scenario (Scenario2)	• TCO analysis was made considering the possible maximum fuel cell efficiency as far as current manufacturer specifications allow for. • High hydrogen price was applied to assess the effectiveness of current maximum fuel cell efficiency in keeping the TCO/Mile of the fuel cell electric RCV cost competitive with the diesel RCV.
Future peak fuel cell efficiency and low hydrogen price scenario (Scenario 3)	• TCO analysis was made for future a future situation considering values of fuel cell efficiency, low hydrogen price and diesel price for 2030. • TCO/Mile analysis was conducted with these parameters to see if cost parity between fuel cell electric RCV and diesel RCV is achievable at a lower annual mileage than the current average annual mileage of the fleet.
Future peak fuel cell efficiency and high hydrogen price scenario (Scenario 4)	• TCO analysis was made to assess the effectiveness of high fuel cell efficiency in mitigating the effects of high hydrogen price

Table 4.4: Values of pre-set parameters for each scenario

Scenario	**Fuel Cell Efficiency (η^{FC})**	**Electric Powertrain Efficiency (η^{e})**	**Hydrogen Price/Kg ($C_{E_{pu}}^{H_2}$)**	**Diesel Price/Gallon ($C_{Diesel}^{V_{pu}}$)**
Baseline **(Scenario 1)**	51%	75%	£7.04	£8.44
Current Max Efficiency and High Hydrogen Price **(Scenario 2)**	57%	75%	£10.30	£8.44
Future Peak Fuel Cell Efficiency and Low Hydrogen Price **(Scenario 3)**	68%	75%	£1.26	£10.73
Future Peak Fuel Cell Efficiency and High Hydrogen Price **(Scenario 4)**	68%	75%	£10.30	£10.73

The value for fuel cell efficiency in the baseline scenario reflected that of a commonly attainable value given the current state of technology at present (2022). This value was based on the average fuel cell efficiency on the Arcola-Ballard 26-tonne fuel cell electric RCV [52], which uses a 70kW FCmove™-HD heavy-duty PEM fuel cell power module that is manufactured by Ballard Power Systems [188]. In the current maximum fuel cell efficiency with high hydrogen price scenario, the fuel cell efficiency value is the maximum attainable efficiency of the FCmove™-HD heavy-duty fuel cell power module. The fuel cell values that are used in the future scenarios accounting for the year 2030 are based on targeted peak PEM fuel cell efficiencies mentioned in [188]. This efficiency value was in line with the projection of increasing fuel cell efficiency in the future because developments in materials and technology are expected.

The electric powertrain efficiency was maintained the same across all the scenarios studied and was obtained by observing average TtW efficiencies of electric powertrains in [189], [190]. The diesel engine efficiency given in [190] was also maintained to be the same for all scenarios in this study, while diesel engine technology is considered an established technology.

The prices of hydrogen/kg (£7.04 & £10.30) were based on real prices provided by the Hydrogen Valley Platform [57]. The Hydrogen Valley Platform is a collaborative project that was initiated by the Clean Hydrogen Partnership and co-funded by the European Union. Values of hydrogen prices used were location specific and statistically reported on frequency of occurrence. The hydrogen price of £7.04 was the most frequently occurring across all monitored hydrogen stations, hence its selection for the study. The value of £10.30 was selected from the data provided from the Hydrogen Valley Platform, this value reflects the average high value as stated in [57]. The expected hydrogen price in the year 2030 is predicted to be around £1.26/kg [57], [59]. Nonetheless, the possibility of hydrogen prices remaining high over time is still a possibility. Hence, the inclusion of the high hydrogen price in future Scenario 2 (£10.30). The price of diesel is expected to increase by around 50 pence/litre by 2030 [191], hence why a diesel price of £10.73/gallon is used in the future Scenarios 1 and 2.

4.5 Results and Discussion of Scenario Studies

4.5.1 Baseline Scenario (Scenario 1)

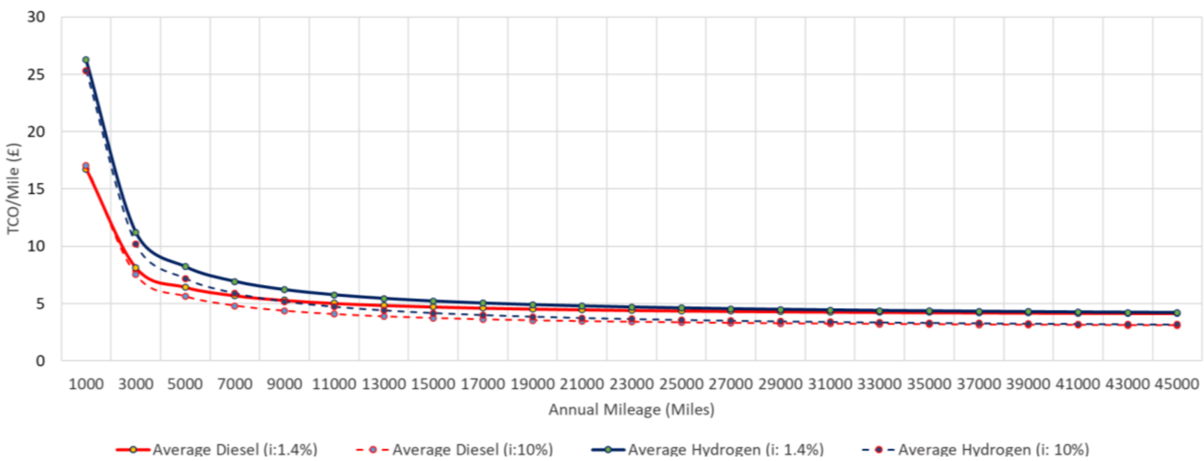

Figure 4.3: Baseline scenario (Scenario 1)

The results in Figure 4.3 show the TCO/Mile for the baseline scenario, where it reflects characteristics of the average hydrogen RCV and average hydrogen price against that of the average diesel RCV and diesel price (current average fuel cell efficiency and current fuel prices).

When comparing hydrogen RCVs and diesel RCVs separately, it is seen that the TCO/Mile of both hydrogen and diesel RCVs are cheaper with greater annual mileage and the TCO/Mile also decreases when discount rate is raised from 1.4% to 10%. When comparing hydrogen RCVs and diesel RCVs, it can be seen that despite a higher initial TCO/Mile for the average hydrogen RCV, its TCO/Mile reaches parity with that of the average diesel RCV at around 27,000 miles/annum.

Given the average annual distance of 9,000 miles for the diesel RCV in Leeds City Council, the TCO/Mile ratio between average diesel RCV and average hydrogen RCV at 9,000 miles for a discount rate of 1.4% is 1.17 and 1.19 for a discount rate of 10%. The monetary difference between the average hydrogen RCV and the average diesel RCV at 9,000 miles is 15% and 16% for a discount rate of 1.4% and 10%, respectively. This indicates that the TCO/Mile of the average hydrogen RCV is already becoming competitive with that of the average diesel RCV. Given the trend of TCO/Mile becoming smaller with greater annual mileage, it is expected that the hydrogen RCVs can eventually become cheaper to own and run than a diesel RCV.

4.5.2 Current Maximum Fuel Cell Efficiency with High Hydrogen Price (Scenario 2)

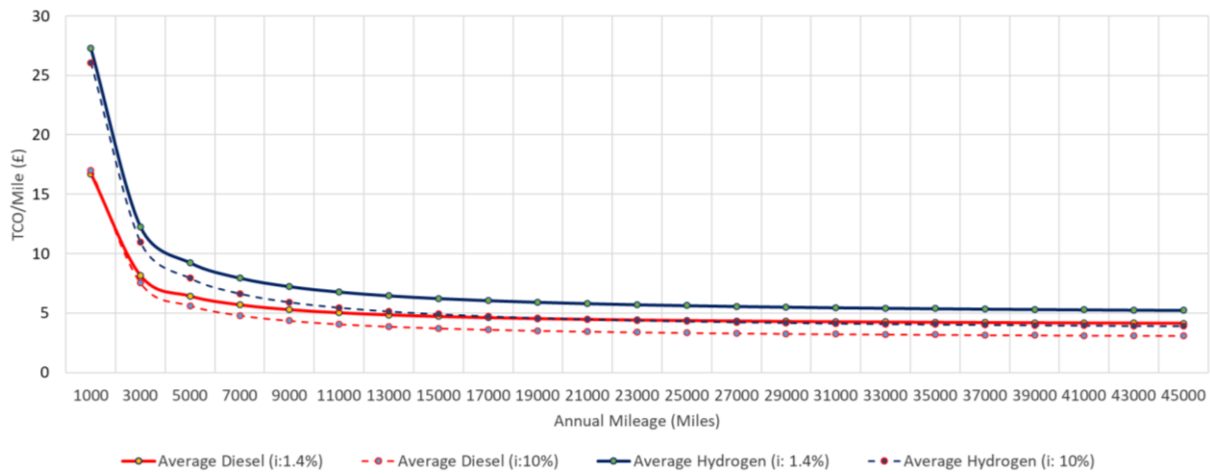

Figure 4.4: Current maximum fuel cell efficiency with high hydrogen price (Scenario 2)

Figure 4.4 presents a comparison of an average hydrogen RCV where maximum current fuel cell efficiency (per manufacturer's standard) is achievable and an average diesel vehicle. The hydrogen price for this scenario is given a high price. This aims to observe the effect of high hydrogen price on the TCO/Mile of a hydrogen RCV and assess its techno-economic performance against the average diesel RCV.

In this scenario, parity between hydrogen TCO/Mile and diesel TCO/Mile is not possible, which is due to the high price of hydrogen (£10.30/kg). The maximum manufacturer's fuel cell efficiency of 57% applied in this scenario. However, judging from the results above, the increase of fuel cell to this nominal value is still not enough to offset the increase in TCO/Mile attributed to the high hydrogen price. At 9,000 miles per annum, the ratio of TCO/Mile of the average hydrogen RCV and average diesel RCV in this scenario is 1.47 and 1.44 for discount rates of 1.4% and 10%, respectively. TCO/Mile of hydrogen for a discount rate of 1.4% is 31% higher than diesel and for a discount rate of 10% it is 31% higher.

Figure 4.4 clearly indicates that the TCO/Mile for the average hydrogen RCV decreases with an increase in annual mileage. However, it does not manage to reach parity with the TCO/Mile of diesel, even at 45,0000 miles per annum. However, this does not conclude that it would be impossible for the TCO/Mile of the hydrogen RCV to reach parity with the TCO/Mile of the diesel RCV because the annual mileage studied in this chapter does not extend further than the 45,000-mile mark.

4.5.3 Future Peak Fuel Cell Efficiency with Low Hydrogen Price (Scenario 3)

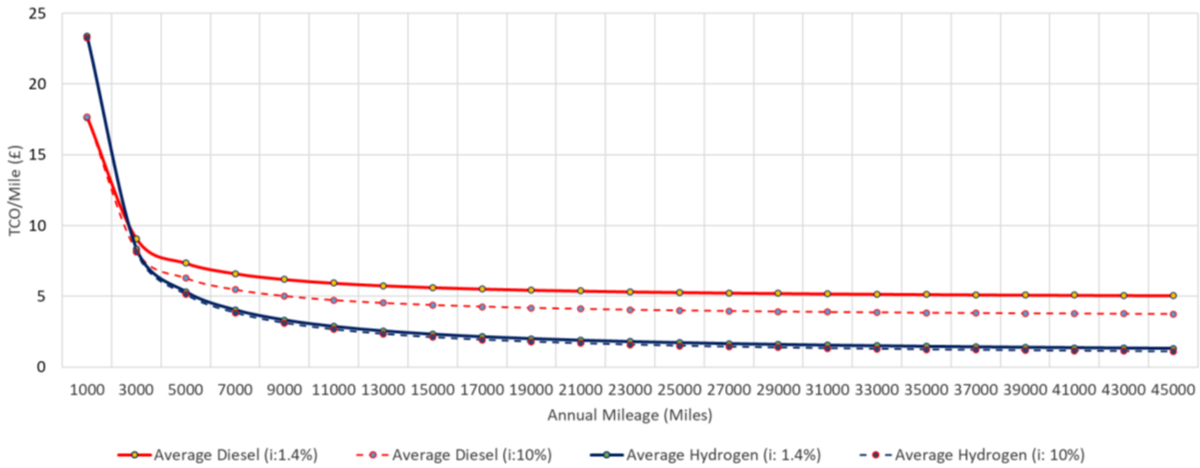

Figure 4.5: Future peak fuel cell efficiency with low hydrogen price (Scenario 3)

This scenario observes hydrogen RCVs and diesel RCVs with conditions reflecting the year 2030 where fuel cell efficiency is around 68%, hydrogen price/kg is £1.26 and diesel price is £10.73/gallon. It can be seen in Figure 4.5 that the TCO/Mile of the average hydrogen RCV manages to reach parity with the average diesel RCV at 3,000 miles per annum.

The TCO/Mile of the average hydrogen RCV becomes lower than the average diesel TCO/Mile as annual mileage increases. This trend is attributed to the low price of hydrogen, high fuel cell efficiency and the higher price of diesel. Furthermore, the TCO/Mile between the average hydrogen vehicles given a discount rate of 1.4% and 10% does not increase significantly with greater annual mileage. At an annual mileage of 9,000, the TCO/Mile ratio of the average hydrogen RCV against the average diesel RCV is 0.54 and 0.62 for a discount rate of 1.4% and 10%, respectively. The TCO/Mile of the average hydrogen RCV is 86% lower than that of the average diesel RCV at a discount rate of 1.4% and 61% lower at a discount rate of 10%.

Given the very low price of hydrogen and high fuel cell efficiency expected in the year 2030, the results presented in this section show very promising potential for the adoption of hydrogen powered RCVs for municipal refuse collection fleets because TCO/Mile parity for the hydrogen RCV with respect to the TCO/Mile of the diesel RCV is reached at a relatively low annual mileage.

4.5.4 Future Peak Fuel Cell Efficiency with High Hydrogen Price (Scenario 4)

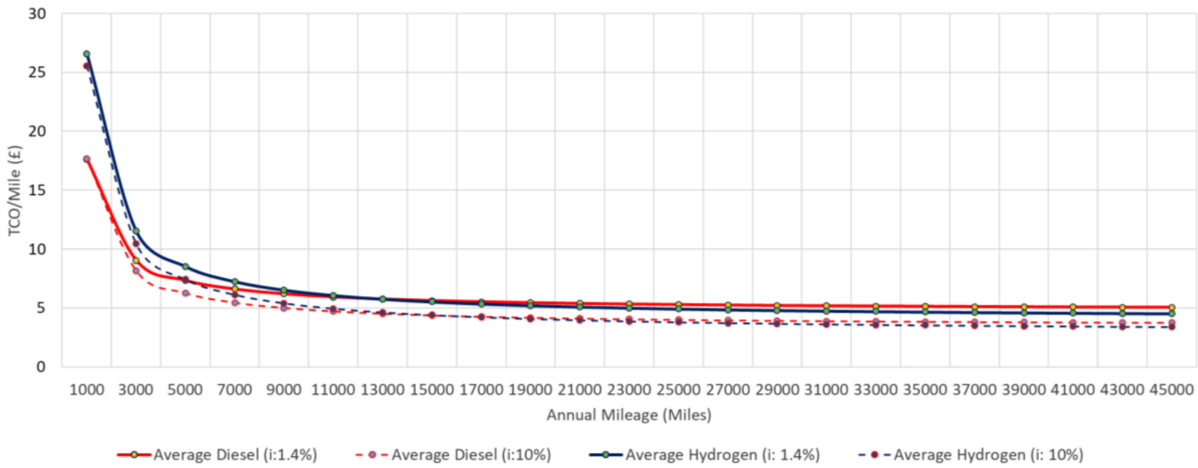

Figure 4.6: Future peak fuel cell efficiency with high hydrogen price (Scenario 4)

The case for 2030 but with high hydrogen price is considered in Figure 4.6. In terms of average hydrogen RCV TCO/Mile, parity with average diesel TCO/Mile is reached at around 11,000 annual miles. The high hydrogen price also affects the TCO/Mile of the average hydrogen RCV with respect to an increase in discount rate. It is seen here that the TCO/Mile of the hydrogen RCV with 10% discount rate becomes lower with higher annual mileage.

Despite the effect of a high hydrogen price on TCO/Mile of the average hydrogen RCV, the TCO/Mile of the average hydrogen RCV can already be considered to be very competitive with the average diesel RCV at 9,000 miles per annum. The high fuel cell efficiency offsets the negative effects of high hydrogen price on the TCO/Mile because the TCO/Mile of the average hydrogen RCV eventually becomes lower than that of the average diesel vehicle beyond the 11,000 annual mileage mark.

The TCO/Mile ratio of between the average hydrogen RCV and average diesel RCV at a discount rate of 1.4% and an annual mileage of 9,000 is 1.05. Similarly, at the same annual mileage at a discount rate of 10%, the TCO/Mile ratio between the average hydrogen RCV and average diesel RCV is 1.08. The TCO/Mile of hydrogen at 9,000 miles per annum for a discount rate of 1.4% is 5% higher than that of the average diesel RCV. At a discount rate of 10% for the same annual mileage, the TCO/Mile of hydrogen is 7% higher than the average diesel RCV.

4.5.5 Summary and Discussion of the Findings from the Scenario Studies

The purpose of observing the TCO/Mile of the hydrogen and diesel powered RCVs at an average annual mileage of 9,000 miles was to give a realistic comparison of TCO/Mile based on the actual average annual mileage of an operational RCV (Leeds City Council RCV fleet). Looking at the results obtained from the scenario studies in Sections 4.5.1–4.5.4, it can be seen that the TCO/Mile of the average hydrogen powered RCV did not manage to reach parity with the TCO/Mile of the average diesel powered RCV at 9,000 miles, except for that in Scenario 3. The TCO/Mile of the hydrogen powered RCV only managed to reach parity with the TCO/Mile of the diesel powered RCV past the 9,000 miles per year mark in Scenarios 1 and 4. However, when looking more closely at the baseline scenario (Scenario 1), the TCO/Mile of the hydrogen powered RCV is only 15%–16% higher than the TCO/Mile of the diesel powered RCV. This indicates that operating a hydrogen powered RCV with an average current fuel cell efficiency under average current hydrogen prices is already cost competitive in comparison to a diesel powered RCV. Furthermore, in the case of Scenario 4 where the expected peak fuel cell efficiency projected for the year 2030 is met and hydrogen price is high, the TCO/Mile of the hydrogen powered RCV is only 5%–7% higher than that of the diesel powered RCV. A study of the TCO/Mile of other ULEVs, such as BEVs, compared to that of diesel vehicles of a similar class was presented in [192]. It was found that the TCO/Mile of BEVs were on average 12%-16% higher than diesel vehicles. Thus, it can be argued that hydrogen powered RCVs are cost competitive with respect to other ULEVs.

Hydrogen fuel demand at 9,000 annual miles for a 10-year period of ownership between the different values of fuel cell efficiency was quantified by Equation (4.7) and the results are shown in Table 4.5.

Table 4.5: Hydrogen demands at 9,000 annual miles and 10-year ownership (lifetime)

Fuel Cell Efficiency (η^{FC})	Hydrogen Demand ($E_D^{H_2}$)
51%	45,329.38 kg
57%	40,557.88 kg
68%	33,99.704 kg

The total fuel demand for a diesel powered RCV (E_D^{Diesel}) of the same annual mileage and ownership period is found to be 31,273.6 gallons. The CO_2 emitted by burning 1 gallon of diesel is around 11.9kg/gallon [193]. Thus, with respect to the scenarios studied, the benefits provided via the use of a hydrogen powered RCV in terms of decarbonisation for a lifetime ownership period of 10 years is a reduction of around 372 tonnes of CO_2 emissions.

4.6 Sensitivity Analysis

4.6.1 Sensitivity of Discount Rates and Ownership Periods Towards TCO

The sensitivity of ownership period and discount rates on the TCO of both average hydrogen RCV and average diesel RCV was studied. Discount rates of 1.4%, 3%, 5%, 7% and 10%, and ownership periods of 3, 4, 5, 7 and 10 years were used. In this sensitivity analysis, the parameters for fuel cell efficiency and fuel prices were set to the baseline to avoid biasing the results. The results of the sensitivity analysis are shown in Figure 4.7.

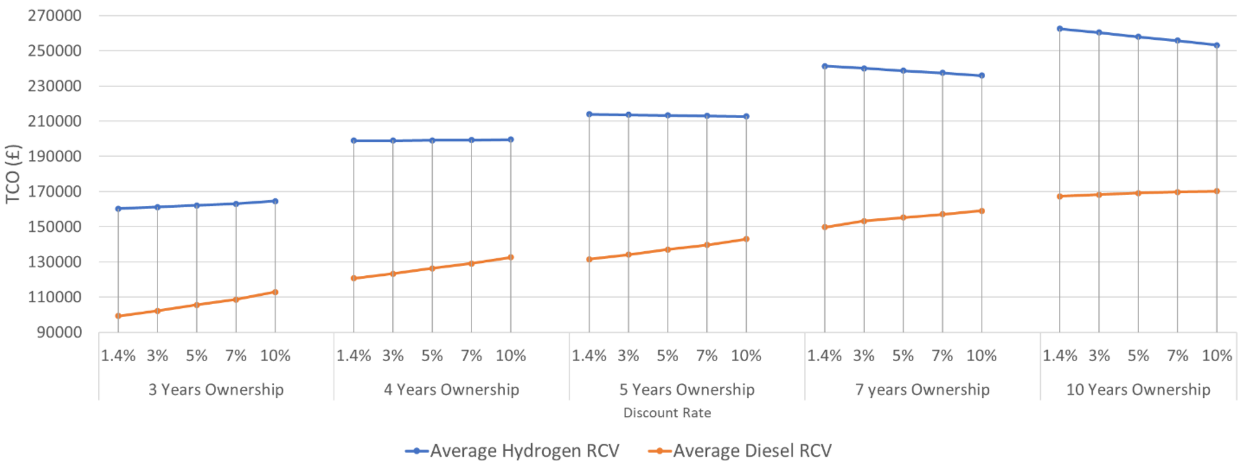

Figure 4.7: Overall TCO subject to increments in discount rates and ownership periods

It can be seen in Figure 4.7 that the overall TCO of both average hydrogen RCV and average diesel RCV increases with respect to increases in discount rate for short ownership periods of 3 to 4 years. This trend of increase in the TCO is due to the increase in discount rate reducing the resale value of the RCVs. Exclusively in the case of the average hydrogen RCV, from an ownership period of 5 year onwards, the TCO decreases with an increase in discount rate. This happens because the discount rate takes into account the effect of inflation, which weakens the value of the associated operating costs.

4.6.2 Sensitivity of Fuel Cell Efficiency on TCO/Mile

The effect of increasing fuel cell efficiency towards TCO/Mile was studied. This was done by keeping hydrogen and diesel price the same as that in the present baseline scenario (Scenario 1) and increasing the fuel cell efficiency to the 2030 fuel cell efficiency of 68% by increments of 1%. The results are shown in Figure 4.8.

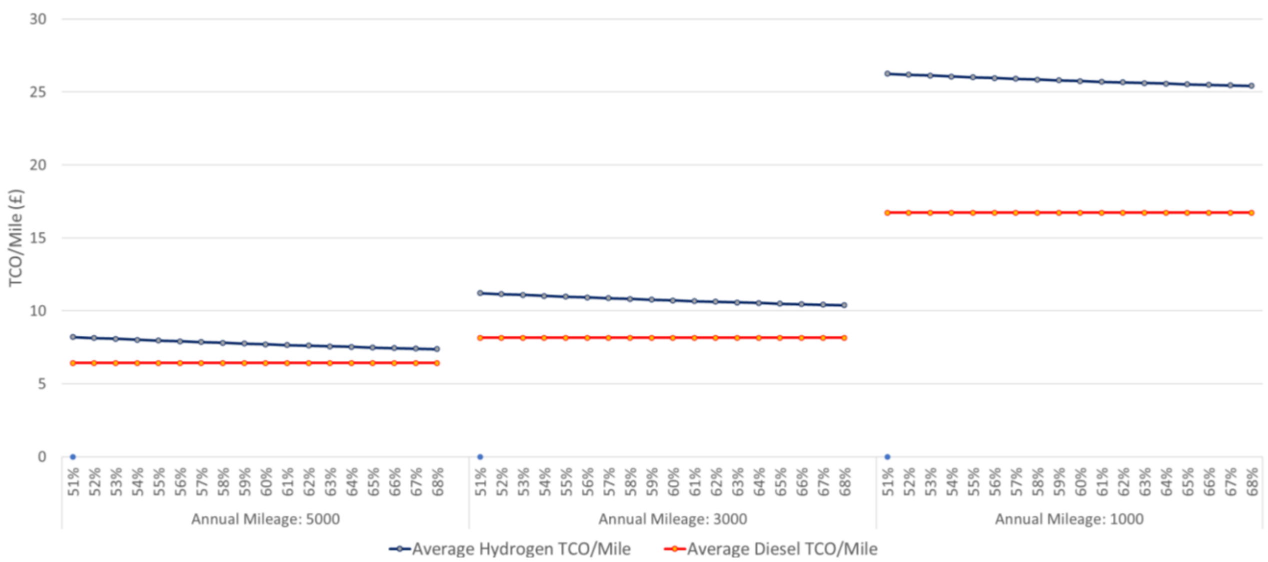

Figure 4.8: TCO/Mile of average hydrogen RCV with increasing efficiency vs TCO/Mile of average diesel RCV

It can be seen in Figure 4.8 that TCO/Mile of average hydrogen becomes closer to the average TCO/Mile of diesel as fuel cell efficiency increases and annual mileage increases. The rate at which TCO/Mile of the average hydrogen RCV decreases also becomes more apparent with an increase in both fuel cell efficiency and annual mileage. TCO/Mile for hydrogen RCV with an annual mileage of 5,000 is around 10% when fuel cell efficiency is increased from 51% to 68%. Similarly for the same increase in fuel cell efficiency, at 3,000 and 1,000 miles per annum, the TCO/Mile of the hydrogen RCV drops by 7.4% and 3.2%, respectively. The sensitivity of the TCO/Mile towards increments in fuel cell efficiency determined that with increasing annual mileage, the reduction in TCO/Mile for the hydrogen RCV increases even more. Table 4.6 summarises these findings.

Table 4.6: TCO/Mile reduction with increase in η_{FC}

Annual Mileage (Miles)	TCO/Mile Reduction at η^{FC} =57%	TCO/Mile Reduction at η^{FC} =68%
1000	1%	3%
3000	3%	8%
5000	4%	11%
7000	5%	14%
9000	6%	15%
11000	6%	17%
13000	7%	18%

It can be seen in Table 4.6 that the effect of increasing fuel cell efficiency does contribute to a reduction in overall TCO/Mile because a better fuel efficiency will reduce the fuel cost/mile. The current maximum η_{FC} does not reduce TCO/Mile as significantly as that of the expected 2030 efficiency of 68%. However, although the rate of reduction TCO/Mile increases with annual mileage, the rate at which the reduction increases slow down because fuel cost per mile (OC_2) cannot be 0.

4.6.3 Sensitivity of Fuel Price to TCO/Mile

The effect of increasing fuel price on TCO/Mile of both average hydrogen RCV and average diesel RCV was studied. This involved using the fuel cell efficiency values of the baseline scenario (Scenario 1), while the fuel price/kWh (C_{Epu}^{Fuel}) for both hydrogen and diesel was gradually increased to 10 pence by increments of 1 penny. The results of this sensitivity study are shown in Figure 4.9.

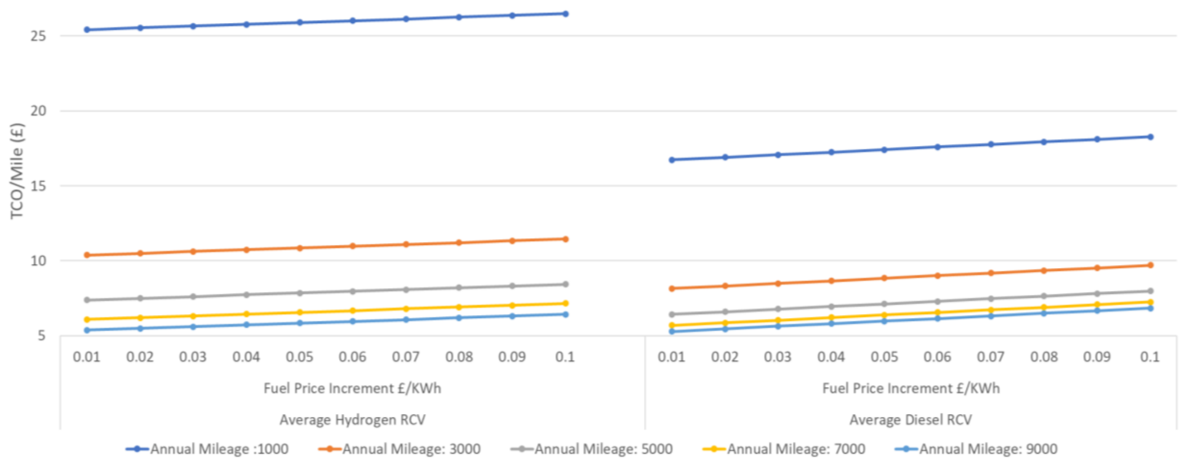

Figure 4.9: TCO/Mile with increasing fuel cost

As expected, by increasing the price/kWh of the fuel, both TCO/Mile of the hydrogen RCV and diesel RCV experience a gradual increase. The TCO/Mile of both RCVs falls upon reaching a higher annual mileage. The increase in TCO/Mile as fuel price/kWh rises to 10 pence is summarised in Table 4.7.

Table 4.7: Increase in TCO/Mile with increase in annual mileage

Hydrogen RCV		Diesel RCV	
Annual Mileage	**TCO/Mile Increase**	**Annual Mileage**	**TCO/Mile Increase**
1000	6%	1000	8%
3000	12%	3000	16%
5000	16%	5000	19%
7000	20%	7000	21%
9000	23%	9000	23%

It can be seen in Table 4.7 that for the same increments of fuel cost/kWh and annual mileage, hydrogen manages to suppress the rise of TCO/Mile when compared to diesel. This can be attributed to the better fuel consumption of the hydrogen RCV when compared to the diesel RCV. Furthermore, the TCO/Mile increase at lower annual mileages is lower for the hydrogen RCV when compared to the diesel RCV. This indicates that hydrogen RCVs can be cost competitive at lower annual mileages because its operational costs are overall lower than the diesel RCV.

4.6.4 Overall Analysis of Sensitivity Study and Proportions of Associated Costs of TCO

Sensitivity analyses were conducted to observe the individual parameters and their effect on the TCO of both a hydrogen RCV and a diesel RCV. The proportions of the associated costs related to the TCO include the capital expenditure, vehicle excise tax, fuel cost/mile and the MSR costs. An analysis of the percentages that contribute to the overall TCO of both a hydrogen RCV and diesel RCV was conducted with variations in fuel cell efficiency, fuel costs/kWh and increasing discount rates, which mirror what has already been done in the previous sections. The results of this analyses are shown in Figure 4.10 and Figure 4.11.

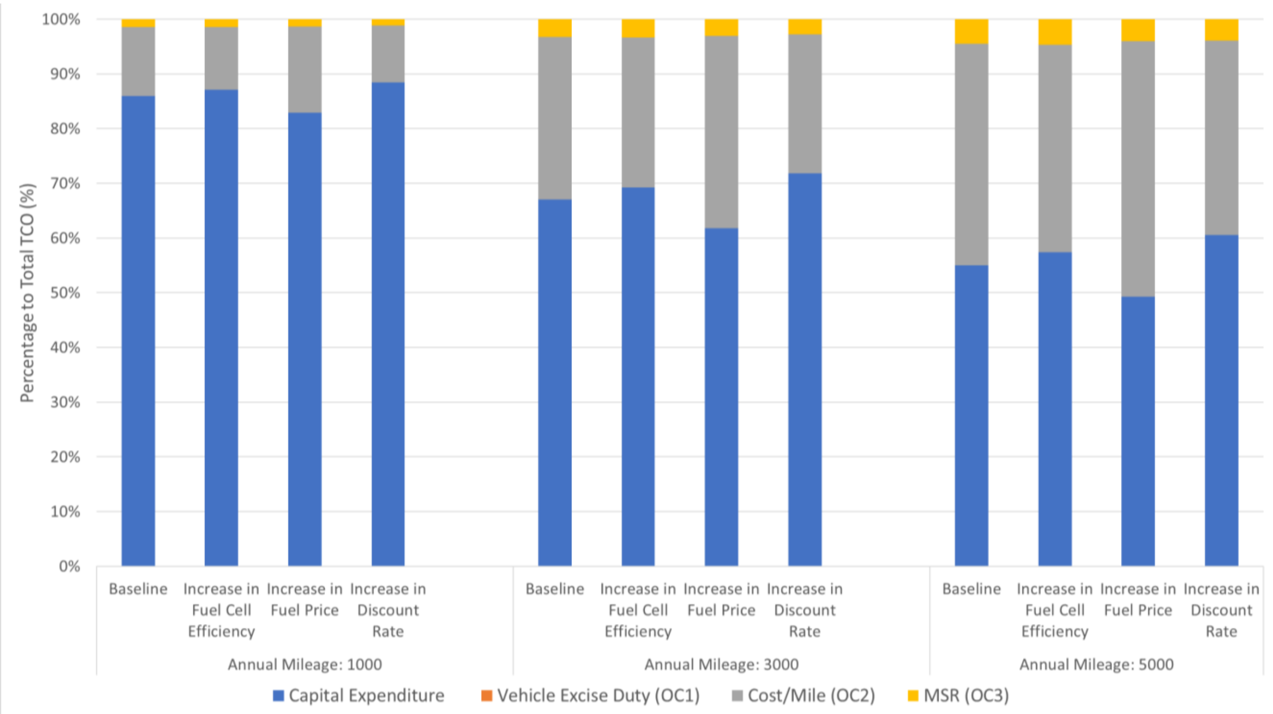

Figure 4.10: Proportions of associated costs contributing to overall TCO (H_2 RCV)

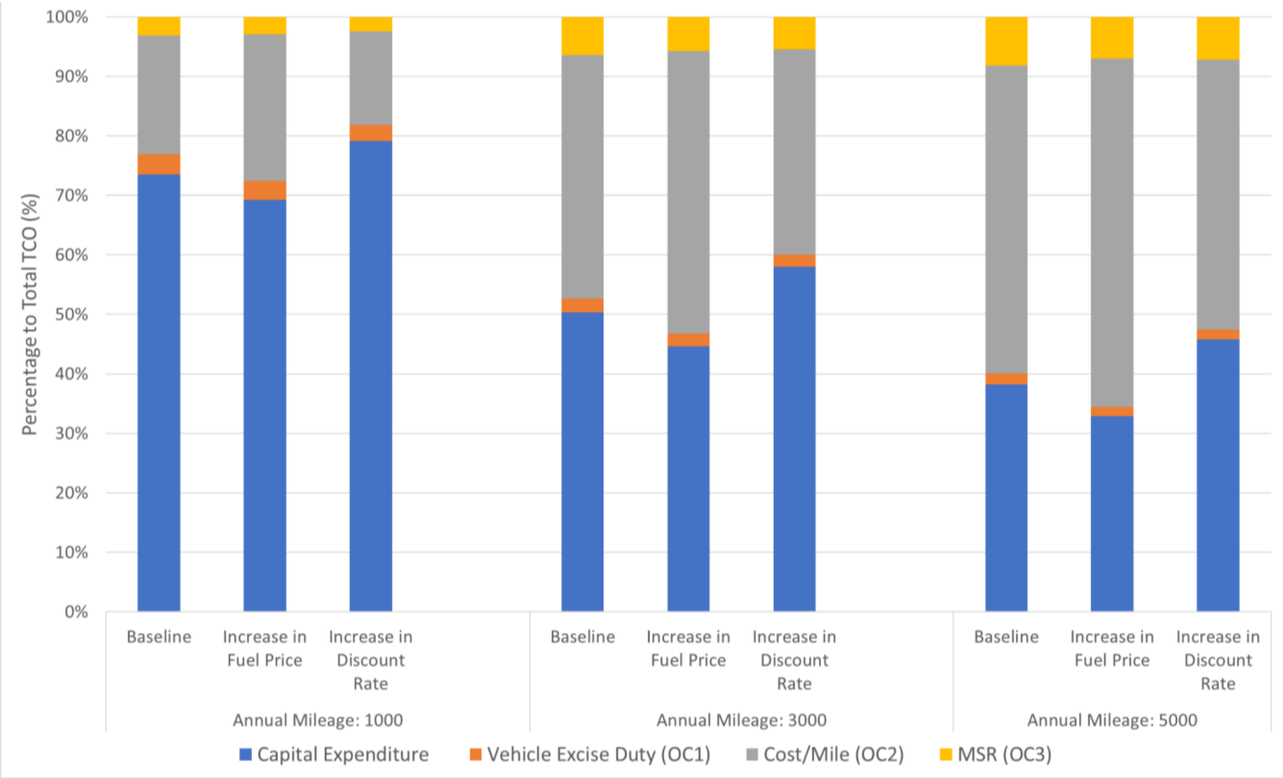

Figure 4.11: Proportions of associated costs contributing to overall TCO (Diesel RCV)

This sensitivity study considered three scenarios for testing. The first is a baseline scenario in which the parameters of fuel cell efficiency, hydrogen price, and diesel price are identical to the values in Scenario 1. The second scenario is where η_{FC} is increased to 57%. In the case for the diesel RCV, this scenario involving efficiency was not conducted for this study because diesel powertrains are an established technology. Therefore, the only powertrain efficiency of interest in this study is that of the hydrogen RCV.

A scenario where $C_{E_{pu}}^{Fuel}$ for both hydrogen and diesel is increased by £0.07 was conducted to compare the effect of increasing fuel cost per unit energy on the overall TCO of the vehicle. Finally, a scenario where the discount rate was increased was conducted, which aimed to show the effect that the discount rate has on both capital expenditure and operating costs. Observations of the proportions of associated costs with respect to the overall TCO subject to the sensitivities discussed in Sections 4.6.1–4.6.3 are shown in the Tables 4.8 and 4.9.

Table 4.8: Proportions of associated costs with overall TCO (Hydrogen RCV)

Hydrogen RCV @Annual Mileage: 1,000				
	Capital Expenditure (*CE*)	**Vehicle Excise Tax (OC_1)**	**Fuel Cost/Mile (OC_2)**	**Maintenance, Service and Repairs (OC_3)**
Baseline	86%	0%	12.68%	1.40%
Increase in η_{FC}	87%	0%	11.50%	1.42%
Increase in $C_{H_2}^{E_{pu}}$	83%	0%	15.72%	1.35%
Increase in Discount Rate (*i*)	88%	0%	15.72%	1.15%

Table 4.9: Proportions of associated costs with overall TCO (Diesel RCV)

Diesel RCV @Annual Mileage: 1,000				
	Capital Expenditure (*CE*)	**Vehicle Excise Tax (OC_1)**	**Fuel Cost/Mile (OC_2)**	**Maintenance, Service and Repairs (OC_3)**
Baseline	73%	3%	20%	3%
Increase in $C_{Diesel}^{E_{pu}}$	69%	3%	25%	3%
Increase in Discount Rate (*i*)	79%	3%	16%	2%

Looking at Table 4.8, the baseline case for the hydrogen RCV and in fact all scenarios involving hydrogen have an OC_1 value of 0%. This is due to the hydrogen RCV not being applicable for vehicle excise tax because it is a zero-emission vehicle. It is clearly seen in both Tables 4.8 and

4.9 that the majority of the overall TCO is comprised of the capital expenditure, which is then followed by OC_2.

Upon increasing $C_{E_{pu}}^{Fuel}$ for both hydrogen and diesel RCVs, it is observed that the share of OC_2 with regards to overall contribution to TCO increases while the *CE* decreases. This happens because the increase in overall fuel costs does not affect the net-present value of the RCV. Exclusively in the case for the hydrogen RCV, an increase in the value of η_{FC} led to a decrease in the proportion of OC_2 out of the overall TCO. This was due to cost savings associated with better fuel efficiency, which means that the bulk of cost will be retained by *CE*. Increasing the discount rate increases the proportion of *CE* with regards to overall TCO because it reduces the resale value of the RCV while accounting for inflation, which in effect lowers the value of the operating costs. Finally, increasing annual mileage will increase the proportion of OC_2 and OC_3 with regards to overall TCO while reducing the proportion of *CE* because a greater distance travelled means that more fuel is consumed, and there is also a greater need for maintenance and repairs.

4.7 Chapter Summary

This chapter addressed the study of total cost of ownership of a hydrogen Refuse Collection Fleet (RCV) for a local council. A methodology and a spreadsheet-based tool was developed to calculate the hydrogen requirements and TCO for converting an existing diesel-fuelled RCV fleet. Real data provided by the Leeds City Council was used to base the fuel consumption profiles and annual mileage assumptions for the hydrogen RCV.

Results from the scenarios discussed demonstrated the potential cost competitiveness of hydrogen powered RCVs as the values for TCO/Mile of the hydrogen-powered RCV came close to that of the diesel powered RCV given current values of fuel cell efficiencies and hydrogen price. In some cases, the hydrogen-powered RCVs managed to reach cost parity with the values of TCO/Mile for diesel powered RCVs after a certain annual mileage.

Scenarios depicting future fuel cell efficiencies and hydrogen prices were studied and the results from these scenarios demonstrate that a hydrogen-powered RCV can be cheaper at lower annual mileages than the average annual mileage of the current RCVs in the Leeds City

Council fleet. Furthermore, it was also demonstrated that the expected peak fuel cell efficiency value for 2030 (68%) managed to offset the effect of high hydrogen price.

Independent variables present in the TCO calculations were put forward for sensitivity analysis. The findings show that long ownership periods for hydrogen RCVs was required for them to be cost-competitive with diesel RCVs. Furthermore, TCO/Mile was analysed with regards to its sensitivities to increasing hydrogen fuel cell efficiencies and fuel cost increases. The results show an inverse relationship with regards to their effects on overall TCO and TCO/Mile. However, the most determining factor in the overall TCO is the price of fuel.

Chapter 5: Constrained Optimisation of a Hydrogen-coupled Integrated Energy System

5.1 Introduction

As global energy demand continues to grow, IESs have become an area of high research interest. Intermittent renewable energy systems such as wind and solar PV that produce electricity are increasingly being used but are subject to geographical constraints and weather changes, which causes the electricity supply to be suffer from the issue of intermittency. Therefore, to provide certainty in supply, sources of dispatchable energy are required to address shortages in electricity supply.

Hydrogen is a potential solution for the issue of intermittent renewable energy supply, as well as a potential solution for providing flexibility in the future energy mix. Hydrogen is being considered for use because of the flexibility of applications that it offers and it does not emit CO_2 when used as a source of dispatchable energy. With the advent of IESs, a hydrogen conversion and storage system can be coupled with wind and solar PV electricity generation infrastructure in an integrated energy system to provide grid balancing services or as a source of fuel for transport.

This chapter will study economic dispatch (i.e., meeting energy demands in the integrated energy system, while simultaneously keeping costs minimal). A mathematical model of an integrated energy system coupled with a hydrogen conversion and storage system will be developed using the real case study data of the Levenmouth Community Energy Project. The model of this system is presented as an optimisation problem where several scenarios were developed to study the behaviour of the system under different levels of available renewable energy supply. Finally, the results and findings of this study are summarised and discussed.

5.2 System Specifications and Methods

5.2.1 Specifications of System Under Study

The system under study is an integrated energy system that has electricity and hydrogen as the main energy vectors. It showcases the utilisation of a hydrogen storage system to provide electricity to satisfy electricity demand of a building site during times when electricity import prices are high or when renewable energy supply is not sufficient. Hydrogen is also supplied as fuel for a fleet of vehicles. Hydrogen is generated from renewable energy sources (wind and solar PV) during times when production of renewable electricity is higher than electricity demand. The stored hydrogen can then either be supplied back to the grid via the fuel cell or used to fuel the fleet of vehicles. The expectation of the system's operation is that hydrogen will be produced when either the availability of renewable electricity is high and/or when the import price of electricity is low. The fuel cell will then enter the operation mode when there is low renewable electricity and high electricity export price. A simple block diagram depicting the system is shown in Figure 5.1.

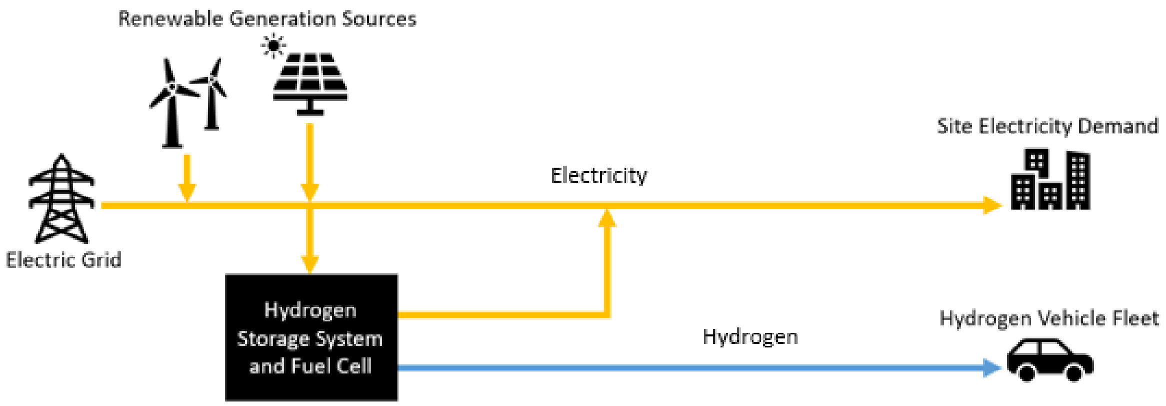

Figure 5.1: Simplified block diagram of the system under study

In Figure 5.1, the yellow lines denote electricity (which can be provided from either the electric grid, renewable electricity sources, the fuel cell, or all simultaneously) and the blue line denotes hydrogen (which is used for a fleet of hydrogen fuelled vehicles).

5.3. Problem Statement and Formulation

5.3.1 Optimisation with Constraints and Mathematical Model of System

The system studied is represented using the energy hub concept as explained in Section 2.6.3.

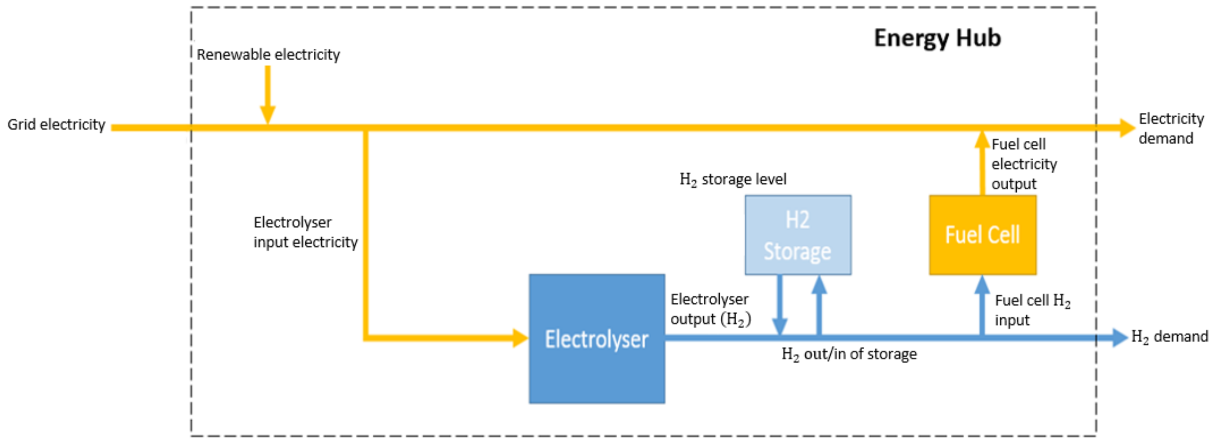

Figure 5.2: Energy hub representation of the integrated energy system under study

Figure 5.2 is an energy hubs block diagram of the test system in Figure 5.1. The respective elements of the energy hub are symbolised below.

- $E^{e}_{grid(t)}$: Grid electricity
- $E^{e}_{D(t)}$: Electricity demand
- $E^{e}_{EL(t)}$: Electrolyser input
- $E^{e}_{WT(t)}$: Wind turbine output
- $E^{e}_{PV(t)}$: Solar PV output
- $E^{e}_{FC(t)}$: Fuel cell output
- $E^{H2}_{D(t)}$: Hydrogen demand
- $E^{H2}_{EL(t)}$: Electrolyser output
- $E^{H2}_{FC(t)}$: Fuel cell input
- $E^{H2}_{inj\ store(t)}$: Hydrogen injected/discharged from hydrogen storage system
- $SL_{H2(t)}$: Storage level

Table 5.1 provides a breakdown of the maximum power outputs of the components present in the system under study. These figures are based on the capacities of the same components that are present in the Levenmouth Community Energy Project [71], [194]

Table 5.1: Maximum power output capacities of the system's components [155]

System Component	Rated Maximum Power Capacity (kW)
Wind Turbine	750
Solar PV	200
Electrolyser	370
Fuel Cell	100
Hydrogen Storage	3333

The problem is formulated as a multi-time period optimal dispatch problem, which is solved via constrained optimisation. The objective of the optimisation is to run the system at the lowest total cost for a certain duration of time. Renewable energy supply profiles, demand (electricity and hydrogen) profiles, and electricity export and import pricing regimes are pre-determined using real data provided by Toshiba Research Europe (from their Levenmouth Community Energy Project) [194].

The objective function "C" (total cost) is defined as follows:

$$C = \sum_{t=1}^{n}(C^{e}_{grid(t)} \times E^{e}_{grid(t)}) \quad (5.1)$$

where, assuming $E^{e}_{grid} < 0$, C^{e}_{grid} is the hourly variable electricity export price and, if $E^{e}_{grid} > 0$, C^{e}_{grid} is instead the hourly variable electricity import price.

The objective function in Equation (5.1) is set against demand constraints (i.e., the energy balance equations), which are mathematically expressed as follows:

Electricity balance equation: $E^{e}_{d(t)} = E^{e}_{grid(t)} + E^{e}_{WT(t)} + E^{e}_{PV(t)} - E^{e}_{EL(t)} + E^{e}_{FC(t)}$ (5.2)

Hydrogen balance equation: $E^{H2}_{D(t)} = E^{e}_{EL(t)}\eta^{e/H2}_{EL} \pm E^{H2}_{inj\ store(t)} - E^{e}_{FC(t)}\frac{1}{\eta^{H2/e}_{FC}}$ (5.3)

where $+E^{H2}_{inj\ store(t)}$ indicates that hydrogen storage is being charged, whereas $-E^{H2}_{inj\ store(t)}$ indicates that hydrogen storage is being discharged.

In matrix form, the system can be represented as follows:

$$\begin{bmatrix} E^{e}_{D(t)} - E^{e}_{WT(t)} - E^{e}_{PV(t)} \\ E^{H2}_{D(t)} \end{bmatrix} = \begin{bmatrix} -1 & 1 & 1 & 0 \\ \eta^{e/H2}_{EL} & 0 & -\frac{1}{\eta^{H2/e}_{FC}} & 1 \end{bmatrix} \begin{bmatrix} E^{e}_{EL(t)} \\ E^{e}_{grid(t)} \\ E^{e}_{FC(t)} \\ \pm E^{H2}_{inj\ store(t)} \end{bmatrix} \tag{5.4}$$

The efficiencies of the converter devices are as follows [148]:

- $\eta^{e/H2}_{EL}$: Efficiency of electrolyser (85%)
- $\eta^{H2/e}_{EL}$: Efficiency of fuel cell (55%)

The elements in the matrix are also subject to upper-bound and lower-bound constraints are categorised and shown below.

Hub input constraints:

- $E^{e}_{grid(min)} \leq E^{e}_{grid} \leq E^{e}_{grid(max)}$ (5.5)
- $E^{e}_{PV(min)} \leq E^{e}_{PV} \leq E^{e}_{PV(max)}$ (5.6)
- $E^{e}_{WT(min)} \leq E^{e}_{WT} \leq E^{e}_{WT(max)}$ (5.7)

Hub converter and storage constraints:

- $E^{e}_{EL(min)} \leq E^{e}_{EL} \leq E^{e}_{EL(max)}$ (5.8)
- $E^{e}_{FC(min)} \leq E^{e}_{FC} \leq E^{e}_{FC(max)}$ (5.9)
- $E^{H2}_{inj\ store(\min)} \leq E^{H2}_{inj\ store} \leq E^{H2}_{inj\ store(max)}$ (5.10)
- $SL_{H2(min)} \leq SL_{H2} \leq SL_{H2(max)}$ (5.11)

Storage level at the initial time step is selected as a value that lies between the minimum and maximum storage capacity. The corresponding storage levels at the subsequent time steps can be mathematically represented as:

$$SL_{H2(t)} = SL_{H2(t-1)} + E^{H2}_{inj\ store(t)} - E^{H2}_{store\ out(t)} \tag{5.12}$$

Equations (5.1–5.3) are coded in MATLAB and are calculated using the built-in ‘fmincon’ function, optimal values for the variables in the energy input matrix considering lowest total cost.

Note: It should be highlighted that the energy efficiency of a fuel cell depends on system loading and may influence the optimisation results. The energy efficiency of a fuel cell can be extrapolated using the Willans line approach [195], which shows the relationship between the energy input and the energy output of a converter [195]. However, a fixed efficiency value has been selected for the electrolyser and fuel cell operation in this chapter to observe the variation of the energy dispatch within the energy system with respect to the loads and renewable energy supply. Consequently, a detailed assessment of the electrolyser and fuel cell, and their performance depending on the load characteristics, although of significance, falls outside the scope of this work.

5.3.2 Present System Operation

Using the data provided on the Levenmouth Community Energy Project [194], [71], the Baseline operation for one week of the actual system with both low and high renewable electricity supply is shown in Figures 5.3 and 5.4.

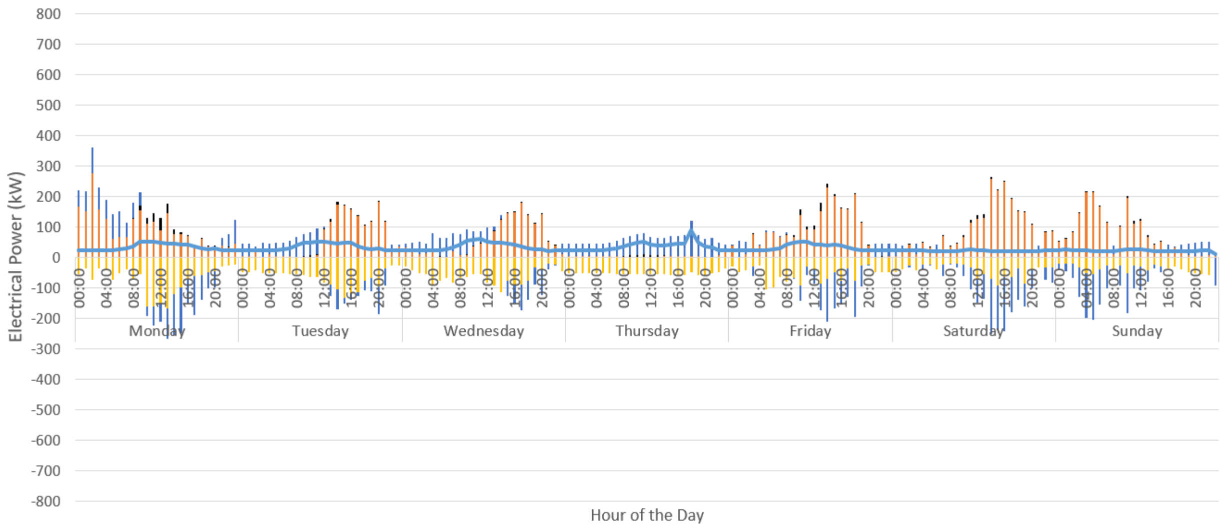

(a) Baseline operation – low renewables scenario

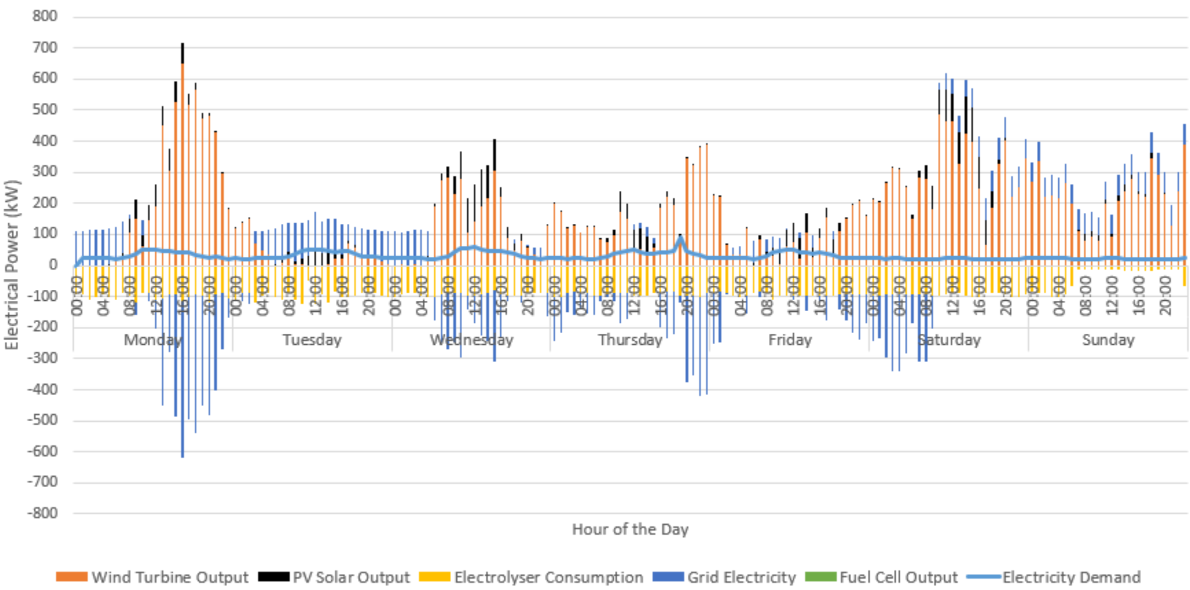

(b) Baseline operation – high renewables scenario

Figure 5.3: Electricity system data for baseline operation: a) low renewables; b) high renewable

Figure 5.3 shows the relevant operational data of the electricity system on-site. It should be emphasised that when grid electricity is on the negative Y-axis, it indicates that electricity is being exported back to the grid; whereas when it is on the positive Y-axis, electricity is being imported from the grid.

The historical data shows the electrolyser is operated throughout the study period. During certain periods (e.g., Tuesday), grid electricity is used to produce hydrogen using the electrolyser and also to meet the on-site electricity demand. Significant quantities of electricity exports are observed, particularly during periods with high renewable supply such as that on Monday between 08:00-20:00.

Figure 5.4 shows the operational data on hydrogen production and consumption on-site.

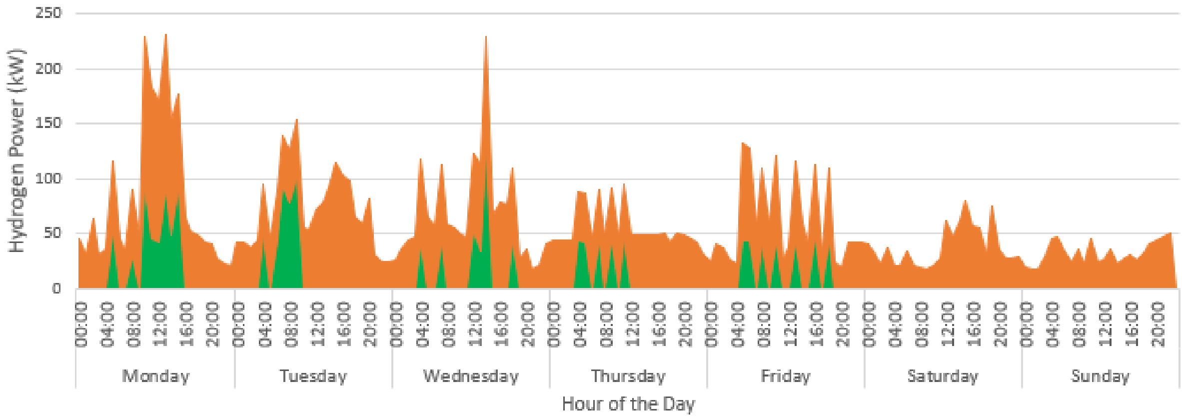

(a) Baseline operation - low renewable generation

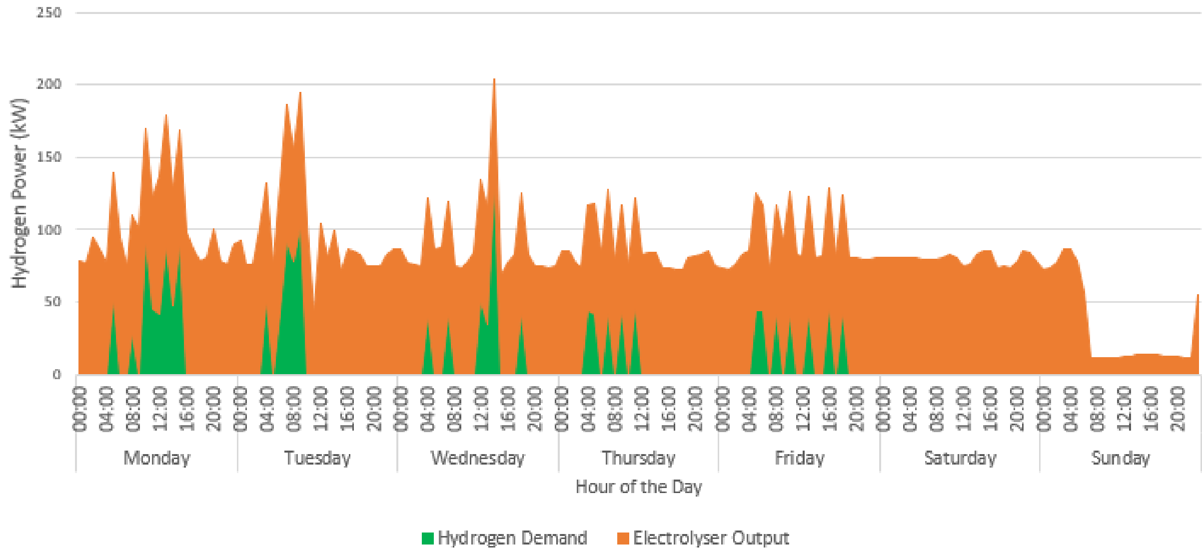

(b) Baseline operation – high renewable generation

Figure 5.4 Hydrogen system data for baseline operation: a) low renewables; b) high renewables

By observing the differences in Figures 5.4a and 5.4b, it is evident that the higher and more consistent electrolyser output levels are attributed to the higher renewable electricity supply.

The available data indicates that the system is not utilising the available onsite hydrogen for grid balancing operations as the hydrogen demand shown in Figure 5.4 only accounts for vehicle refuelling. Therefore, optimisation scenarios using the baseline performance data which demonstrate the potential of using the onsite hydrogen for grid balancing whilst satisfying both site electricity and hydrogen vehicle refuelling demands are to modelled and investigated.

5.3.3 Optimisation Scenarios

Given the baseline operation of the Levenmouth system, 2 scenarios are developed to demonstrate how the installed hydrogen conversion and storage system can be used to decrease grid electricity imports and satisfy both demands for site electricity consumption and vehicle refuelling. These scenarios are summarised in Table 5.2.

Table 5.2: Optimisation Scenarios

Scenario	Description
One week cost optimal operation of the test system with low renewable electricity supply.	• Electricity demand accounts for 42% of on-site renewable electricity supply. • Electricity and hydrogen demand as in base scenario. • Electrolyser, hydrogen storage and fuel cell operated for cost minimisation.
One week cost optimal operation of the test system with high renewable electricity supply.	• Electricity demand accounts for 16% of on-site renewable electricity supply. • Electricity and hydrogen demand as in base scenario. • Electrolyser, hydrogen storage and fuel cell operated for cost minimisation.

The purpose of the optimisation is to study the optimal operation of the electrolyser and fuel cell, and the energy management of the hydrogen storage unit. The results of optimal operation are compared with the baseline scenario to enable opportunities for improvements in system operation. The motivation behind the scenarios is that a variation in renewable energy supply profiles should result in different operational behaviours for the electrolyser, hydrogen storage, and fuel cell systems. These scenarios will allow a comprehensive assessment of the positive impact that renewable energy supply has on the integrated energy system by reducing total operational costs and carbon emissions.

It should be highlighted that the electricity and hydrogen demand profiles for the different scenarios are kept the same as in the baseline operation of the system (Section 5.3.2). Specifically, the hydrogen demand is derived from the refuelling data of seven vehicles because this information is available from the historical datasets. This is done so that the difference in behaviour of the different technologies within the energy system becomes apparent.

The optimisation problem considers electricity and hydrogen demands as a constraint. Therefore, the results will reflect a balancing act of hydrogen production and supply with electricity demands and the availability of renewable energy. This provides a better insight into the utilisation of renewable energy production for the purpose of hydrogen production, unlike in references [147] and [148] where hydrogen is simply a consequential product of excess renewable energy production and does not act as a factor that is detrimental to the optimal operation of the system.

Further constraints in the optimisation problem which are considered are the maximum generation capacities of the onsite renewables (wind turbine and solar PV system), electrolyser and fuel cell. Furthermore, the maximum storage capacity is a constraint that cannot be exceeded either. The values of these constraints are listed in Table 5.1.

Electricity export and import price profiles are also kept the same for the same reason and reflect typical prices in the UK. Each scenario is run for 2 weeks within the model at hourly time granularity. A period of one week comprising the optimisation results of the second week has been extracted to avoid start-stop effects of the optimisation in the first week. This was done to prevent bias in the data analysis.

In comparison, [108] provides an optimisation study period of a year. This is very helpful in terms of determining the seasonal behaviour of an integrated energy system but does not provide a clear image of how such systems work on a day-to-day basis. Furthermore, with such a long optimisation window, it would be difficult to exactly observe the difference in behaviour between weekdays and weekends. References [156] and [157] take the approach of using a 24-hour optimisation window. Although this provides insight as to how an integrated energy system would behave for a day very accurately, it does not allow for the optimisation to run to the following day, and this makes it harder to do an analysis of day-ahead scheduling. This chapter tries to tackle these issues by providing a detailed day-to-day representation of system operation on hourly time steps. This enables day-ahead scheduling and enables the variation in behaviour between weekdays and weekends to be observed. Observing the differences between weekdays and weekends is of interest because energy consumption demands are expected to vary between them because the load demands are based on building sites, which may consume more energy during weekdays and working hours when compared to weekends.

5.4 Results and Discussion

5.4.1 Optimal Cost Operation for Low and High Renewable Electricity Generation Scenarios

These scenarios depict the test system optimal operation during a week for both low and high renewable energy supply on-site. Figure 5.5 shows the optimisation results for the electricity system in these scenarios.

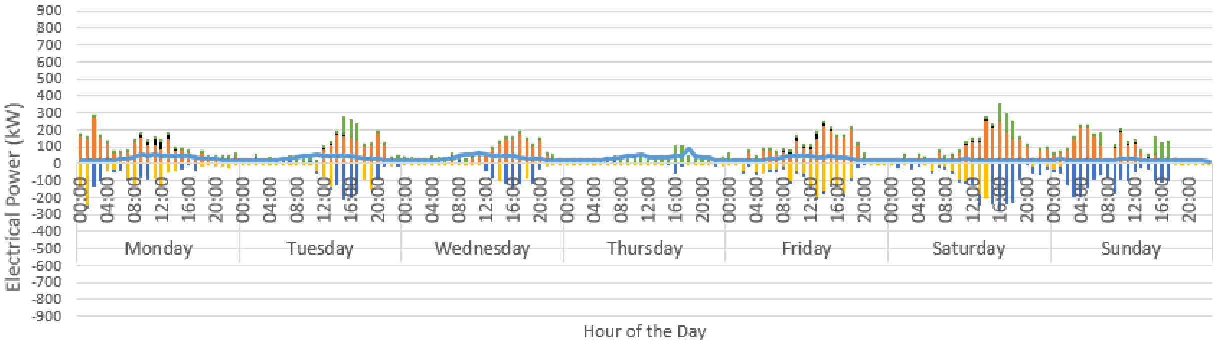

(a) Optimal operation - low renewable scenario

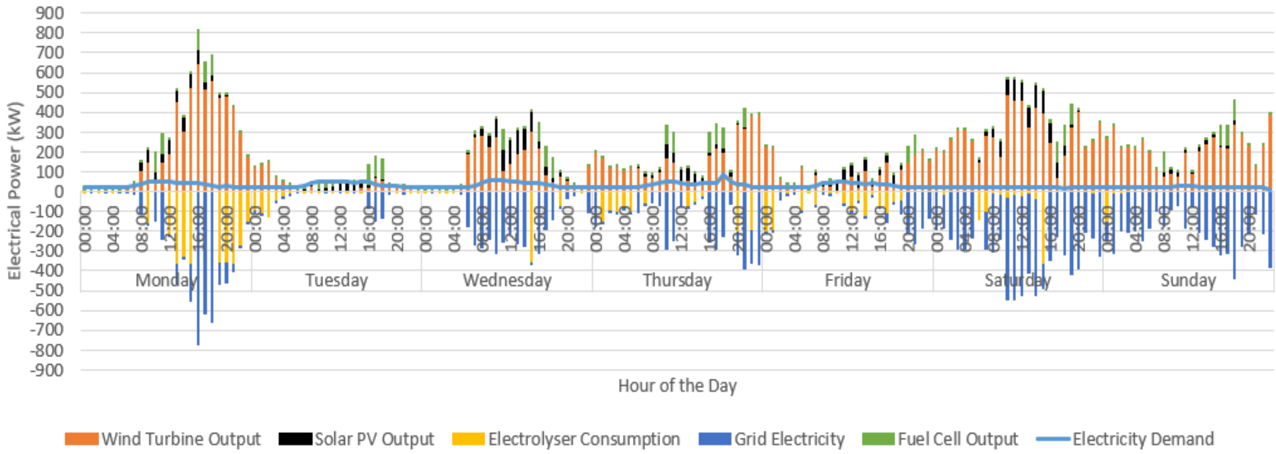

(b) Optimal operation - high renewable scenario

Figure 5.5: Electricity system data for optimal operation: a) low renewables; b) high renewables

Looking at Figure 5.5 a,b, when the renewable power outputs are high, the electrolyser load increases at the same time (see 5.5 a, Friday, between the hours of 4 am and 6 pm). This happens because the system converts excess renewable generation into hydrogen for storage. The fuel cell output follows high electricity import/export prices (16:00–19:00 h) to reduce costs and increase electricity export revenues. It also compensates for periods with lower renewable electricity generation on-site. This is seen on Thursday in Figure 5.5 a because there is continuous fuel cell utilisation between the hours of 08:00 to 22:00. A foresight of a low renewable electricity generation period triggers the fuel cell to consume stored hydrogen for electricity load balancing purposes to avoid importing electricity from the grid. There is a noticeable difference in the availability of renewable electricity supply in Figure 5.5b when compared to Figure 5.5a. Consequently, higher amounts of electricity are being exported in a high renewable electricity supply when compared to the low supply scenario, where the highest amount of electricity export is around 250 kW. In the high renewables scenario, electricity export averages around 500 kW.

Figure 5.6 shows the optimisation results for the hydrogen system in the optimal operation scenarios.

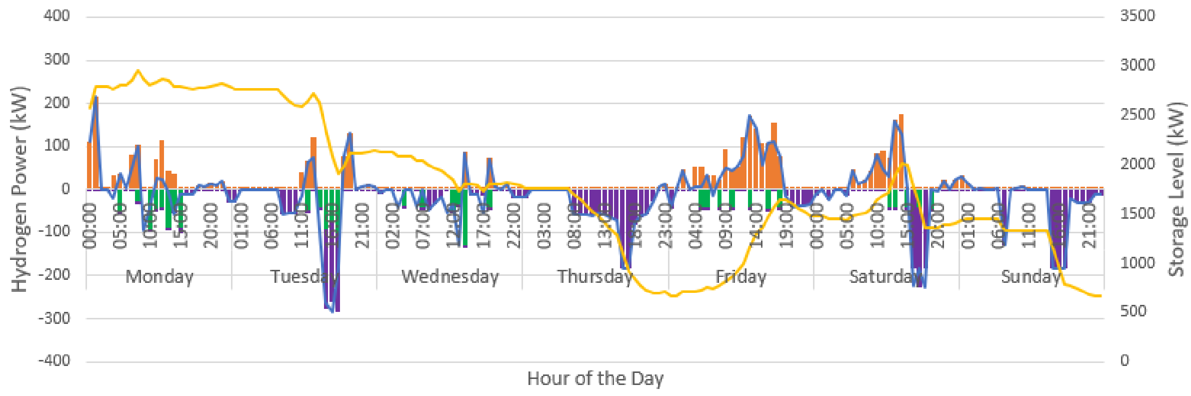

(a) Optimal operation - low renewable scenario

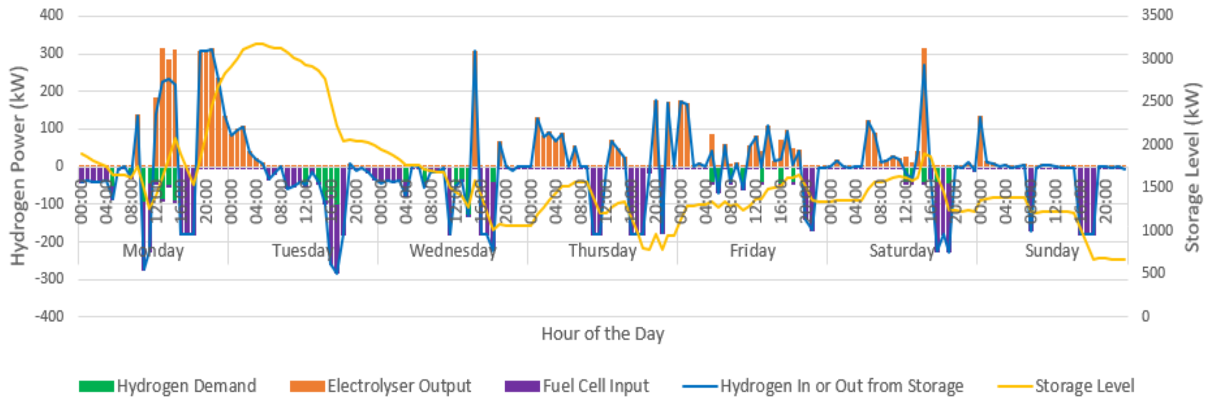

(b) Optimal operation - high renewable scenario

Figure 5.6: Hydrogen system data for optimal operation: a) low renewables; b) high renewables (the hydrogen storage level is on the right-hand Y-axis)

As shown in Figure 5.6a, the hydrogen storage level is at a minimum on Thursday due to the utilisation of the fuel cell for electricity generation during the low renewables period. The storage system then re-charges again on Friday when there is significant excess renewable electricity supply. In Figure 5.6b, the behaviour of the hydrogen storage system is consistent with the behaviour shown in Figure 5.6a, where hydrogen is stored during periods of excess renewable electricity available and is then discharged to cover high electricity price periods and periods of low renewable supply. Figure 5.5b shows that the higher availability of renewable electricity supply allows for a steadier storage level to be maintained throughout the period of optimisation.

Figure 5.7 depicts the behaviour of the electrolyser and fuel cell and grid electricity against the import and export prices of electricity. In addition, the renewable electricity available after serving the site electricity load (net renewable energy) is shown in the graphs as a measure of how much electricity can potentially be used for the electrolyser energy consumption or as electricity exported to the grid.

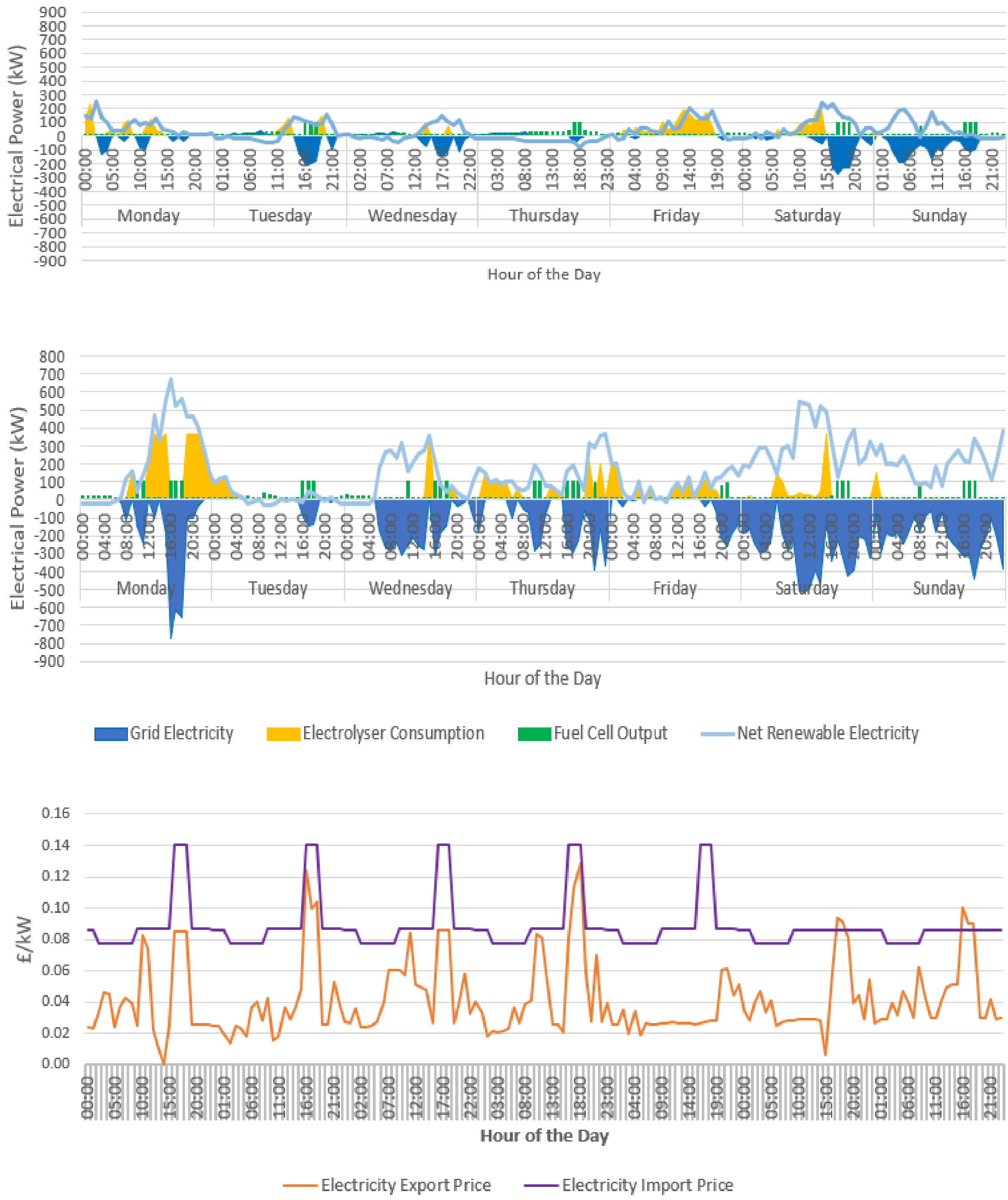

Figure 5.7: Fuel cell and electrolyser operation against electricity import and export prices

In Figure 5.7, the electrolyser electricity consumption peaks match with high levels of net renewable supply. The maximum electrolyser electricity consumption at a single instance is seen in the high renewable electricity supply scenario. This is expected because there is more net renewable electricity available in this scenario. In the low renewable energy supply on Thursday, where there is a period of low renewable electricity supply, the system imports electricity between the 00:00 to 11:00. This period coincides the period when electricity import prices are low. After 11:00, the system starts using the stored hydrogen in the fuel cell to convert it to electricity. Figure 5.7 also shows that peaks in import and export prices match with one another most of the time. This constrains the site operation to export electricity during these high price periods. The system is exporting electricity during the peak of electricity export price on each day.

5.4.2 Summary of Baseline and Optimal Cost Operation Scenarios

Table 5.3 presents a summary of the results for the different scenarios that were studied.

Table 5.3: Summary of baseline and optimisation results

	Low Renewables		**High Renewables**	
	Baseline operation	Optimal operation	Baseline operation	Optimal operation
Site Electricity Demand (kW)	5228.37	5228.37	5051.71	5051.71
Site Hydrogen Demand (kW)	1722.41	1722.41	1722.41	1722.41
Renewable Electricity Available (kW)	11981.66	11981.66	31734.60	31734.60
Electrolyser Energy Consumption (kW)	9526.21	4280.08	14629.35	7437.03
Fuel Cell Output (kW)	-	2049.66	-	3231.74
Stored Hydrogen (kW)	-	2846.2	-	5643.5
Discharged Hydrogen (kW)	-	4657.2	-	6920.3
Total Electricity Imports (kW)	4081.20	515.82	6372	0.03
Total Electricity Exports (kW)	5061.20	5066.20	10718	22858
Total Cost of Operation (£)	-	-239.8	-	-1118

From these results, it can be observed that there is more than 2.5 times renewable electricity generation available in the high renewables scenario compared to the low renewables scenario. The reason behind this is that electricity and hydrogen demand followed a fixed profile to facilitate the performance comparison of system operation for the different scenarios.

There is a significant reduction in electricity imports in the optimal cost operation compared to the baseline operation for both low renewables (87% reduction) and high renewables (almost 100%) cases. This is due to smart energy management within the site by storing available excess renewable electricity generation using hydrogen storage and its reconversion to electricity using the fuel cell when renewable electricity from the wind turbine and solar PV system is not available. The significant reduction in electricity imports translate to avoided costs. In addition, electricity imports are reduced, and system revenue is maximised by exporting electricity from excess renewable electricity and fuel cell output to make use of high export prices (during 16:00–19:00 hrs). The amount of electricity exported was 4.5 times more in the high renewables scenario compared to the low renewables case.

The electrolyser utilisation was optimised in the optimal cost operation scenarios and showed lower utilisation compared to the baseline operation cases. It is evident that in the baseline scenarios the electrolyser also uses electricity imported from the grid at a high cost, which is mostly avoided in the optimal cost operation.

The fuel cell plays an important role in balancing the system. It has shown it can help provide electricity to meet electricity demands when renewable generation is not available and, in addition, support revenue generation. The high renewables scenario shows higher utilisation of the fuel cell compared to the low renewables scenario, as expected.

It can be said that the availability of high-quality site data allowed for a realistic depiction of the system operation. However, given a situation where there is missing electricity demand data, hydrogen demand data and/or outlier data for either one at specific time steps, the methods in developed in chapters 3 and for can be used to fill in missing data within a wider body of data or correct any outlier data.

Hydrogen storage is a key enabler for the integrated electricity-hydrogen energy balancing system and has shown that, when designed with the correct capacities, is able to support storage of excess renewable electricity, meet hydrogen demand, and discharge to the fuel cell to convert back to electricity when required. The overall system hinges on the smart management of the hydrogen storage to facilitate energy-cost and carbon savings. Therefore, the ability to better forecast electricity prices and renewable generation ahead of time is an important need for realising this optimised operation.

5.5 Chapter Summary

The optimal cost operation of an integrated renewable-electricity-hydrogen energy system was demonstrated in the studies conducted in this chapter. A model of a hydrogen-coupled energy system with hydrogen conversion and storage systems that was based on the real case study of the Levenmouth Community Energy Project was developed using the energy hubs concept.

A set of scenarios considering the real operational data and seasonal variations in renewable electricity supply were developed. The function of hydrogen as an energy vector to capture excess electricity and use for backup during periods of low renewable electricity and to supply a clean vehicle fuel while meeting system energy balance constraints has been demonstrated. This was done via a constrained optimisation study in MATLAB. The effect of the seasonal variations of renewable energy supply on the energy dispatch and total cost of system operation were then summarised and discussed.

The results show that by integration of renewable technologies, electrolyser, hydrogen storage, and fuel cell technologies, the site energy system can gain significant operational cost and carbon savings particularly during periods of high renewable generation. The results indicate the need for operation scheduling and advanced control of the integrated system considering forecasts of renewable generation and electricity prices to ensure that low periods of renewable generation and high electricity price periods are managed effectively. The results show that optimum operation involves modulating the electrolyser to follow on-site renewable generation and modulating the fuel cell output to reduce electricity imports and generate revenue during periods of high prices. Hydrogen storage is a central part of the overall electricity and hydrogen system integration and to the ability to time-shift renewable energy to periods of electricity and hydrogen demands. It is important to note that actual operation savings may deviate from the results shown as this study assumes perfect foresight of system conditions.

The methodology presented is transferrable and scalable to sites of similar structure and the general findings will be applicable. The optimisation results shown are applicable to the UK conditions where time-varying import and export prices are utilised. The grid prices are a determining external factor for site operation and should reflect the local conditions when applied.

Chapter 6: Conclusions and Future Work

This chapter provides an overview of the contributions, conclusions, and makes some suggestions for future work.

6.1 Overview of the Research Goals and Contributions Provided by the Thesis

The main goal of this research was to develop methods of quantifying energy demands to address the lack of real data from demonstration projects where hydrogen conversion and storage systems are operated in an integrated energy system running on intermittent renewable energy and to describe their optimal operation.

The contributions of the thesis are summarised in the following bullet points:

- The benefits and challenges of utilising hydrogen in the transport sector and IES were presented and discussed.
- The state-of-the-art regarding the deployment of hydrogen-based technologies in the transport sector and IES was discussed.
- A simple method for developing electricity-demand profiles for sites that do not yet have monitoring infrastructure was developed.
- A method for developing fuel consumption and fuel cost/mile characteristics of a FCEV based on real technical data was developed.
- The techno-economic feasibility of deploying hydrogen fuelled RCVs in a current and future scenario was demonstrated.
- A real case study of on the optimal dispatch and cost minimisation of an IES with a hydrogen conversion and storage system was presented. The benefits of deploying hydrogen as an additional energy vector in the IES were quantified and discussed.

The conclusions derived from each technical contribution chapter are summarised in the following section.

6.2 Conclusions from the Research Work

The conclusions from the research undertaken are summarised in the following subsections.

6.2.1 Literature Review of Hydrogen Use for Decarbonisation of the Transportation Sector and Local Energy Systems

The literature review aimed to identify the potential benefits of using hydrogen for decarbonising the transport sector, as well as for use in IESs. It was found that there is a need to better understand the challenges and potential benefits of using hydrogen in both the transport sector and in IESs. A list of projects involving hydrogen for grid balancing services and transportation in Europe was studied. From this list, it was found that the UK only accounted for around 10% of the listed projects. Out of all of the hydrogen demonstration projects listed in the Table 2.1 that are based in the UK, only three projects involve systems that use hydrogen for both transport and grid electricity services. Thus, further research is required to assess the techno-economic challenges and benefits of using hydrogen for transport and grid electricity services.

The literature concerning the methods and models for analysing the cost optimal dispatch of hydrogen in IESs and for transport was also reviewed. The available literature on the subject showed a distinct lack of studies of the use of hydrogen in a localised energy system where hydrogen is stored and dispatched based on site electricity demand and vehicle refuelling demand, while considering electricity export and import prices. Most of the reviewed literature showed that hydrogen is only used for either grid balancing services or transport. Those studies that did look at both uses of hydrogen under a single system either had the hydrogen storage off-site or only consisted of an analysis horizon of 24 hours. This highlights the need for studies of the cost optimal dispatch of stored hydrogen in an integrated energy system that caters for both grid balancing services and transport in a localised IES that have a time horizon longer than 1 day.

6.2.2 Developing Representative Renewable Electricity-demand Profiles

A method was developed to generate a building site's representative electricity demand using a minimal number of parameters, which are typically available from an electricity invoice. This method was implemented to generate a set of scaling factors that show the hourly proportion of electricity demand for a 24-hour granularity. The scaling factors that are generated from this method considered hourly behaviour of electricity demand between weekdays and weekends. Another set of scaling factors were then developed with this method that took into consideration the demand behaviour of each specific day of the week. These scaling factors were generated and validated using historical data that were provided by the Rotherham and QEH sites.

The validation of the scaling factors was done over a series of seven scenarios that accounted for the electricity demand specifications of both the Rotherham and QEH sites, seasonal electricity-demand variations in the two sites, and then used scaling factors of one site to determine the representative electricity profile of the other site. The historical data of the sites were compared with the representative demand profiles that were generated by the scaling factors. Accuracy was measured by calculating the mean percentage error between the generated representative profiles and the historical demand profiles at each hour. It was found that there is a reasonable level of accuracy between the generated representative profiles with the historical data.

6.2.3 Hydrogen Powered Refuse Collection Vehicles: Total Cost of Ownership Analysis and Sensitivity Analysis

Using real operational data of diesel RCVs in the Leeds City Council fleet, a method for quantifying hydrogen fuel consumption in hydrogen powered RCVs of the same class was developed. Scenarios considering present and future values of fuel cell efficiency and fuel prices were developed to aid in the development of a case study of the difference in TCO for both hydrogen and diesel powered RCVs.

The results of the total cost per mile analysis show that the hydrogen powered refuse collection vehicle was cost competitive in most of the scenarios. With an increase in annual mileage, the hydrogen powered refuse collection vehicle also managed to reach cost parity and even became cheaper to own and run than the diesel powered refuse collection vehicle. Given the predicted high fuel cell efficiency and low fuel values predicted for 2030, the hydrogen powered refuse collection vehicle was able to reach cost parity with the diesel powered refuse collection vehicle before reaching the average annual mileage of the vehicles studied in the Leeds City Council fleet.

Sensitivity analysis of the refuse vehicles showed that reduction in TCO required longer ownership periods, higher powertrain efficiencies and higher annual mileage (these variables can be decided from the operator's or owner's side). However, it was evident in the case of the hydrogen refuse collection vehicle that the TCO is most sensitive to increase in fuel price.

6.2.4 Optimal Operation of a Hydrogen Storage and Fuel Cell Coupled Integrated Energy System

A steady-state model of an integrated energy system that utilises a hydrogen conversion and storage system for grid balancing operations and vehicle refuelling was developed. The mathematical representation of the model was based on the energy hubs method. The purpose of developing the model was to conduct an optimal cost and dispatch study of the system considering the individual upper-bound and lower-bound constraints for the system components (i.e., fuel cell generation capacity, maximum storage capacity, electrolyser capacity), while fulfilling demands for both electricity and hydrogen.

The model that was studied and presented in this thesis was based on the Levenmouth Community Energy Project, where wind power and solar PV electricity generation was connected to a microgrid to supply electricity for a group of buildings present on-site. This is further augmented by the use of a hydrogen conversion and storage system that fulfils grid supply and demand balancing, while also providing a source of green fuel for a set of dual fuel hydrogen vehicles.

Three scenarios were developed to study the system and its capabilities of satisfying the demands with the present constraints. The scenarios looked at the system's behaviour over the course of a week at an hourly granularity. These scenarios included a baseline scenario where the actual system operation data from the Levenmouth Community Energy Project was presented. In this scenario, the hydrogen conversion and storage system were not yet operational. However, the following scenarios considered the hydrogen conversion and storage system to be operational and also incorporated the actual building electricity demands, hydrogen demands and seasonal renewable electricity generation from the

Levenmouth Community Energy Project. The low and high renewable electricity supply scenarios were then optimised for the objective of cost minimisation on MATLAB.

It was found that for both low and high renewable electricity supply scenarios, the grid electricity export was significantly lower than that in the baseline scenario where the hydrogen conversion and storage system was not operational. In both the low and high renewable electricity supply scenarios, the system was running at a net profit because more electricity was exported than imported. Specifically, in the high renewable scenario it was found that the system was fully running on the available on-site generated renewable energy and the total grid electricity imports for this scenario were almost 0.

6.4 Future Work

This research has added to the current body of knowledge on the utilisation of hydrogen-based technologies in the decarbonisation of the transport and energy sectors. The methods that were developed and the analyses have demonstrated the use of hydrogen-based technologies as a means of decarbonisation, they can also save energy costs. A list of recommendations for further work to compliment and strengthen the contributions in this thesis can be found in the following points:

- Adding additional uncertainties for developing representative demand profiles such as building occupant behaviour method can increase accuracy as well as the adjustability of the scaling factors between same category buildings. In the future, the scaling factor method can be used in unison with stochastic methods especially in early building planning stages as it is a method which can be deployed quickly with minimum data. This would help providing an early picture to planners as to what the demand profile would roughly look like before acquiring enough data to employ more complex stochastic models.
- In terms of the techno-economic related studies of hydrogen fuel cell vehicles, a thorough investigation of the maintenance, service and repair costs should be conducted. At present most academic literature indicate that these costs are lower compared to the same costs for conventionally fuelled vehicles. However, there are manufacturers of such vehicles who indicate that due to the higher capital costs of

fuel cells, the maintenance, service, and repair costs end up being higher than that of conventionally fuelled vehicles.

- Given the high capital costs of hydrogen fuel cell vehicles, it would be difficult to justify the economics of using them for commercial private transport. The rate at which battery electric cars are getting cheaper would make it difficult for hydrogen fuel cell vehicles to compete in the market. Battery electric technology in the heavy transport industry is in its very early stages. Thus, taking advantage of the high energy density of hydrogen, further investigation for hydrogen as a transport fuel for shipping, large logistical vehicles and air transport would be an important area of research heading into the future.
- With the increase of distributed energy systems, hydrogen can play a more prominent role in both the electricity and gas sectors as it can be used for both. At present, it is quite understood that hydrogen technologies have a lot of potential being a future major player in the ancillary services market due to their fast dynamics. However, going into the future, optimisation studies of hydrogen in the context of integrated energy systems should also investigate the potential of hydrogen for energy arbitrage and peer-to-peer energy trading for both electricity and gas.

References

[1] L. A. Yarzábal, L. M. B. Salazar, and R. A. Batista-García, ‘Climate change, melting cryosphere and frozen pathogens: Should we worry…?’, *Environmental Sustainability*, vol. 4, no. 3, pp. 489–501, Sep. 2021, doi: 10.1007/s42398-021-00184-8.

[2] B. Burson, ‘DISPLACEMENT IN A CHANGING CLIMATE-Localized humanitarian action at the forefront of the climate crisis’, Geneva, 2021.

[3] V. Martin and W. Spry, ‘Energy Trends UK, January to March 2023’, 2023.

[4] I. MacLeay, K. Harris, and A. Annut, ‘Digest of United Kingdom Energy Statistics 2013’, London, 2013.

[5] H. Edwards, I. Stewart, B. Mawhood, and P. Bolton, ‘Electric vehicles and infrastructure’, Feb. 2023.

[6] B. Nykvist and O. Olsson, ‘The feasibility of heavy battery electric trucks’, *Joule*, vol. 5, no. 4, pp. 901–913, Apr. 2021, doi: 10.1016/j.joule.2021.03.007.

[7] M. de las N. Camacho, D. Jurburg, and M. Tanco, ‘Hydrogen fuel cell heavy-duty trucks: Review of main research topics’, *Int J Hydrogen Energy*, vol. 47, no. 68, pp. 29505–29525, Aug. 2022, doi: 10.1016/j.ijhydene.2022.06.271.

[8] HM Government, ‘Hydrogen Net Zero Investment Roadmap’, Apr. 2023.

[9] Sandia National Laboratories and T. Nguyen, ‘DOE Global Energy Storage Database’. Accessed: Feb. 24, 2023. [Online]. Available: https://sandia.gov/ess-ssl/gesdb/public/

[10] M. Abeysekera, ‘Combined Analysis of Coupled Energy Networks’, PhD Thesis, Cardiff University, Cardiff, 2016.

[11] The Royal Society, ‘Options for producing low-carbon hydrogen at scale’, London, 2018.

[12] T. Wang, X. Cao, and L. Jiao, ‘PEM water electrolysis for hydrogen production: fundamentals, advances, and prospects’, *Carbon Neutrality*, vol. 1, no. 1, p. 21, Dec. 2022, doi: 10.1007/s43979-022-00022-8.

[13] A. Velazquez Abad and P. E. Dodds, ‘Production of Hydrogen’, in *Encyclopedia of Sustainable Technologies*, Elsevier, 2017, pp. 293–304. doi: 10.1016/B978-0-12-409548-9.10117-4.

[14] K. T. Møller, T. R. Jensen, E. Akiba, and H. Li, ‘Hydrogen - A sustainable energy carrier’, *Progress in Natural Science: Materials International*, vol. 27, no. 1, pp. 34–40, Feb. 2017, doi: 10.1016/j.pnsc.2016.12.014.

[15] M. ŞAHBAZ and E. SULUKAN, ‘Biyokütle bazlı Biyoyakıt üretiminin modellenmesi ve Türkiye’de tarım sektörü için referans enerji sisteminin geliştirilmesi’, *Ege Üniversitesi Ziraat Fakültesi Dergisi*, pp. 61–70, Jun. 2021, doi: 10.20289/zfdergi.731470.

[16] U.S Department of Energy, 'Alternative Fuels Data Center Fuel Properties Comparison'.

[17] I. N. Kessides and D. C. Wade, 'Deriving an Improved Dynamic EROI to Provide Better Information for Energy Planners', *Sustainability*, vol. 3, no. 12, pp. 2339–2357, Dec. 2011, doi: 10.3390/su3122339.

[18] K. Mazloomi and C. Gomes, 'Hydrogen as an energy carrier: Prospects and challenges', *Renewable and Sustainable Energy Reviews*, vol. 16, no. 5, pp. 3024–3033, Jun. 2012, doi: 10.1016/j.rser.2012.02.028.

[19] J. Twitchell, K. DeSomber, and D. Bhatnagar, 'Defining long duration energy storage', *J Energy Storage*, vol. 60, p. 105787, Apr. 2023, doi: 10.1016/j.est.2022.105787.

[20] British Petroleum (BP), 'Fact Sheet - A guide to storing fuel'.

[21] E. D. Christensen, T. Alleman, and R. L. McCormick, 'Re-Additization of Commercial Biodiesel Blends During Long-Term Storage ', Denver, Nov. 2020.

[22] D. Rudland, B. Thomas, C. Brewer, K. Toomer, L. Siddorn, and R. Norbury, 'Garages and Filling Stations - A Guide for Developers', 2020.

[23] California Hydrogen Business Council, 'Power-to-Gas: The Case for Hydrogen--White Paper', 2015.

[24] M. A. Pellow, C. J. M. Emmott, C. J. Barnhart, and S. M. Benson, 'Hydrogen or batteries for grid storage? A net energy analysis', *Energy Environ Sci*, vol. 8, no. 7, pp. 1938–1952, 2015, doi: 10.1039/C4EE04041D.

[25] M. Penev and C. Hunter, 'Energy Storage Analysis', Apr. 2019.

[26] J. Moore and B. Shabani, 'A Critical Study of Stationary Energy Storage Policies in Australia in an International Context: The Role of Hydrogen and Battery Technologies', *Energies (Basel)*, vol. 9, no. 9, p. 674, Aug. 2016, doi: 10.3390/en9090674.

[27] M. Abeysekera, J. Wu, and N. Jenkins, 'Integrated energy systems: An overview of benefits, analysis methods, research gaps and opportunities', 2016.

[28] U. of T. Department of Thermal and Fluid Engineering, 'Energy Systems Integration'. Accessed: Feb. 08, 2023. [Online]. Available: https://www.utwente.nl/en/et/tfe/research-groups/TE/research/research/Energy_Systems_Integration/

[29] F. Kachirayil, J. M. Weinand, F. Scheller, and R. McKenna, 'Reviewing local and integrated energy system models: insights into flexibility and robustness challenges', *Appl Energy*, vol. 324, p. 119666, Oct. 2022, doi: 10.1016/j.apenergy.2022.119666.

[30] IEA, 'Energy end-use data collection methodologies and the emerging role of digital technologies', 2019.

[31] W. Seward, W. Hua, and M. Qadrdan, ‘Electricity Storage in Local Energy Systems’, in *Microgrids and Local Energy Systems*, IntechOpen, 2021. doi: 10.5772/intechopen.99350.

[32] O. M. Babatunde, J. L. Munda, and Y. Hamam, ‘Power system flexibility: A review’, *Energy Reports*, vol. 6, pp. 101–106, Feb. 2020, doi: 10.1016/j.egyr.2019.11.048.

[33] H. Holttinen *et al.*, ‘The Flexibility Workout: Managing Variable Resources and Assessing the Need for Power System Modification’, *IEEE Power and Energy Magazine*, vol. 11, no. 6, pp. 53–62, Nov. 2013, doi: 10.1109/MPE.2013.2278000.

[34] S. Impram, S. Varbak Nese, and B. Oral, ‘Challenges of renewable energy penetration on power system flexibility: A survey’, *Energy Strategy Reviews*, vol. 31, p. 100539, Sep. 2020, doi: 10.1016/j.esr.2020.100539.

[35] E. & I. S. Department for Business, ‘Energy Trends UK, July to September 2022’, 2022.

[36] I. Staffel, R. Green, T. Green, R. Gross, and J. Malte, ‘October to December 2020 Electric Insights Quarterly’, 2020.

[37] M. Joos and I. Staffell, ‘Short-term integration costs of variable renewable energy: Wind curtailment and balancing in Britain and Germany’, *Renewable and Sustainable Energy Reviews*, vol. 86, pp. 45–65, Apr. 2018, doi: 10.1016/j.rser.2018.01.009.

[38] C. Budny, R. Madlener, and C. Hilgers, ‘Economic Feasibility of Pipe Storage and Underground Reservoir Storage Options for Power-to-Gas Load Balancing’, *Energy Procedia*, vol. 61, pp. 2201–2205, 2014, doi: 10.1016/j.egypro.2014.12.109.

[39] S. Gill, E. Barbour, I. A. G. Wilson, and D. Infield, ‘Maximising revenue for non-firm distributed wind generation with energy storage in an active management scheme’, *IET Renewable Power Generation*, vol. 7, no. 5, pp. 421–430, Sep. 2013, doi: 10.1049/iet-rpg.2012.0036.

[40] T.-T. Nguyen, V. Martin, A. Malmquist, and C. A. S. Silva, ‘A review on technology maturity of small scale energy storage technologies’, *Renewable Energy and Environmental Sustainability*, vol. 2, p. 36, Sep. 2017, doi: 10.1051/rees/2017039.

[41] J. Moore and B. Shabani, ‘A Critical Study of Stationary Energy Storage Policies in Australia in an International Context: The Role of Hydrogen and Battery Technologies’, *Energies (Basel)*, vol. 9, no. 9, p. 674, Aug. 2016, doi: 10.3390/en9090674.

[42] H. Steinmüller *et al.*, *Power to Gas – eine Systemanalyse. Markt- und Technologiescouting und -analyse*. 2014.

[43] V. Vartiainen, ‘Screening of Power to Gas Projects’, Lappeenranta University of Technology, Lappeenranta, 2016.

[44] C. Wulf, P. Zapp, and A. Schreiber, ‘Review of Power-to-X Demonstration Projects in Europe’, *Front Energy Res*, vol. 8, Sep. 2020, doi: 10.3389/fenrg.2020.00191.

[45] NREL, 'ESIF 2018', 2018.

[46] U.S Department of Energy, 'Developing Renewable Energy Projects Larger Than 10 MWs at Federal Facilities -A Practical Guide to Getting Large-Scale Renewable Energy Projects Financed with Private Capital', 2013.

[47] H. W. Langmi, N. Engelbrecht, P. M. Modisha, and D. Bessarabov, 'Hydrogen storage', in *Electrochemical Power Sources: Fundamentals, Systems, and Applications*, Elsevier, 2022, pp. 455–486. doi: 10.1016/B978-0-12-819424-9.00006-9.

[48] Department for Transport, 'Official Statistics--Transport and Environment Statistics 2022', Oct. 2022.

[49] Deloitte Monitor, 'Fueling the Future of Mobility: Hydrogen and Fuel Cell Solutions for Heavy Duty and Long-Haul Freight Transportation', Paris, 2020.

[50] J. Jones, A. Genovese, and A. Tob-Ogu, 'Hydrogen vehicles in urban logistics: A total cost of ownership analysis and some policy implications', *Renewable and Sustainable Energy Reviews*, vol. 119, p. 109595, Mar. 2020, doi: 10.1016/j.rser.2019.109595.

[51] M. Sayer, A. Ajanovic, and R. Haas, 'On the economics of a hydrogen bus fleet powered by a wind park – A case study for Austria', *Int J Hydrogen Energy*, vol. 47, no. 78, pp. 33153–33166, Sep. 2022, doi: 10.1016/j.ijhydene.2022.07.195.

[52] Ballard Power Systems and Arcola Energy, 'Zero Emission Fuel Cell Electric Refuse Collection Vehicles '.

[53] Automotive Council UK and Advanced Propulsion Centre UK, 'Fuel Cell Roadmap 2020', Feb. 2021.

[54] T. Endacott, 'EST Fleet Review-Electric Refuse Collection Vehicles Manchester City Council EST Fleet Report | Manchester City Council', 2019. [Online]. Available: http://www.energysavingtrust.org.uk/

[55] M. Yue, H. Lambert, E. Pahon, R. Roche, S. Jemei, and D. Hissel, 'Hydrogen energy systems: A critical review of technologies, applications, trends and challenges', *Renewable and Sustainable Energy Reviews*, vol. 146, p. 111180, Aug. 2021, doi: 10.1016/j.rser.2021.111180.

[56] D. J. MacKay, *Sustainable Energy - Without the Hot Air*. Cambridge: UIT Cambridge Ltd, 2009.

[57] U. Weichenhain, M. Kaufman, A. Benz, and G. Matute-Gomez, 'Hydrogen Valleys Insights into the Emerging Hydrogen Economies Around the World', Brussels, 2021.

[58] E. & I. S. Department for Business, 'Hydrogen Production Costs 2021', London, 2021.

[59] E. Taibi, H. Blanco, R. Miranda, and M. Carmo, 'Green Hydrogen Cost Reduction Scaling Up Electrolysers to Meet 1.5'C Climate Goal', Abu Dhabi, 2020.

[60] AA Limited (Formerly: The Automobile Association), 'Fuel Price Report (May 2022)', 2022.

[61] E. & I. S. Department for Business, 'BEIS 2017 Fossil Fuel Price Assumptions', London, 2017.

[62] E. & I. S. Department for Business, 'Monthly and Annual Prices of Road Fuels and Petroleum Products'. Accessed: Dec. 26, 2022. [Online]. Available: https://www.gov.uk/government/statistical-data-sets/oil-and-petroleum-products-monthly-statistics

[63] Organization of the Petroleum Exporting Countries, 'OPEC Basket Price'. Accessed: Dec. 26, 2022. [Online]. Available: https://www.opec.org/opec_web/en/data_graphs/40.htm

[64] CENEX, 'Preparing for Fuel Cell Vehicle Rollout: Trial, Analysis and Deployment Planning for Hydrogen Fleets', 2022.

[65] HM Government, 'Transitioning to Zero Emission Cars', 2020.

[66] C. J. Oglieve, M. Mohammadpour, and H. Rahnejat, 'Optimisation of the vehicle transmission and the gear-shifting strategy for the minimum fuel consumption and the minimum nitrogen oxide emissions', *Proceedings of the Institution of Mechanical Engineers, Part D: Journal of Automobile Engineering*, vol. 231, no. 7, pp. 883–899, Jun. 2017, doi: 10.1177/0954407017702985.

[67] S. He, X. Fan, Q. Wang, X. Chen, and S. Zhu, 'Review on Torque Distribution Scheme of Four-Wheel In-Wheel Motor Electric Vehicle', *Machines*, vol. 10, no. 8, p. 619, Jul. 2022, doi: 10.3390/machines10080619.

[68] K. T. Chau, 'Pure electric vehicles', in *Alternative Fuels and Advanced Vehicle Technologies for Improved Environmental Performance*, Elsevier, 2014, pp. 655–684. doi: 10.1533/9780857097422.3.655.

[69] Q. Lu, W. Zhou, and Y. Zheng, 'Regenerative Braking Control Strategy with Real-Time Wavelet Transform for Composite Energy Buses', *Machines*, vol. 10, no. 8, p. 673, Aug. 2022, doi: 10.3390/machines10080673.

[70] G. Gahleitner, 'Hydrogen from renewable electricity: An international review of power-to-gas pilot plants for stationary applications', *Int J Hydrogen Energy*, vol. 38, no. 5, pp. 2039–2061, Feb. 2013, doi: 10.1016/j.ijhydene.2012.12.010.

[71] 'Levenmouth Community Energy Project'. Accessed: Dec. 30, 2022. [Online]. Available: https://www.brightgreenhydrogen.org.uk/levenmouth-community-energy-project/

[72] H. Ritchie, M. Roser, and P. Rosado, 'Energy', OurWorldInData. Accessed: Feb. 20, 2023. [Online]. Available: https://ourworldindata.org/energy/country/

[73] J. Arnal, M. Isasa, and L. Glielmo, 'HAEOLUS DELIVERABLE D5.4 Environmental performance analysis', Mar. 2023.

[74] P. Marocco, D. Ferrero, A. Lanzini, and M. Santarelli, 'The role of hydrogen in the optimal design of off-grid hybrid renewable energy systems', *J Energy Storage*, vol. 46, p. 103893, Feb. 2022, doi: 10.1016/j.est.2021.103893.

[75] Orkney Renewable Energy Forum, 'Orkney Hydrogen Strategy The Hydrogen Islands 2019 – 2025 ', Orkney, 2019.

[76] K. H. Sirviö, H. Laaksonen, K. Kauhaniemi, and N. Hatziargyriou, 'Evolution of the Electricity Distribution Networks—Active Management Architecture Schemes and Microgrid Control Functionalities', *Applied Sciences*, vol. 11, no. 6, p. 2793, Mar. 2021, doi: 10.3390/app11062793.

[77] W. Cheng and S. Lee, 'How Green Are the National Hydrogen Strategies?', *Sustainability*, vol. 14, no. 3, p. 1930, Feb. 2022, doi: 10.3390/su14031930.

[78] G. Gahleitner, 'Hydrogen from renewable electricity: An international review of power-to-gas pilot plants for stationary applications', *Int J Hydrogen Energy*, vol. 38, no. 5, pp. 2039–2061, Feb. 2013, doi: 10.1016/j.ijhydene.2012.12.010.

[79] IEA, M. Schoenfisch, and A. Dasgupta, 'Grid-Scale Storage', Paris, 2022.

[80] U.S Department of Energy, 'Energy Storage Grand Challenge: Energy Storage Market Report', 2020.

[81] I. Staffell and S. Pfenninger, 'The increasing impact of weather on electricity supply and demand', *Energy*, vol. 145, pp. 65–78, Feb. 2018, doi: 10.1016/j.energy.2017.12.051.

[82] A. Almuhtady, A. Alshwawra, M. Alfaouri, W. Al-Kouz, and I. Al-Hinti, 'Investigation of the trends of electricity demands in Jordan and its susceptibility to the ambient air temperature towards sustainable electricity generation', *Energy Sustain Soc*, vol. 9, no. 1, p. 39, Dec. 2019, doi: 10.1186/s13705-019-0224-1.

[83] M. Anvari, E. Proedrou, B. Schäfer, C. Beck, H. Kantz, and M. Timme, 'Data-driven load profiles and the dynamics of residential electricity consumption', *Nat Commun*, vol. 13, no. 1, p. 4593, Aug. 2022, doi: 10.1038/s41467-022-31942-9.

[84] T. H. Ruggles, D. J. Farnham, D. Tong, and K. Caldeira, 'Developing reliable hourly electricity demand data through screening and imputation', *Sci Data*, vol. 7, no. 1, p. 155, May 2020, doi: 10.1038/s41597-020-0483-x.

[85] IEA, 'Digitalisation and Energy', Paris, 2017.

[86] H. Maammeur, A. Hamidat, and L. Loukarfi, 'A Numerical Resolution of the Current-Voltage Equation for a Real Photovoltaic Cell', in *TerraGreen 13 International Conference 2013*, Advancements in Renewable Energy and Clean Environment, 2013.

[87] S. Dubey, J. Sarvaiya, and B. Seshadri, 'Temperature Dependent Photovoltaic (PV) Efficiency and Its Effect on PV Production in the World A Review', in *PV Asia Pacific Conference 2012*, 2012, pp. 313–316.

[88] C. Carl, 'Calculating Solar Photovoltaic Potential on Residential Rooftops in Kailua Kona, Hawaii', Master of Science, University of Southern California, 2014.

[89] RWE npower Renewables, 'Wind Turbine Power Calculations '.

[90] P. E. Bett and H. E. Thornton, 'The climatological relationships between wind and solar energy supply in Britain', *Renew Energy*, vol. 87, pp. 96–110, Mar. 2016, doi: 10.1016/j.renene.2015.10.006.

[91] H. C. Bloomfield, D. J. Brayshaw, P. L. M. Gonzalez, and A. Charlton-Perez, 'Sub-seasonal forecasts of demand and wind power and solar power generation for 28 European countries', *Earth Syst Sci Data*, vol. 13, no. 5, pp. 2259–2274, May 2021, doi: 10.5194/essd-13-2259-2021.

[92] IEA, 'Harnessing Variable Renewables', 2011.

[93] Eurelectric, 'Flexibility and Aggregation Requirements for their interaction in the market', Jan. 2014.

[94] C. Jin, J. Xiao, J. Hou, X. Wu, J. Zhang, and E. Du, 'Flexibility improvement evaluation of hydrogen storage based on electricity–hydrogen coupled energy model', *Global Energy Interconnection*, vol. 4, no. 4, pp. 371–383, Aug. 2021, doi: 10.1016/j.gloei.2021.09.004.

[95] T. H. Ruggles, J. A. Dowling, N. S. Lewis, and K. Caldeira, 'Opportunities for flexible electricity loads such as hydrogen production from curtailed generation', *Advances in Applied Energy*, vol. 3, p. 100051, Aug. 2021, doi: 10.1016/j.adapen.2021.100051.

[96] S. S. Farahani, C. Bleeker, A. van Wijk, and Z. Lukszo, 'Hydrogen-based integrated energy and mobility system for a real-life office environment', *Appl Energy*, vol. 264, p. 114695, Apr. 2020, doi: 10.1016/j.apenergy.2020.114695.

[97] I. Staffell *et al.*, 'The role of hydrogen and fuel cells in the global energy system', *Energy Environ Sci*, vol. 12, no. 2, pp. 463–491, 2019, doi: 10.1039/C8EE01157E.

[98] M. M. Whiston, I. Azevedo, S. Litster, K. Whitefoot, C. Samaras, and J. Whitacre, 'Total Cost of Ownership of Fuel Cell Electric Vehicles Using Expert Assessments', *ECS Meeting Abstracts*, vol. MA2018-02, no. 42, pp. 1419–1419, Jul. 2018, doi: 10.1149/MA2018-02/42/1419.

[99] H. Blanco, J. J. Gómez Vilchez, W. Nijs, C. Thiel, and A. Faaij, 'Soft-linking of a behavioral model for transport with energy system cost optimization applied to hydrogen in EU', *Renewable and Sustainable Energy Reviews*, vol. 115, p. 109349, Nov. 2019, doi: 10.1016/j.rser.2019.109349.

[100] S. Bhagavathy and J. Thakur, 'Green Hydrogen: Challenges for Commercialization', *IEEE Smart Grid*, Feb. 2021.

[101] M. Younas, S. Shafique, A. Hafeez, F. Javed, and F. Rehman, 'An Overview of Hydrogen Production: Current Status, Potential, and Challenges', *Fuel*, vol. 316, p. 123317, May 2022, doi: 10.1016/j.fuel.2022.123317.

[102] P. S. Roy, J. Song, K. Kim, C. S. Park, and A. S. K. Raju, 'CO2 conversion to syngas through the steam-biogas reforming process', *Journal of CO_2 Utilization*, vol. 25, pp. 275–282, May 2018, doi: 10.1016/j.jcou.2018.04.013.

[103] K. Bareiß, C. de la Rua, M. Möckl, and T. Hamacher, 'Life cycle assessment of hydrogen from proton exchange membrane water electrolysis in future energy systems', *Appl Energy*, vol. 237, pp. 862–872, Mar. 2019, doi: 10.1016/j.apenergy.2019.01.001.

[104] K. Kendall, 'Green Hydrogen in the UK: Progress and Prospects', *Clean Technologies*, vol. 4, no. 2, pp. 345–355, Apr. 2022, doi: 10.3390/cleantechnol4020020.

[105] Department for Transport, 'Electric vehicle charging device statistics: January 2022', 2022.

[106] PRA, 'Market Review 2022', Uckfield, 2022.

[107] L. G. Swan and V. I. Ugursal, 'Modeling of end-use energy consumption in the residential sector: A review of modeling techniques', *Renewable and Sustainable Energy Reviews*, vol. 13, no. 8, pp. 1819–1835, Oct. 2009, doi: 10.1016/j.rser.2008.09.033.

[108] W. Li *et al.*, 'Modeling urban building energy use: A review of modeling approaches and procedures', *Energy*, vol. 141, pp. 2445–2457, Dec. 2017, doi: 10.1016/j.energy.2017.11.071.

[109] O. Adeoye and C. Spataru, 'Modelling and forecasting hourly electricity demand in West African countries', *Appl Energy*, vol. 242, pp. 311–333, May 2019, doi: 10.1016/j.apenergy.2019.03.057.

[110] 'Building energy demand modeling', in *Urban Energy Systems for Low-Carbon Cities*, Elsevier, 2019, pp. 79–136. doi: 10.1016/B978-0-12-811553-4.00003-2.

[111] B. van Ruijven, B. de Vries, D. P. van Vuuren, and J. P. van der Sluijs, 'A global model for residential energy use: Uncertainty in calibration to regional data', *Energy*, vol. 35, no. 1, pp. 269–282, Jan. 2010, doi: 10.1016/j.energy.2009.09.019.

[112] M. Bourdeau, X. qiang Zhai, E. Nefzaoui, X. Guo, and P. Chatellier, 'Modeling and forecasting building energy consumption: A review of data-driven techniques', *Sustain Cities Soc*, vol. 48, p. 101533, Jul. 2019, doi: 10.1016/j.scs.2019.101533.

[113] M. A. Mat Daut, M. Y. Hassan, H. Abdullah, H. A. Rahman, M. P. Abdullah, and F. Hussin, 'Building electrical energy consumption forecasting analysis using

conventional and artificial intelligence methods: A review', *Renewable and Sustainable Energy Reviews*, vol. 70, pp. 1108–1118, Apr. 2017, doi: 10.1016/j.rser.2016.12.015.

[114] C. Li, X. Zheng, Z. Yang, and L. Kuang, 'Predicting Short-Term Electricity Demand by Combining the Advantages of ARMA and XGBoost in Fog Computing Environment', *Wirel Commun Mob Comput*, vol. 2018, pp. 1–18, 2018, doi: 10.1155/2018/5018053.

[115] S. Liu, A. Zeng, K. Lau, C. Ren, P. Chan, and E. Ng, 'Predicting long-term monthly electricity demand under future climatic and socioeconomic changes using data-driven methods: A case study of Hong Kong', *Sustain Cities Soc*, vol. 70, p. 102936, Jul. 2021, doi: 10.1016/j.scs.2021.102936.

[116] S. K. Dash, M. Roccotelli, R. R. Khansama, M. P. Fanti, and A. M. Mangini, 'Long Term Household Electricity Demand Forecasting Based on RNN-GBRT Model and a Novel Energy Theft Detection Method', *Applied Sciences*, vol. 11, no. 18, p. 8612, Sep. 2021, doi: 10.3390/app11188612.

[117] I. Ozer, S. B. Efe, and H. Ozbay, 'A combined deep learning application for short term load forecasting', *Alexandria Engineering Journal*, vol. 60, no. 4, pp. 3807–3818, Aug. 2021, doi: 10.1016/j.aej.2021.02.050.

[118] J. Pavlovic, G. Fontaras, S. Broekaert, B. Ciuffo, M. A. Ktistakis, and T. Grigoratos, 'How accurately can we measure vehicle fuel consumption in real world operation?', *Transp Res D Transp Environ*, vol. 90, p. 102666, Jan. 2021, doi: 10.1016/j.trd.2020.102666.

[119] S. M. M. Al-Chalabi and K. A. Al-Dhahiri, 'System Design for Measuring and Monitoring Fuel Consumption Remotely Using Embedded System', *J Phys Conf Ser*, vol. 1804, no. 1, p. 012113, Feb. 2021, doi: 10.1088/1742-6596/1804/1/012113.

[120] E. I. Toropov, Y. P. Trusov, A. S. Vashurin, and P. S. Moshkov, 'Estimation of the accuracy of fuel consumption measurement based on data from the on-board CAN-bus', *J Phys Conf Ser*, vol. 2061, no. 1, p. 012072, Oct. 2021, doi: 10.1088/1742-6596/2061/1/012072.

[121] A. Khan Ankur, S. Kraus, T. Grube, R. Castro, and D. Stolten, 'A Versatile Model for Estimating the Fuel Consumption of a Wide Range of Transport Modes', *Energies (Basel)*, vol. 15, no. 6, p. 2232, Mar. 2022, doi: 10.3390/en15062232.

[122] C. Hissler, 'How to determine the fuel consumption for a hydrogen light commercial vehicle project to be competitive?', KTH Royal Institute of Technology, Stockholm, 2022.

[123] H. Lohse-Busch *et al.*, 'Automotive fuel cell stack and system efficiency and fuel consumption based on vehicle testing on a chassis dynamometer at minus 18 °C to positive 35 °C temperatures', *Int J Hydrogen Energy*, vol. 45, no. 1, pp. 861–872, Jan. 2020, doi: 10.1016/j.ijhydene.2019.10.150.

[124] G. Guandalini and S. Campanari, 'Well-to-wheel driving cycle simulations for freight transportation: battery and hydrogen fuel cell electric vehicles', in *2018 International Conference of Electrical and Electronic Technologies for Automotive*, IEEE, Jul. 2018, pp. 1–6. doi: 10.23919/EETA.2018.8493216.

[125] Cenex, 'Project Report North East Scotland Fleet Review (Hydrogen Demand) ', Loughborough , Mar. 2021.

[126] T. Ramsden, 'An Evaluation of the Total Cost of Ownership of Fuel Cell Powered Material Handling Equipment', Colorado, 2014.

[127] A. Stewart and T. Dodson, 'Low Carbon Cars in the 2020s: Consumer Impacts and EU Policy Implications', Nov. 2016.

[128] Ballard Motive Solutions, 'Fuel Cell Maintenance and the "Moving Parts" Fallacy'. Accessed: Nov. 20, 2022. [Online]. Available: https://www.ballardmotivesolutions.com/insights/fuel-cell-maintenance-and-the-moving-parts-fallacy

[129] X. Hao *et al.*, 'Evaluating the current perceived cost of ownership for buses and trucks in China', *Energy*, vol. 254, p. 124383, Sep. 2022, doi: 10.1016/j.energy.2022.124383.

[130] M. Scorrano, R. Danielis, and M. Giansoldati, 'Dissecting the total cost of ownership of fully electric cars in Italy: The impact of annual distance travelled, home charging and urban driving', *Research in Transportation Economics*, vol. 80, p. 100799, May 2020, doi: 10.1016/j.retrec.2019.100799.

[131] E. Figenbaum, 'Retrospective Total cost of ownership analysis of battery electric vehicles in Norway', *Transp Res D Transp Environ*, vol. 105, p. 103246, Apr. 2022, doi: 10.1016/j.trd.2022.103246.

[132] F. Schmid, L. Taube, J. Rieck, and F. Behrendt, 'Electrification of Waste Collection Vehicles: Technoeconomic Analysis Based on an Energy Demand Simulation Using Real-Life Operational Data', *IEEE Transactions on Transportation Electrification*, vol. 7, no. 2, pp. 604–615, Jun. 2021, doi: 10.1109/TTE.2020.3031072.

[133] M. Chang *et al.*, 'Trends in tools and approaches for modelling the energy transition', *Appl Energy*, vol. 290, p. 116731, May 2021, doi: 10.1016/j.apenergy.2021.116731.

[134] M. A. Chang-Ojeda, J. Thellufsen, B. Zakeri, and H. Lund, 'Survey of Energy Systems Modelling Tools', 2021. doi: 10.17632/6s59gbxh6p.1.

[135] T. Lee, 'Optimization v.s Simulation '.

[136] M. Welsch, M. Howells, M. Bazilian, J. F. DeCarolis, S. Hermann, and H. H. Rogner, 'Modelling elements of Smart Grids – Enhancing the OSeMOSYS (Open Source Energy Modelling System) code', *Energy*, vol. 46, no. 1, pp. 337–350, Oct. 2012, doi: 10.1016/j.energy.2012.08.017.

[137] K. Poncelet, E. Delarue, J. Duernick, D. Six, and W. D'haeseleer, 'The Importance of Integrating the Variability of Renewables in Long-term Energy Planning Models', in *IAEE European Energy Conference*, Rome: IAEE, Oct. 2014.

[138] G. Haydt, V. Leal, A. Pina, and C. A. Silva, 'The relevance of the energy resource dynamics in the mid/long-term energy planning models', *Renew Energy*, vol. 36, no. 11, pp. 3068–3074, Nov. 2011, doi: 10.1016/j.renene.2011.03.028.

[139] P. A. Østergaard, 'Reviewing EnergyPLAN simulations and performance indicator applications in EnergyPLAN simulations', *Appl Energy*, vol. 154, pp. 921–933, Sep. 2015, doi: 10.1016/j.apenergy.2015.05.086.

[140] M. Z. Jacobson, M. A. Delucchi, M. A. Cameron, and B. A. Frew, 'Low-cost solution to the grid reliability problem with 100% penetration of intermittent wind, water, and solar for all purposes', *Proceedings of the National Academy of Sciences*, vol. 112, no. 49, pp. 15060–15065, Dec. 2015, doi: 10.1073/pnas.1510028112.

[141] N. Qamar, T. N. Malik, F. Qamar, M. Ali, and M. Naeem, 'Energy hub: modeling, control, and optimization', in *Renewable Energy Systems*, Elsevier, 2021, pp. 339–362. doi: 10.1016/B978-0-12-820004-9.00018-8.

[142] M. Geidl and G. Andersson, 'Optimal Power Flow of Multiple Energy Carriers', *IEEE Transactions on Power Systems*, vol. 22, no. 1, pp. 145–155, Feb. 2007, doi: 10.1109/TPWRS.2006.888988.

[143] A. A. Bayod-Rújula, Y. Yuan, A. Martínez-Gracia, J. Wang, J. Uche, and H. Chen, 'Modelling and Simulation of a Building Energy Hub', in *The 2nd International Research Conference on Sustainable Energy, Engineering, Materials and Environment*, Basel Switzerland: MDPI, Nov. 2018, p. 1431. doi: 10.3390/proceedings2231431.

[144] A. Mansour-Saatloo, M. A. Mirzaei, B. Mohammadi-Ivatloo, and K. Zare, 'A Risk-Averse Hybrid Approach for Optimal Participation of Power-to-Hydrogen Technology-Based Multi-Energy Microgrid in Multi-Energy Markets', *Sustain Cities Soc*, vol. 63, p. 102421, Dec. 2020, doi: 10.1016/j.scs.2020.102421.

[145] M. Geidl, 'Integrated Modeling and Optimization of Multi-Carrier Energy Systems', PhD Thesis, ETH Zurich, Zurich, 2007.

[146] Y. Cheng, M. Liu, H. Chen, and Z. Yang, 'Optimization of multi-carrier energy system based on new operation mechanism modelling of power-to-gas integrated with CO_2-based electrothermal energy storage', *Energy*, vol. 216, p. 119269, Feb. 2021, doi: 10.1016/j.energy.2020.119269.

[147] X. Ding, W. Sun, G. P. Harrison, X. Lv, and Y. Weng, 'Multi-objective optimization for an integrated renewable, power-to-gas and solid oxide fuel cell/gas turbine hybrid system in microgrid', *Energy*, vol. 213, p. 118804, Dec. 2020, doi: 10.1016/j.energy.2020.118804.

[148] A. Hajimiragha, C. Canizares, M. Fowler, M. Geidl, and G. Andersson, ‘Optimal Energy Flow of integrated energy systems with hydrogen economy considerations’, in *2007 iREP Symposium - Bulk Power System Dynamics and Control - VII. Revitalizing Operational Reliability*, IEEE, Aug. 2007, pp. 1–11. doi: 10.1109/IREP.2007.4410517.

[149] F. Kholardi, M. Assili, M. A. Lasemi, and A. Hajizadeh, ‘Optimal Management of Energy Hub with Considering Hydrogen Network’, in *2018 International Conference on Smart Energy Systems and Technologies (SEST)*, IEEE, Sep. 2018, pp. 1–6. doi: 10.1109/SEST.2018.8495664.

[150] A. Mansour-Saatloo, M. Agabalaye-Rahvar, M. A. Mirzaei, B. Mohammadi-Ivatloo, M. Abapour, and K. Zare, ‘Robust scheduling of hydrogen based smart micro energy hub with integrated demand response’, *J Clean Prod*, vol. 267, p. 122041, Sep. 2020, doi: 10.1016/j.jclepro.2020.122041.

[151] M. Haji Akhoundzadeh *et al.*, ‘A Conceptualized Hydrail Powertrain: A Case Study of the Union Pearson Express Route’, *World Electric Vehicle Journal*, vol. 10, no. 2, p. 32, May 2019, doi: 10.3390/wevj10020032.

[152] G. Zhao and E. R. Nielsen, ‘Social Impact Assessment of BIG HIT: A report into the societal impact of the project’, 2018.

[153] H. T. ARAT and M. G. SÜRER, ‘State of art of hydrogen usage as a fuel on aviation’, *European Mechanical Science*, vol. 2, no. 1, pp. 20–30, Dec. 2017, doi: 10.26701/ems.364286.

[154] W. Zhang *et al.*, ‘Optimal operation of wind-solar-hydrogen storage system based on energy hub’, in *2017 IEEE Conference on Energy Internet and Energy System Integration (EI2)*, IEEE, Nov. 2017, pp. 1–5. doi: 10.1109/EI2.2017.8245493.

[155] K. AlRafea, M. Fowler, A. Elkamel, and A. Hajimiragha, ‘Integration of renewable energy sources into combined cycle power plants through electrolysis generated hydrogen in a new designed energy hub’, *Int J Hydrogen Energy*, vol. 41, no. 38, pp. 16718–16728, Oct. 2016, doi: 10.1016/j.ijhydene.2016.06.256.

[156] M. Daraei, P. E. Campana, and E. Thorin, ‘Power-to-hydrogen storage integrated with rooftop photovoltaic systems and combined heat and power plants’, *Appl Energy*, vol. 276, p. 115499, Oct. 2020, doi: 10.1016/j.apenergy.2020.115499.

[157] P. R. da C. Mendes, J. E. Normey-Rico, and C. B. Alba, ‘Economic energy management of a microgrid including electric vehicles’, in *2015 IEEE PES Innovative Smart Grid Technologies Latin America (ISGT LATAM)*, IEEE, Oct. 2015, pp. 869–874. doi: 10.1109/ISGT-LA.2015.7381269.

[158] R. Proietto *et al.*, ‘Mixed heuristic-non linear optimization of energy management for hydrogen storage-based multi carrier hubs’, in *2014 IEEE International Energy Conference (ENERGYCON)*, IEEE, May 2014, pp. 1019–1026. doi: 10.1109/ENERGYCON.2014.6850550.

[159] M. Gökçek and C. Kale, 'Optimal design of a Hydrogen Refuelling Station (HRFS) powered by Hybrid Power System', *Energy Convers Manag*, vol. 161, pp. 215–224, Apr. 2018, doi: 10.1016/j.enconman.2018.02.007.

[160] S. Geng, M. Vrakopoulou, and I. A. Hiskens, 'Optimal Capacity Design and Operation of Energy Hub Systems', *Proceedings of the IEEE*, vol. 108, no. 9, pp. 1475–1495, Sep. 2020, doi: 10.1109/JPROC.2020.3009323.

[161] G. Chicco, S. Riaz, A. Mazza, and P. Mancarella, 'Flexibility From Distributed Multienergy Systems', *Proceedings of the IEEE*, vol. 108, no. 9, pp. 1496–1517, Sep. 2020, doi: 10.1109/JPROC.2020.2986378.

[162] S. M. Nosratabadi, M. Jahandide, and R. K. Nejad, 'Simultaneous planning of energy carriers by employing efficient storages within main and auxiliary energy hubs via a comprehensive MILP modeling in distribution network', *J Energy Storage*, vol. 30, p. 101585, Aug. 2020, doi: 10.1016/j.est.2020.101585.

[163] A. Vian, F. Bignucolo, and M. de Carli, 'Modelling and Optimization Approach of Residential Energy Hub: The GHOTEM Project', in *2019 1st International Conference on Energy Transition in the Mediterranean Area (SyNERGY MED)*, IEEE, May 2019, pp. 1–6. doi: 10.1109/SyNERGY-MED.2019.8764149.

[164] F. Schmid, L. Taube, J. Rieck, and F. Behrendt, 'Electrification of Waste Collection Vehicles: Technoeconomic Analysis Based on an Energy Demand Simulation Using Real-Life Operational Data', *IEEE Transactions on Transportation Electrification*, vol. 7, no. 2, pp. 604–615, Jun. 2021, doi: 10.1109/TTE.2020.3031072.

[165] R. Ewert, A. Grahle, K. Martins-Turner, A. M. Syré, K. Nagel, and D. Göhlich, 'Electrification of Urban Waste Collection: Introducing a Simulation-Based Methodology for Technical Feasibility, Impact and Cost Analysis', *World Electric Vehicle Journal*, vol. 12, no. 3, p. 122, Aug. 2021, doi: 10.3390/wevj12030122.

[166] A. Fattahi, J. Sijm, and A. Faaij, 'A systemic approach to analyze integrated energy system modeling tools: A review of national models', *Renewable and Sustainable Energy Reviews*, vol. 133, p. 110195, Nov. 2020, doi: 10.1016/j.rser.2020.110195.

[167] CIBSE, *CIBSE Guide A - Environmental Design*. 2006.

[168] European Comission, 'PHOTOVOLTAIC GEOGRAPHICAL INFORMATION SYSTEM (PVGIS)'. Accessed: Mar. 03, 2022. [Online]. Available: https://joint-research-centre.ec.europa.eu/pvgis-photovoltaic-geographical-information-system_en

[169] Hyundai, 'Hyundai HiS-S260MG (Data Sheet)'. 2013.

[170] K. Rao, *Wind Energy for Power Generation*. Springer International Publishing, 2019.

[171] G. Lente and K. Ősz, 'Barometric formulas: various derivations and comparisons to environmentally relevant observations', *ChemTexts*, vol. 6, no. 2, p. 13, Jun. 2020, doi: 10.1007/s40828-020-0111-6.

[172] ‘Data.ceda.ac.uk’. Accessed: Apr. 18, 2022. [Online]. Available: https://data.ceda.ac.uk/badc/ukmo-midas-open/data/uk-mean-wind-obs/dataset-version-202007/fife/00235_leuchars/qc-version-1

[173] Elexon, ‘Elexon Data flows available from BSC Systems’. Accessed: Oct. 04, 2023. [Online]. Available: https://www.elexon.co.uk/data/key-data-reports/data-flows-available-from-bsc-systems/

[174] Elexon, ‘UKERC Energy Data Centre: Data Catalogue’. Accessed: Oct. 04, 2023. [Online]. Available: https://ukerc.rl.ac.uk/DC/cgi-bin/edc_search.pl/?WantComp=42

[175] K. Morita, H. Shiromaru, Y. Manabe, T. Kato, T. Funabashi, and Y. Suzuoki, ‘A study on estimation of aggregated electricity demand for one-hour-ahead forecast’, *Appl Therm Eng*, vol. 114, pp. 1443–1448, Mar. 2017, doi: 10.1016/j.applthermaleng.2016.09.162.

[176] S. Patterson, ‘Do hospital admission rates increase in colder winters? A decadal analysis from an eastern county in England’, *J Public Health (Bangkok)*, vol. 40, no. 2, pp. 221–228, Jun. 2018, doi: 10.1093/pubmed/fdx076.

[177] J. R. Cancelo, A. Espasa, and R. Grafe, ‘Forecasting from one day to one week ahead for the Spanish system operator’, Getafe, 2008.

[178] M. Sajjad *et al.*, ‘A Novel CNN-GRU-Based Hybrid Approach for Short-Term Residential Load Forecasting’, *IEEE Access*, vol. 8, pp. 143759–143768, 2020, doi: 10.1109/ACCESS.2020.3009537.

[179] M. Alhussein, K. Aurangzeb, and S. I. Haider, ‘Hybrid CNN-LSTM Model for Short-Term Individual Household Load Forecasting’, *IEEE Access*, vol. 8, pp. 180544–180557, 2020, doi: 10.1109/ACCESS.2020.3028281.

[180] J. Pirie, J. Stenning, C. Cluzel, T. Dodson, and A. Zanre, ‘The Impact of a 2030 ICE Phase-Out in the UK’, Cambridge, Nov. 2020.

[181] HM Government, ‘Low-emission vehicles eligible for a plug-in grant’. Accessed: Feb. 28, 2023. [Online]. Available: https://www.gov.uk/plug-in-vehicle-grants/trucks

[182] HM Revenue & Customs, ‘Vehicle Excise Duty’, 2015.

[183] P. Lebeau, C. Macharis, and J. van Mierlo, ‘How to Improve the Total Cost of Ownership of Electric Vehicles: An Analysis of the Light Commercial Vehicle Segment’, *World Electric Vehicle Journal*, vol. 10, no. 4, p. 90, Dec. 2019, doi: 10.3390/wevj10040090.

[184] L. Rush, Y. Zhou, and D. Gohlke, ‘Vehicle Residual Value Analysis by Powertrain Type and Impacts on Total Cost of Ownership’, 2022.

[185] Leeds City Council, ‘Fleet Vehicles’, Dataset. Accessed: Feb. 16, 2023. [Online]. Available: https://datamillnorth.org/dataset/fleet-vehicles

[186] Leeds City Council, 'Fleet Vehicles Fuel Consumption', Dataset. Accessed: Feb. 16, 2023. [Online]. Available: https://datamillnorth.org/dataset/fleet-vehicles-fuel-consumption

[187] Y. Wang, Y. Pang, H. Xu, A. Martinez, and K. S. Chen, 'PEM Fuel cell and electrolysis cell technologies and hydrogen infrastructure development – a review', *Energy Environ Sci*, vol. 15, no. 6, pp. 2288–2328, 2022, doi: 10.1039/D2EE00790H.

[188] Ballard Power Systems, 'Fuel Cell Power Module for Heavy Duty Motive Applications'. Ballard Power Systems.

[189] M. Weiss, K. C. Cloos, and E. Helmers, 'Energy efficiency trade-offs in small to large electric vehicles', *Environ Sci Eur*, vol. 32, no. 1, p. 46, Dec. 2020, doi: 10.1186/s12302-020-00307-8.

[190] O. A. Hjelkrem, P. Arnesen, T. Aarseth Bø, and R. S. Sondell, 'Estimation of tank-to-wheel efficiency functions based on type approval data', *Appl Energy*, vol. 276, p. 115463, Oct. 2020, doi: 10.1016/j.apenergy.2020.115463.

[191] J. Stenning, D. Fazekas, U. Chewpreecha, B. Molnar, A. Vu, and Á. D. Hartvig, 'Exploring the trade-offs in different paths to reduce transport and heating emissions in Europe', Cambridge, May 2021.

[192] C. Rout, H. Li, V. Dupont, and Z. Wadud, 'A comparative total cost of ownership analysis of heavy duty on-road and off-road vehicles powered by hydrogen, electricity, and diesel', *Heliyon*, vol. 8, no. 12, p. e12417, Dec. 2022, doi: 10.1016/j.heliyon.2022.e12417.

[193] I. Staffel, 'The Energy and Fuel Data Sheet', Birmingham, Mar. 2011.

[194] Toshiba Europe, 'Pzip—Data Repository Site'. Accessed: Jan. 19, 2021. [Online]. Available: ftp://ldr.toshiba-trel.com/1073

[195] S. J. Pachernegg, 'A Closer Look at the Willans-Line', Feb. 1969. doi: 10.4271/690182.